Treg-Specific deletion of the phosphate SHP-1 impairs control of inflammation *in vivo*:

The role of SHP-1 in regulating regulatory T cell function and immune tolerance

QinLei Gu
Suzhou, China

M.S. University of Virginia, 2020

B.S., University of Wisconsin-Madison 2016

A Dissertation presented to the Graduate Faculty

of the University of Virginia in Candidacy for the Degree of

Doctor of Philosophy

Department of Microbiology, Immunology, and Cancer Biology

University of Virginia
March 2023

Abstract

In the immune system, regulatory T cells (Treg cells) are one of the crucial players contributing to the maintenance of immunological tolerance and homeostasis. A delicate balance is achieved between the activation of conventional T cells (Tcon cells) and the suppression by Treg cells to support a healthy and functional immune system. Previous studies demonstrated that the tyrosine phosphatase SHP-1, a negative regulator of TCR signaling, modulates Tcon cell resistance to Treg-mediated suppression, thereby shaping this activation-suppression balance. However, the role of SHP-1 in Treg cells is still not fully understood.

In this work, we revealed how SHP-1 affects the functional phenotype of Treg cells and modulates Treg suppressive function. At the intracellular signaling level, SHP-1 attenuates Treg Akt phosphorylation, and loss of SHP-1 drives Treg cells towards a glycolysis pathway. At the functional Treg cell level, SHP-1 limits the *in vivo* accumulation of $CD44^{hi}CD62L^{lo}$ T cells with the CD8+ and CD4+ Tcon cell populations under steady state condition. Interestingly under challenge, SHP-1-deficient Treg cells are less efficient in suppressing inflammation *in vivo,* once transferred, they may not survive or migrate to peripheral inflammation sites.

In addition, this study investigates the role of SHP-1 in Treg cells in aged mice. Incidental observations suggest that FOXP3+ Treg cell specific SHP-1 deficient mice may develop splenomegaly. Instead, preliminary results suggest a trend of FOXP3+ Treg loss and down regulation of ICOS expression in the aged mice.

Overall, this work identifies SHP-1 as a critical player in mediating the balance between T cell activation and suppression. Therefore, SHP-1 could potentially become a

promising therapeutic target for fine-tuning the balance between Treg-mediated suppression and Tcon activation/resistance to suppression.

Acknowledgements

I would like to thank my PI Dr. Ulrike Lorenz for her guidance and help in both my scientific pursuits and my life in Charlottesville.

I would also like to express my gratitude to our collaborator Dr. Kenneth Tung, whose expertise in mice pathology has been a great help to my project.

In addition, I am thankful for my committee members, Dr. Melanie Rutkowski, Dr. Kodi Ravichandran, Dr. Tajie Harris and Dr. Loren Erickson for their perspectives and input, which helped to shape my work. I am also grateful to all the individuals who provided technical support, shared their protocols and reagents and gave helpful advice for the experiments I conducted, including Christopher Medina, Marissa Gonzales, Jessica Harakal, Ranjit Sahu, Maile Hollinger, Hui Qiao and Ray Zeng.

Furthermore, I would also like to thank the current and previous members of our lab: Dr. Emily Mercadante, Darya lavashova, Mahmut Parlak, and Tabish Khan for their support and friendship, as well as the staff members in the research histology core for processing all my paraffin samples and previous MIC and CIC staff members Peggy Morris, Sandy Weirich, Amy Anderson for their assistance.

I am grateful for the support of my family, especially my parents. Without their support and encouragement, I would not have come this far. I would also like to remember my grandpa and my uncle, who first nurtured my interest in science and living beings, but passed away during my year in PhD program.

Lastly, I would like to thank all the mice that I have used during my graduate studies. I hope that my work has justified their sacrifice.

Table of contents

List of Abbreviations

Ab	Antibody
ADAP	Adhesion and degranulation-promoting adapter protein
Ag	Antigen
AIG	Autoimmune gastritis
AIRE	Autoimmune regulator
Akt	Protein kinase B
ANOVA	Analysis of variance
APC	Antigen presenting cell
cAMP	cyclic adenosine monophosphate
CD	Cluster of differentiation
cDNA	Complementary deoxyribonucleic acid
CNS	Conserved non-coding sequences
Crk II	CT10 regulator of kinase II
CTLA-4	Cytotoxic T lymphocyte antigen 4
CTV	Cell trace violet
DC(s)	Dendritic cell(s)
DEREG	DEpletion of REGulatory T cells
dLck	Distal promoter of Lck
DN	Double negative thymocyte
DP	Double positive thymocyte

ELISA	Enzyme-linked immunosorbent assay
FBS	Fetal bovine serum
fl	floxed
FOXP3	Forkhead box P3
FR4	Folate receptor 4
GITR	Glucocorticoid-induced TNFR-related protein
Gzmb	Granzyme B gene
HRP	Horseradish Peroxidase
ICAM-1	Intercellular adhesion molecule 1
ICOS	Inducible T cell costimulator
ICOSL	Inducible T cell costimulator ligand
IDO	Indoleamine 2,3-dioxygenase
IFN	Interferon
IFNγ	Interferon gamma
IL	Interleukin
IPEX	Immune dysregulation, polyendocrinopathy, enteropathy, X-linked
iTreg	induced Treg
JAK	Janus kinase proteins
LAG-3	Lymphocyte-activation gene 3
Lck	Lymphocyte-specific protein tyrosine kinase
LFA-1	Lymphocyte function-associated antigen 1
LN	Lymph node(s)

MACS	Magnetic activated cell sorting
me/me	*motheaten* mice
MFI	Mean fluorescence intensity
MHC I/II	Major histocompatibility complex class I or class II
miR	microRNA
mRNA	Messenger ribonucleic acid
mTOR	Mechanistic target of rapamycin
OX-40	Tumor necrosis factor receptor superfamily member 4
PBS	Phosphate buffered saline
PE	phycoerythrin
PI3K	Phosphoinositide 3-kinase
pTreg	peripheral Treg
RAG1/2	Recombination activating gene 1/2
RBC	red blood cell
RNA-seq	Ribonucleic acid sequencing
S.D.	Standard deviation
s.e.m	Standard error of the mean
S473	Serine 473 (in AKT)
SLP-76	Lymphocyte cytosolic protein 2
SSG	Sodium stibogluconate
STAT	Signal transducer and activator of transcription proteins
T-bet	T-box expressed in T cells
Tc cells	Cytotoxic T lymphocyte

Tcon cells	Conventional T lymphocyte
tdTomato	tandem dimer Tomato fluorescent protein
Teff cells	Effector T lymphocyte
Tfh cells	T follicular helper cells
TGF	Transforming Growth Factor
Th cells	Helper T lymphocytes
Tigit	gene coding for T-cell immunoglobulin and ITIM domain
TLR	Toll-like receptor
Treg cells	Regulatory T lymphocyte
tTreg	thymic Treg
WT	Wildtype
Ebi3	Epstein-Barr Virus Induced gene 3
Zap-70	Zeta-chain-associated protein kinase 70
TRAF6	TNF receptor associated factor 6
Tnfrsf18	TNF Receptor Superfamily Member 18, gene coding for GITR
Ikzf2	IKAROS Family Zinc Finger 2, gene coding for Helios
mLN	mesenteric lymph nodes
NRP-1	**Neuropilin-1**
isoDCA	3β-hydroxydeoxycholic acid
FXR	Farnesoid X eceptor
EV	Extracellular vesicles
A2AR	Adenosine receptor 2A

SHP-1	Src homology region 2 domain-containing phosphatase 1
TCR	T cell receptor
RPMI	Roswell Park Memorial Institute medium
H&E	hematoxylin and eosin
PAS	Periodic Acid Schiff stain
AAI	allergic airway inflammation
HDM	house dust mite
DT	Diphtheria Toxin
OCAR	Oxygen consumption rate
ECAR	Extracellular acidification rate
PD-1	Programmed cell death protein 1
GATA3	GATA binding protein 3
RORγt	Retineic-acid-receptor-related orphan receptor gamma
qPCR	Quantitative polymerase chain rection
loxP	locus of x-over, P1
pAKT	phosphorylated AKT
LSD	Least significant difference
FOXO	Forkhead box protein O
Tvm cells	Virtual memory T cells
IRIP	Inducible and reversible *in vivo* protein degradation
c-SMAC	central supramolecular activation cluster
p-SMAC	peripheral supramolecular activation cluster
C3G	Rap guanine nucleotide exchange factor 1 (RAPGEF1)

Rap1	Ras-proximate-1/Ras-related protein 1
FAK	Focal adhesion kinase
PYK2	protein tyrosine kinase 2-beta
SKAP1	Src kinase-associated phosphoprotein 1
Bim	BCL2-interacting mediator of cell death
GRB1	Growth-factor receptor-bound protein-2

List of Figures

Chapter 1

Introduction

The Immune System

Our immune system relies on multiple levels of control to balance its response to danger while maintaining self-tolerance. The evolution of the immune system has been driven by the need to protect organisms from a wide variety of pathogens, including viruses, bacteria, fungi, and parasites. Pathogens have evolved in parallel to evade the immune system's surveillance, leading to a constant race between the immune system and pathogens.

The immune system has evolved alongside the first evidence of organisms 3.5 billion years ago (1) and has proven to help the host adapt to changes in the environment and the emergence of new pathogens. In early unicellular organisms such as bacteria and archaea, prokaryotes utilize the clustered regularly interspaced short palindromic repeat (CRISPR)/Cas (CRISPR-associated system) to generate resistance against invading foreign DNA (1). The evolutionary history of the immune system can be traced back to the earliest multicellular organisms, such as sponges and cnidarians (2), which possess a primitive innate immune system. Innate immunity is the first line of the host defense system and includes mainly short-lived myeloid cells, such as monocytes, mast cells, macrophages, neutrophils, basophils, and eosinophils, as well as some lymphoid cells, such as natural killer (NK) cells and innate lymphoid cells (ILCs) (3,4,5). The majority of these cells (except ILCs) express pattern recognition receptors (PRRs) that can identify pathogen-associated molecular patterns (PAMPs) from various pathogens, including viral materials and bacterial and fungal components (5). This allows them to quickly identify and upregulate inflammatory mechanisms in response to numerous invading pathogens.

The emergence of adaptive immunity during chordate evolution about 500 million years ago added a new level of complexity to immune defenses (1,6). The expression of somatically diversified antigen receptors, a key component providing an additional layer of defense specificity, appears in all vertebrate animals (6,7,8). The unique development of the major cellular effectors, lymphocytes, in adaptive immunity allows the recognition of antigens triggering the activation of the immune response (7). Each lymphocyte has a unique antigen recognition receptor that is generated combinatorially, resulting in a highly diverse receptor repertoire (3,8). This enables vertebrate hosts to recognize and respond to a vast range of potential pathogens or toxins in an antigen-specific manner.

B cells and T cells are the two major lymphocyte lineages shared by the adaptive immune system in all vertebrate animals (7,8). After sensing dangerous signals, such as microbes with PRRs, the players in the innate immune system instruct the activation of T cells and B cells in the immune response (9). These two types of lymphocytes are highly specific in recognizing and combating pathogens with the help of the innate immune system. T cells express T cell receptors (TCR) that recognize foreign and self-antigens bound to major histocompatibility complex molecules (MHC) on host cells leading to various effector functions (see below), while B cells express immunoglobulin (Ig) receptors that recognize intact antigens. Upon activation and maturation, B cells secrete antibodies that facilitate the clearance of pathogens by blocking their access to cells and aiding in their recognition and clearance by phagocytes. The T and B cell arms of the adaptive immune responses share common features, including V(D)J recombination of antigen receptors and the establishment of immune memory, which differentiate them from the innate immune response (4,10). During V(D)J recombination, one V (variable)

gene segment joins to one J (joining) gene segment. In the case of BCR heavy chains or certain TCR chains, such as alpha chains, a D (diversity) gene segment is also included (11,12). The TCR and BCR recombination processes both involve the RAG1/2 enzymes and the recognition and cleavage of RSS sequences flanking the gene segments. This process happens in the thymus for T cells, while B cell development occurs in the bone marrow (4,12). The end result is the generation of a diverse repertoire of antigen receptors that allows T and B cells to recognize and respond to a wide range of foreign antigens.

In addition to recognizing a diverse range of antigens, immune memory is also a critical component of the adaptive immune system, enabling a more rapid and efficient response upon re-exposure to a pathogen. T and B cells undergo clonal expansion and differentiate into effector cells, which can directly combat the pathogen. Memory B cells are produced after the initial contact of the naïve B cells with antigen-specific T follicular helper (TFH) cells, which stimulate the formation of germinal centers in the pre-GC phase. During the germinal center reaction, B cells undergo multiple rounds of B cell receptor (BCR) diversification, clonal expansion, and class-switch recombination (GC phase), resulting in the selection of high-affinity GC B cell variants that contribute to the memory B cell compartment (12).

Naive T cells become activated when they encounter cognate antigens presented by antigen-presenting cells (APCs) (13). This results in the T cells undergoing clonal expansion and differentiation into effector T cells, which then travel to the site of infection. Once the infection is cleared, a small proportion of the effector T cells differentiate into central memory T cells, which can be found in the circulation and

lymphoid organs, and effector memory T cells, which are localized in peripheral tissues and circulate in the blood throughout the host body (9,14). However, not all lymphocytes actively migrate throughout the system. These so-called “tissue-resident” T cells, which include conventional T cells (Tcon), regulatory T cells (Treg), or “innate-like” T cells, such as MAIT cells, γδ T cells, and iNKT cells (15), have been found to permanently reside in the skin, gut, liver, lung, brain and other tissues in the body (14,16,17)

T cells

T cells are one of the major participants in the adaptive immune system and were named after their discovery in the thymus, a primary lymphoid organ (10,18). The thymus is an ancient and anatomically homogenous lymphoid organ, evolutionarily specialized in normal T cell development and selection (7). Both the thymus in jawed vertebrates and the thymoid tissue in lamprey larvae express FOXN1 (19,20), which likely further regulates the expression of chemokines, such as CXCL12 in lampre, or CXCL12, CCL25, and CCL21 in mouse embryos (19,20) to attract hematopoietic progenitor cells to the thymic rudiment. Within the thymus, Delta-like 4 (DLL4) is expressed on local epithelial cells and functions as the ligand for NOTCH1, the T cell lineage-specification molecule, to activate the NOTCH signaling pathway (7,21).

T cell composition changes throughout the lifespan of a host. In early life, naive T cells and thymic derived regulatory T cells, which will be discussed in a later section of this introduction, are produced from the thymus and spread across significant lymphoid and mucosal areas of the body. In contrast to the adult tissues, where memory T cells are the dominant population due to repeated antigen exposure and infections experienced by the host system, during the first two years of life, the pediatric tissues and blood are

mainly populated by naïve T cells recently emigrated out from the thymus. In these young and immunologically naïve hosts, memory T cells predominantly accumulate in mucosal sites like the small intestine and lungs (22,23). As an individual ages, memory T cells increase in frequency throughout the body, including secondary lymphoid organs, and this accumulation is even more pronounced at mucosal and barrier sites (24, 25)

The helper T cells (Th) and cytotoxic T cells (Tc) are two major types of effector T cells. Helper T cells are characterized by the expression of CD4 and activate and coordinate immune responses by recognizing and binding to specific antigens presented by MHC class II molecules on the surface of APCs (25,26). Upon activation, T cells undergo clonal expansion and exhibit various effector functions, as described below. TCR signaling, together with signaling pathways from other molecules such as cytokines, costimulatory molecules, chemokines, integrins, and metabolites, drives the differentiation of activated CD4+ T helper cells into specific subtypes (Figure 1.1), such as Th1 (28), Th2 (29), Th17 (29), follicular helper T (30), and Treg cells (26, 27). Each of these subtypes of Th cells produces a specific panel of cytokines that define their subtype and activate other immune cells, such as B cells, cytotoxic T cells, and macrophages, and help them to differentiate and function more effectively (26, 27). For example, Th1 cells are skewed by IL-12 and interferon-γ (IFN-γ) and secrete IFN-γ, which helps fight intracellular viruses and pathogens (31). Th2 cells, skewed by IL-25, IL-33, and IL-4 *in vivo*, produce IL-4, IL-5, and IL-13 cytokines to help fight extracellular bacteria and parasitic pathogens and promote antibody production (32). Th9 cells generate IL-9 cytokine and have a controversial role in both parasitic infections and

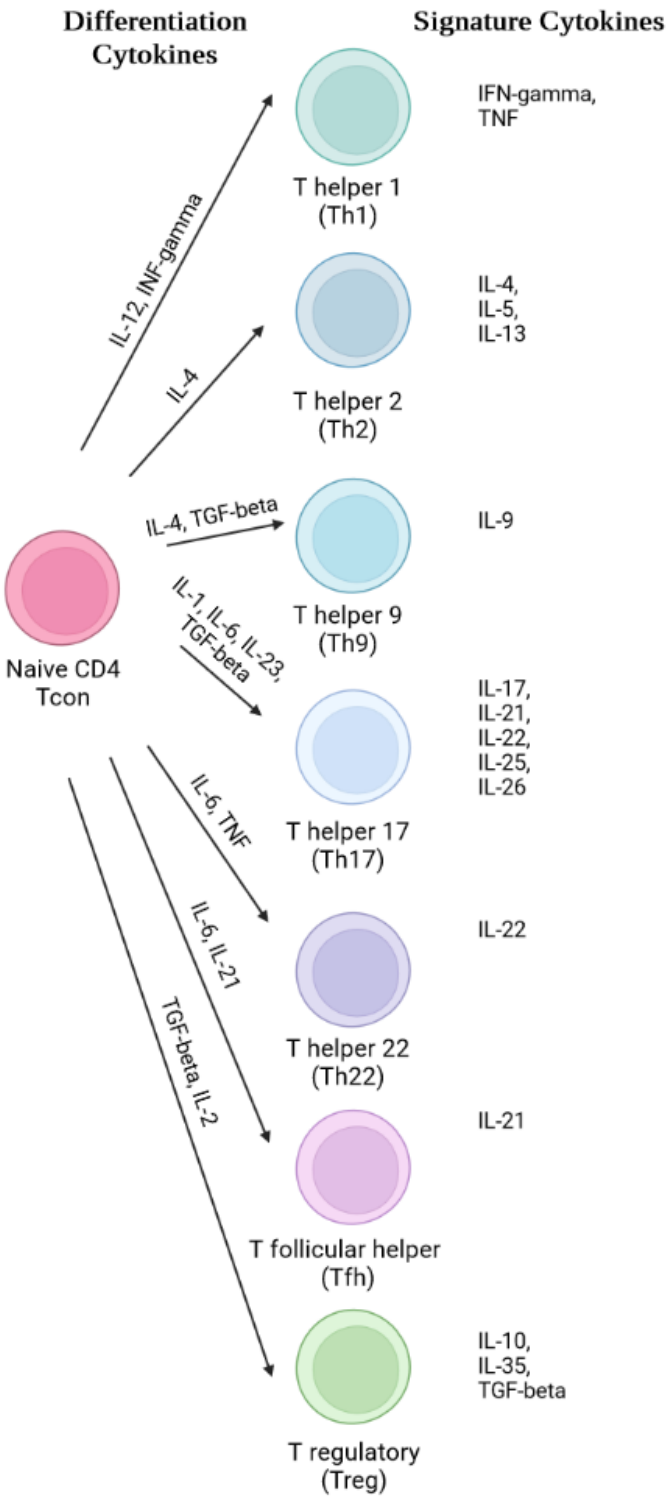

Figure 1.1: CD4+ helper T cell subsets derived from naïve conventional CD4 cells. Th1, Th2, Th9, Th17, Th22, Tfh and peripheral Treg cells can be differentiated from naïve CD4 Tcon cells via stimulation with indicated combinations of differentiation-

driving cytokines. Each differentiated T cell subset produces a distinct set of signature cytokines. Figure adapted from (225).

cancer settings (33-35). Th17 cells, induced by IL-6, IL-21, IL-23 and TGF-β, produce IL-17A, IL-17F, and IL-22 cytokines for bacterial pathogen control (36). Different transcriptional master regulators are expressed following the skewing of naïve CD4 cells by respective cytokines, and each transcriptional master regulator is critical for Th cell differentiation, cytokine production, and lineage commitment. Th1 cell differentiation is regulated by the T-box transcription factor T-bet (37). Th2 cell differentiation is regulated by GATA-binding protein 3 (GATA3) (38). Th17 cells are defined by expression of the master transcription factor RORγt (39). Tfh cells play an important role in modulating B cell maturation and are defined by B cell lymphoma 6 (BCL-6), which induces CXCR5 and ICOS expression and promotes the migration of Tfh cells to the B cell follicle (40,41). The master transcription factor for Treg cells is forkhead box P3 (FOXP3) (42,43). Interestingly, certain subsets of T cells, such as Th17 and Treg cells, are not permanently committed to one subtype and can be transformed into other lineages when exposed to specific stimuli or in the presence of inflammatory disease conditions (44-46). For example, BCL-6 can maintain a low level of background expression in the Th1 cell population despite high T-bet expression (71,72) during conditions such as Listeria monocytogenes infection, which allows for the quick alteration between Th1 and Tfh populations and provides more flexibility for responsive Th 1 and Tfh cells (46).

In contrast to CD4+ Th cells, Tc cells express CD8 and recognize the cognate peptide presented by MHC I molecules. Upon activation, CD8 T cells directly attack and kill infected cells through the release of lytic granules that contain cytotoxic substances such as serglycin, perforin and granzymes, leading to the induction of apoptosis in the infected cells (25, 47-49). In addition to the lytic granules, Tc cells can also initiate

killing by delivering extracellular vehicles (EVs) containing Fas ligand (FasL) (50, 51) or by contacting target cells with Fas ligand on their plasma membrane during immunological synapse formation (51, 52). This process exploits the Fas receptor expressed on the target cells and triggers a signaling cascade that leads to the activation of a caspase-dependent cell death pathway, together with the release of APO2 ligand/TRAIL also in EVs (53). Recently, supramolecular attack particles (SMAPs) were identified as another Tc killing pathway (51, 54, 55), which has a longer half-life (52, 54) and can deliver killing autonomously.

After acute infection or vaccination, most effector CD8 T cells (Teff) undergo apoptosis following antigen clearance, but a small population of memory precursor T cells remains, which can further differentiate into memory CD8 T cells (56). These memory T cells are distributed throughout the body to provide immune protection, and some of them become tissue-resident memory T cells, which are maintained in tissues and epithelial regions and are poised to respond to secondary antigen exposure (57-59). These memory CD8 T cells downregulate their cytotoxic effector function and alter their cytokine profile, coinciding with the upregulation of transcription factors Eomes and Tcf-1. Additionally, they acquire the ability to self-renew in response to IL-7 and IL-15 (27, 56, 57). Some memory CD8 T cells remain in local tissues to become resident memory CD8 T cells (Trm) and express high levels of CD69 and CD103 and low levels of CD127 (56). However, during chronic infections or tumor conditions where the antigens persist, failure in the memory T cell development can lead to so-called CD8 exhaustion (56, 60). Exhausted T cells lose their effector functions and exhibit elevated and sustained expression of inhibitory receptors (IRs). They also have unique metabolism and display

epigenetic and transcriptional characteristics that distinguish them from Teff and memory T cells (60-62)

Thymic T cell differentiation

Early T cell programming begins with the migration of multipotent hematopoietic progenitor cells to the thymus, where they receive NOTCH pathway signals from the thymic microenvironment and start to proliferate (63,64). T cell development starts with double-negative (DN) cell form that lacks expression of both CD4 and CD8 (65). These cells then progress through a double negative 1 (DN1) stage and become early thymic progenitor (ETP) cells, which are characterized as KIT+CD44+CD25– cells (65,66). The ETP cells then transition through DN2a, DN2b, DN3a, DN3b, and DN4 stages and lose the ability to become non-T lymphocytes even if removed to a non-NOTCH signaling environment (66,67). The differentiation of fate-committed T cells is driven by NOTCH 1 signaling, along with other transcription factors, such as TCF1, GATA-3, RUNX proteins, E-box proteins, and potentially BCL-11B (26, 63, 68,69). The different DN stages: DN2a, DN2b, DN3a, DN3b, DN4 are defined by the presence or absence of growth factor receptor CD117 Kit, CD127, CD44, and CD25 expression on the cells (66,67). During the DN3 stage of T cell development, a complex of pre-TCRα and mature β chains appears in the plasma membrane. The mature β chain is generated by somatic DNA rearrangement via RAG 1 or RAG 2 (73- 75).

Positive selection:

Positive selection of T cells with a functional pre-TCR occurs through β selection, leading to massive proliferation and TCRa gene rearrangement (68, 76). The DN pro T

cells acquire CD4 and CD8 expression to become double-positive (DP) cells (68), which will eventually differentiate into mature CD4 or CD8 single-positive (SP) cells. The affinity of each TCR for encountered MHC-peptide complexes becomes crucial for the fate of the thymocyte from this point on. Thymocytes whose TCRs do not bind to the MHC-peptide complex will not receive survival signals and die quickly due to neglect, while those expressing TCRs with low affinity for MHC-peptide will be positively selected (26, 63).

Negative selection:

After TCR rearrangement, immature CD4+CD8+ DP thymocytes undergo selection and maturation processes in the thymic cortex and medulla (80, 81). DP T cells interact with cortical thymic epithelial cells (cTECs) and bone marrow-derived antigen-presenting cells, such as dendritic cells (DCs) (82). DP T cells that recognize high-affinity self-peptide-MHC complexes undergo clonal deletion, a process of programmed cell death (4, 68). DP T cells that express TCRs with lower affinity for self-peptide-MHC complexes are positively selected (as described above) and differentiate into CD4+ or CD8+ single-positive (SP) cells as they migrate from the cortex to the medulla (4,81). In the medulla, SP cells continue to sample antigens presented by medullary thymic epithelial cells (mTECs) and DCs. In contrast to the cTECs, which play a critical role in the positive selection of T cells in the outer cortex region, the mTECs are responsible for inducing negative selection at the inner medulla area (83). mTECs express the transcription factor AIRE, promoting the expression of tissue-specific antigens (TSAs) (4, 82, 83, 84). Lack of AIRE in host mTECs has been shown to be associated with autoimmune diseases affecting multiple organs, including type 1 autoimmune

polyglandular syndrome (APS-1), or autoimmune polyendocrinopathy-candidiasis-ectodermal dystrophy (APECED) syndrome, which results in underactive parathyroid gland and dysfunction in the gastrointestinal tract, and Sjögren's syndrome, which disrupts the normal function of lacrimal and salivary gland (85,86, 87). Recent findings suggest that the transcriptional regulator, FEZ family zinc finger 2(Fezf2), may compensate for AIRE function (83, 85). This process is known as promiscuous gene expression and is essential for generating self-tolerance and removing self-reacting T cells (83). While most αβ T cells differentiate into CD4+ T cells restricted by MHC class II or CD8+ Tc cells restricted by MHC class I molecules (68), a few T cell subsets, such as invariant natural killer T cells are selected by lipid-bound MHC class I–like CD1d molecules presented in the medullary microenvironments (88-90).

Regulatory T cell

Regulatory T (Treg) cells are one of the crucial participants in controlling various immune responses (91), including allergy, autoimmunity, anti-tumor immunity, metabolic regulation, and tissue repair (92-96). Treg cells are primarily recognized for their suppressive function that keeps excessive inflammatory responses under control. However, emerging data suggest additional roles of Treg cells in non-immune settings during tissue regeneration, such as in stimulating hair follicle regeneration (97) and muscle repairment (98).

Since the initial identification of FOXP3 as a Treg master transcription factor (42-43, 99-102), additional types of regulatory T cells have been discovered (103). In humans, FOXP3 can also be upregulated in activated effector conventional T cells (Tcon)

without any associated suppressive activities (80, 103-105). However, in mice, FOXP3 is still considered the exclusive master transcription factor of Treg cells (106).

The term “regulatory T cells” can refer to different T cells exhibiting suppressive activities (107), including the most widely recognized CD4+CD25+FOXP3+ suppressive Th cells (42, 106), CD4+FOXP3-IL10+ T regulatory type 1 cells (108,109), and the CD8 +FOXP3+ cells (110-112). In this study, we focus primarily on the CD4+ FOXP3+ CD25+ Treg cells, which are characterized by constitutive expression of nuclear Foxp3 and the surface proteins CD25, CD45RO, GITR, CD122, HLA-DR, CCR4, and CTLA-4 in human (101) and CD25, CD45RBlow, CTLA-4, and GITR in mice (43). Treg cells can either be derived from the thymus as part of thymic T cell development or differentiated from naïve conventional CD4+ T cells in the periphery. Moreover, Treg cells can also be artificially induced *ex vivo* in therapeutic or experimental settings (113, 81).

Regulatory T cell differentiation

Although the thymic exposure of the developing T cells to high-affinity self-antigens has been shown to induce clonal deletion of T cells (68), in the current prevailing perspective of the Treg cell differentiation model, a higher TCR affinity interaction with self-antigen and the resulting stronger TCR signaling strength also favor thymic-derived regulatory T (tTreg) differentiation. This affinity hypothesis proposes that stronger TCR signaling engaging with precursor cells induces CD4+ SP cells to preferentially differentiate into tTreg cells, as opposed to the negative selection or Tcon cell differentiation (82, 114). Some studies suggest that the TCR signaling strength required for Treg development appears to be lower than that for clonal deletion during the negative selection (114,115). While FOXP3 is considered the “master regulator” of Treg

cells, their fate in the thymus may be determined far prior before the FOXP3 expression (116). For instance, some Treg cell signature genes, such as Tnfrsf18 encoding for GITR (117) and Ikzf2 encoding for Helios (116) are upregulated in human thymic Treg precursor cells long before FOXP3 expression (118). In CD25−Foxp3− CD4+ SP thymocytes, strong agonist antigen binding to the TCR induces the upregulation of IL-2Ra (CD25), leading to the IL-2 dependent CD25+Foxp3− type of Treg precursor cells (119, 120). In this "two-step" model of Treg precursor cell to Treg cell differentiation, CD25+Foxp3− Treg precursor cells do not require further TCR-driven stimulation but are induced by the IL-2-STAT5 signaling pathway, eventually leading to stable FOXP3 expression both in vivo and in vitro (116, 120, 121).

In the periphery, the majority of Treg cells are thymic-derived (t) Treg cells (116). Another type of Treg, known as peripheral (p) Treg cells, can be derived from naïve CD4 T cells in many peripheral organs. Following thymic differentiation, naïve CD4+ SP Tcon cells migrate out of the thymus and enter the peripheral lymphoid tissues (82). In order to differentiate into the pTreg cells, these naïve CD4 Tcon cells encounter high-affinity agonist antigens at a sub-immunogenic concentration (82) in the presence of a Treg-inducing environment such as cytokines and/or metabolic products (116) (Figure 1.2). For instance, in the peripheral intestinal mucosa, DCs attract naïve T cells by controlling the expression of homing receptors (122). Upon reaching the site, naïve T cells encounter the tolerance-inducing cytokine IL-10, which is constitutively produced by various immune cell types, including macrophages, T cells, neutrophils, mast cells, and DCs (25,122), and also bind to regular food antigens presented by DCs in the

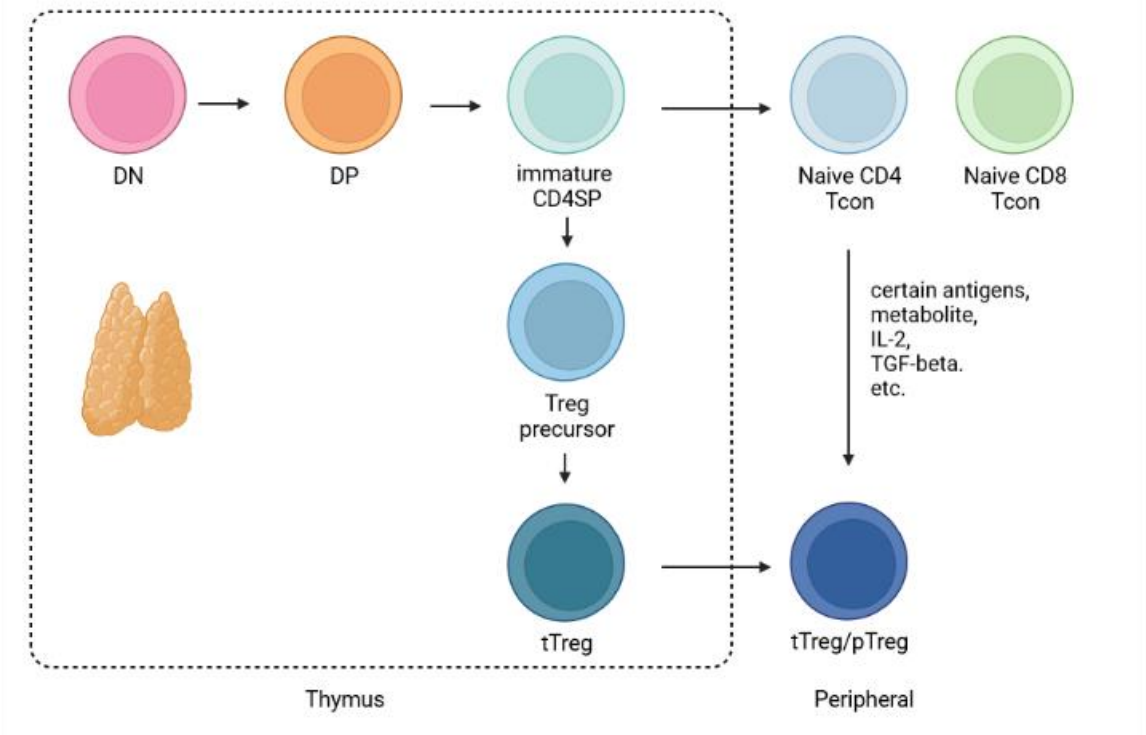

Figure 1.2: Schematic representation of thymic Treg cell development. DN: double negative T cells; DP: double positive T cells; Immature CD4SP: immature CD4 single positive cells; Treg precursor: FOXP3+ CD25- and CD25+ FOXP3- Treg precursor cells; tTreg: thymic derived Treg cells; pTreg: peripheral derived Treg cells. Thymus produces both tTreg and Tcon cells. Naïve CD4 Tcon cells encounter IL-2, TGF-β and/or certain tolerogenic antigens and metabolites in the periphery and differentiate into pTreg cells.

mesenteric lymph nodes (mLN) (123) leading to their differentiation into pTreg cells. Commensal bacteria in the gut also produce metabolites that promote pTreg differentiation. For instance, the secondary bile acid 3β-hydroxydeoxycholic acid (isoDCA) signals through DCs to downregulate farnesoid X receptor (FXR) and skew the DCs to an anti-inflammatory phenotype, which facilitates Treg cell accumulation in the colon (125). In experimental settings, Treg cells can be induced from CD4 Tcon cells with IL-2 and TGF-β1 *in vivo*.

Although there is no clear marker that differentiates developed pTreg cells from the tTreg cells - Helios and NRP-1 are used as potential tTreg markers, but are not constantly reliable, especially in the transgenic mouse model - genetic enhancers required for their development differ. The conserved non-coding sequences 1 (CNS 1) in the Foxp3 intron that responds to TGF-β and promotes upregulation of FOXP3 expression in pTregs (126) are not part of the process during tTreg generation (127).

Treg suppression and immune tolerance

First identified as “suppressor T cells” in contrast to the “helper T cells” during the 1970s (10, 128), Treg cells have since been recognized as the key player among immunological tolerance-promoting cells. Mutations in the Treg master regulator, “FOXP3”, lead to severe autoimmune diseases in both humans and mice (97). Under normal physiological conditions, the activation of CD8 and CD4 Tcons and their suppression by Treg cells balance each other, contributing to a well-regulated immune response and homeostasis. However, an imbalance in this Tcon-Treg equilibrium can result in pathophysiological phenotypes. For example, failure in suppression favors

autoimmune diseases, such as IPEX (129), while a hyper-suppressive environment within the tumor site may hinder anti-tumor immunity (130).

Although the exact details of Treg-mediated suppression are complex and not completely understood, several potential suppressive mechanisms have been described (Figure 1.3). Firstly, Treg cells out-compete Tcon cells for IL-2 by expressing higher levels of IL-2R (CD25) on their surface, thereby reducing the amount of IL-2 available for Tcon cell expansion and activation (131-133). Secondly, Treg cells secrete immunosuppressive cytokines such as TGF-β, IL-10, and IL-35 (134-137). Thirdly, Treg cells generate additional molecules, such as immunosuppressive micro RNAs (miRNAs) - for example, miR-142-3p is produced by Treg and delivered to DCs to induce a more tolerance-promoting cytokine production profile, and miR-449a-5 is produced by induced Treg (iTreg) cells, which inhibits Th17 differentiation through targeting the Notch1 signaling pathway (138-142) – as well as cAMP (143-145) and adenosine (146,147). Fourthly, Treg cells modulate the expression of co-stimulatory molecules on APCs (148-151). Fifthly, Treg cells can induce cell death by releasing extracellular vehicles (EVs) loaded with immunosuppressive molecules such as granzyme B (152,153).

Despite the fact that many mechanisms of suppression have been reported over the years, our understanding of the signaling pathways that regulate Treg activity is still relatively limited, and thus is the main topic of this thesis.

SHP-1 and TCR signaling

Src homology region 2 domain-containing phosphatase 1 (SHP-1) is a tyrosine phosphatase that is expressed ubiquitously in all hematopoietic cell lineages (154). SHP-1

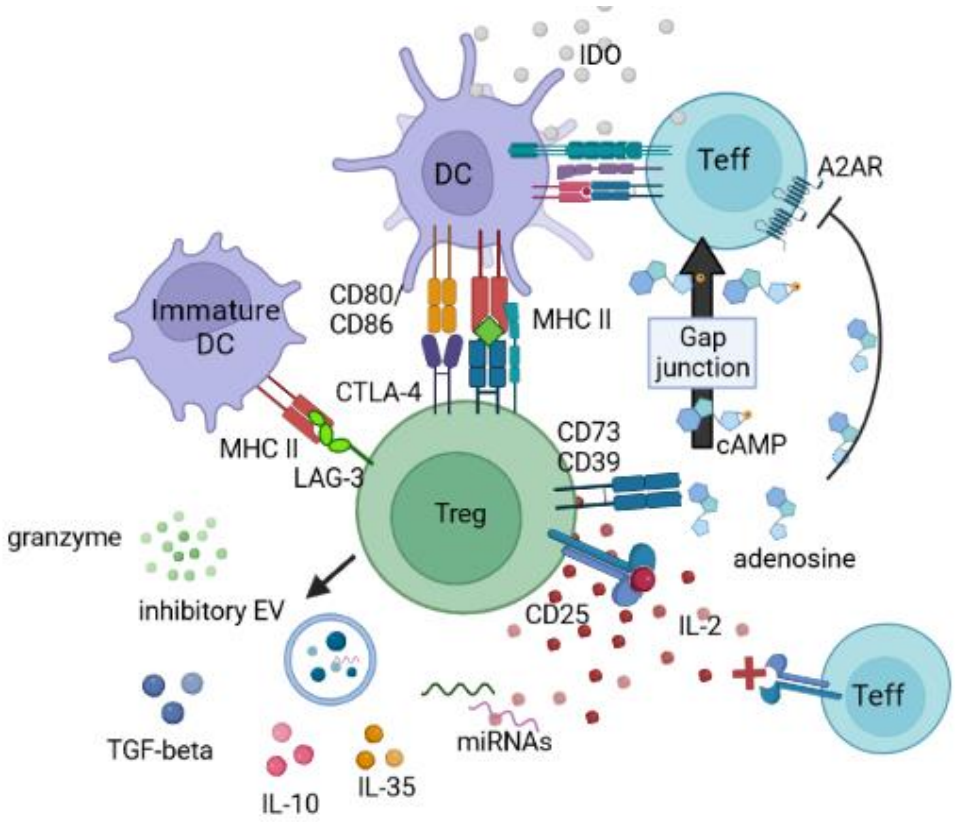

Figure 1.3: Mechanisms of Treg-mediated suppression. Treg cells have been shown to be able to suppress T effector cells through several independent mechanisms, as depicted in this schematic. Increased CD25 expression on the Treg cell surfaces provides a competitive advantage leading to IL-2 deprivation of Teff cells. Treg cells have been shown to secrete immunosuppressive cytokines such as TGF-β, IL-10, IL-35, and to produce additional suppressive molecules such as granzyme B, miRNAs, cAMP and adenosine suppressing both the activation status of antigen-presenting cells as well as directly T effector cell activation. Treg cells also upregulate CTLA-4 to form long-lasting binding with CD80/CD86 on dendritic cells (DCs) and induce suppressive enzyme IDO production by DCs, thereby increasing the Teff cell activation threshold (227). Activated Treg cells also express high level of LAG-3, which binds to MHCII molecule preventing

the maturation of DCs (228). EV: extracellular vesicles; A2AR: Adenosine receptor 2A. Figure adapted from (229)

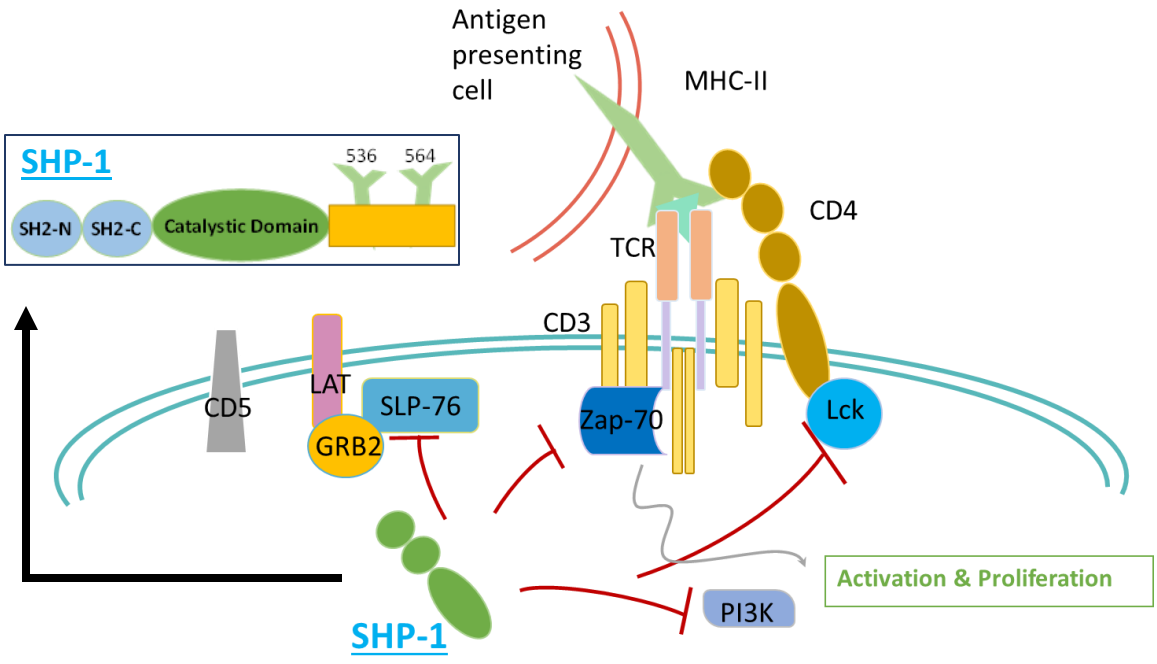

Figure 1.4: SHP-1 in TCR signaling. SHP-1 negatively regulates early components downstream of the TCR signaling pathway, including Zap-70, Lck, SLP-76 and PI3K, and modulates T cell activation and proliferation. SHP-1 structure: SHP-1 has two SH2 domains at the N-terminal end, one catalytic domain, and a C-terminus with two tyrosine residues associated with SHP-1 activation.

can localize to the lipid rafts and interact with early components downstream of the TCR signaling (155), such as Lck (156) and Zap-70 (157) (Figure 1.4). Through these interactions, SHP-1 negatively regulates the TCR signaling pathway (158-160), thereby affecting the downstream T cell functions, including proliferation, cell death, T cell differentiation, cytokine production, and adhesion (161-163).

Previous data from our lab demonstrated that the *motheaten* mouse strain, which globally lacks SHP-1 due to a splicing mutation (164), carries hyper-active Treg cells both *in vitro* and *in vivo* (165). However, global loss of SHP-1 in the *motheaten* mice causes spontaneous inflammation and autoimmunity at a young age (166); this complicates our goal of discerning phenotypes that are cell intrinsic and those emerging from the overall inflammatory environment. Moreover, we have observed that SHP-1 can also modulate signaling in Tcon cells, which further regulates the susceptibility to Treg-mediated suppression (167), suggesting a critical role for SHP-1 as an immune-balance modifier. In addition, elevated SHP-1 expression has been associated with several types of tumors, such as epithelial ovarian cancers (168) and high-grade breast cancers (169), indicating SHP-1 as a potential therapeutic target. Therefore, to better understand the role of SHP-1 in regulating Treg cell function, we utilized the Treg-specific SHP-1-deletion *Foxp3*$^{Cre+}$ *Shp-1*$^{f/f}$ mouse model to investigate how SHP-1 in Treg influences Treg suppression, plasticity and immune balance in general.

Chapter 2

Materials and methods

Mice

SHP1$^{f/f}$ mice (170), *Foxp3*^{YFP}*-cre* mice (171), CD45.1 mice (172–174) and *DEREG* mice (175) were purchased from the Jackson Laboratory. CAG-tdTomato Ai14 Foxp3 (176) mice were kindly provided by Dr. Kipnis (Washington University in St. Louis). *SHP1*$^{f/f}$ mice were crossed to *Foxp3*^{YFP}*-cre* mice and tdTomato mice to generate *Foxp3*^{YFP}*-cre* x *SHP1*$^{f/f}$ mice and exTreg lineage-tracing *Foxp3*^{YFP}*-cre* x *SHP1*$^{f/f}$ x *tdTomato* mice. Mice used throughout these studies are 6 to 8 weeks old, unless specified otherwise. All experimental mice are age and sex matched and housed and bred in the specific pathogen-free facility at the University of Virginia. Experiments were approved by the Animal Care and Use Committee of the University of Virginia.

T cell isolation

Lymph nodes and spleens were harvested from naïve 6-8 weeks old mice unless specified otherwise. Tissues were grinded and filtered through 100 µm and 30µm filters. To isolate splenocytes, red blood cell (RBC) lysis was performed using the RBC lysis kit (Invitrogen) according to the manufacturer's protocol. CD4/CD8 T cells were further isolated using magnetic CD4+ or CD8a+ T cell isolation kits (Miltenyi Biotech) respectively according to the manufacturer's protocol. Splenocytes were labeled using the kit-provided antibody cocktail and T cells were negatively isolated using the manual LS column. Labeled cells remaining on the column after CD4 isolation were purged out and used as antigen presenting cells following irradiation. Isolated CD4 cells were positively enriched for CD25+ Treg cells using CD25-PE and anti-PE beads (Miltenyi) and for the CD4+CD44+CD25- Tcon isolation, CD4+CD25- cells (derived following CD25 cells depletion) were labeled with CD44-beads (Miltenyi). Populations were isolated *via* a

AutoMACS Pro separator (Miltenyi) using Posseld2 program for CD4+ CD25+ Treg and CD4+CD44+ or Deplete program for CD4+CD44- T cells.

Flow cytometry analysis

Isolated cells were filtered through 30μM separator to get single-cell suspension. Single-cell suspensions were incubated with 2.4G2 Ab (Biolegend) for FcγRII/III blocking and stained with surface staining including: CD3 (BD biosciences/Invitrogen), CD4, CD8 (BD/eBioscience/Biolegend), CD11b, CD137, OX-40, CD28, CD80, CD127, CD45.1, CD45.2 (BD Biosciences), B220, CD279, ICOS, FR4 (Biolegend), CD25 (BD/Biolegend), HELIOS (Invitrogen) in FACS buffer (1% BSA and 0.5mM EDTA). Fixable live/dead staining (Invitrogen) were performed after surface staining in PBS. Cell samples were then fixed in fix/lyse solution (BD Biosciences) or 2% paraformaldehyde for later analysis. For samples stained intracellularly, samples were fixed and permeabilized with BD cytofix/cytoperm kit (BD Biosciences) or Foxp3 transcription factor staining buffer set (eBioscience) according to the manufacturer's protocol. Intracellular or nuclei staining for pAKT (Cell Signaling), Foxp3 (eBioscience/Invitrogen), ki67 (eBioscience/Biolegend), RORγt, Gata3, Tbet (Biolegend) were performed following the fix/perm treatment. Fixed samples are stored in 4°C until analyzed. Flow cytometry data were acquired on a BD FACSCanto II or Attune Nxt flow cytometer and analyzed using FCS express 7 (research edition) flow software.

Western blot

Isolated cells with or without stimulation were washed with phosphate-buffered saline (PBS) and lysed with NP-40 buffer (NaCl 150 mM, Tris 50 mM, Nonidet P-40 1%, sodium pyrophosphate 4 mM) or RIPA buffer (NaCl 150 mM, Tris 50 mM, Nonidet P-40 1%, sodium deoxycholate 0.5%, SDS 0.1%) supplemented with a Protease Inhibitors cocktail (Sigma) plus 1mM sodium vanadate, 1mM sodium fluoride, 1 mM PMSF. Lysed samples were spun down at 10,000 g to remove debris and boiled at 100°C for 10 min, with Tris-Glycine buffer (SDS 2%, Bromophenol Blue 0.01%) containing 0.1 M DTT. Aliquots were separated *via* SDS-PAGE. transferred onto PVDF membrane using the Trans-Blot semi-dry transfer system (Bio-Rad). Samples probed for phosphorylation were specially blocked with 5% phosphoBLOCKER (Cell Biolabs) before probing with the following antibodies: anti-SHP-1 (Invitrogen), anti-AKT, or anti-S473-pAKT (Cell Signaling). Blots were re-probed with anti-β-actin HRP (Sigma) to control for loading.

In vitro suppression assay and T cell stimulation

CD4+CD25+ (Treg) cells were isolated from spleens of *Foxp3*$^{Cre+}$ *Shp-1*$^{f/f}$ mutant mice or *Foxp3*$^{Cre+}$ *Shp-1*$^{wt/wt}$ control mice. Where indicated, we also used *Cre*$^{-}$ *SHP1*$^{f/f}$ mice as controls. Since we discovered differences in the levels of Foxp3 protein expression between *Foxp3*$^{Cre+}$ bearing and Cre^{-} mice (Figure 1.2C bottom panel), we included *Foxp3*$^{Cre+}$ *Shp-1*$^{wt/wt}$ as controls throughout the studies to normalize for any effect introduced by *Foxp3-Cre*. 2.5x10^{4} CD4+ CD25- Tcon cells from control SHP-1-sufficient mice were labeled with 5μL CellTrace Violet (Life Technologies) and co-cultured with SHP-1-sufficient (control) or SHP-1-deficient (mutant) Treg cells at 1:0, 2:1, 4:1, 8:1, 16:1 and 32:1 ratios in the presence of 150ng/mL anti-CD3 Ab (Cedar Lane

Laboratories) in the presence of $5x10^4$ irradiated (2000 rads) CD4+ T cell-depleted splenocytes in 200µL 1640 RPMI complete media (RPMI, Gibco; supplemented with 10% heat inactivated FBS (Seradium), 2mM L-glutamine, 10mM HEPES, 1mM MEM sodium pyruvate, 100µM non-essential amino acids, 50µM 2-mercaptoethanol, and concentration penicillin-streptomycin) in 96-well round bottom plates. After 4 days, cultures were harvested and prepared for flow cytometric analyses. Proliferation was calculated based on CellTrace Violet staining using the proliferation analysis tool in FCS Express research edition. Percentages of suppression were calculated using the following formula:

$$\left[1 - \left(\frac{\%divided\ of\ the\ sample}{\%divided\ with\ no\ Treg\ sample}\right)\right] * 100\%$$

To stimulate isolated T cells overnight, 96-well plates were coated with goat anti-hamster IgG (5µg/mL, Jackson Lab) and plate-bound anti-CD3 mAb (1µg/mL, Cedarlane Laboratories) overnight before adding $1x10^5$ of the indicated T cells with 2µg/mL soluble anti-CD28 mAb (BD Biosciences) in 200µL RPMI complete media. For experiments that required higher cell numbers, the conditions were scaled up to 24-well plates with 800µL media each.

Real-time qPCR

Total RNA was extracted from isolated cells using TRIzol reagent and Real-time PCR PureLink-RNA mini kit (Invitrogen). DNA impurities in extracted RNA were removed with DNA-free RNA treatment kit (Applied Biosystems). cDNA was prepared with Applied Biotech cDNA kit according to the manufacturer's protocols. Quantitative

expressions of *shp-1, il-2, il-4, il-10, ebi-3, tgfb-1, tnf, ifng, gapdh,* were measured with TaqMan probes and TaqMan Fast Universal PCR Master Mix (Applied Biosystems) in 96-well plate (US scientific) using QuantStudio 6 Flex system. Relative fold changes were analyzed with QuantStudio Real-Time PCR software, using *gapdh* expression for normalization.

House dust mite (HDM)-induced allergic airways inflammation (AAI) model

Foxp3^{Cre+} *Shp-1*$^{f/f}$ mutant mice or *Foxp3*$^{Cre+}$*Shp-1*$^{wt/wt}$ control mice from both sexes aged 10 to 12 weeks were used in this 2-week AAI induction model. Mice were anesthetized in isoflurane air flow and then given intranasal instillation. Experimental groups were sensitized intranasally with 10 µg low endotoxin HDM extract (Indoor Biotechnologies) in 50µL sterile PBS while inhaled into the non-AAI control group inhaled PBS at days 0, 2, and 4. During challenge phase, mice were given the same concentration and volume of HDM (or PBS in the non-AAI control group) intranasally at days 10, 12, and14.

At day 16 (24-36 hours after the last challenge), lungs were harvested. To collect BAL fluid, trachea was slit open and flushed with ice cold PBS. BAL fluid was treated with RBC lysis to remove any contaminating red blood cells before flow cytometric analyses. For lung histology, 4% paraformaldehyde fixative was slowly injected through trachea into the lung. To keep lungs inflated, a thread was tied below the opening. Lungs were soaked in the 4% paraformaldehyde for 4 days and processed by the Research Histology Core at the University of Virginia. Samples were embedded in paraffin, sectioned into slides, and stained by H&E or Periodic Acid Schiff (PAS) as indicated.

H&E slides were blindly scored by a pathologist following the methods described previously (177). PAS-stained slides were blindly scored using a semi-quantitatively methods as previously described (178), with a modified scale 0-4 representing 0%, 25%, 50%, 75% and 100% of airway epithelium positive for PAS stain.

Induced autoimmune gastritis (AIG)

DEREG mice (175) were obtained from Jackson Lab. To deplete Treg cells and induce AIG, 12-13 weeks old DEREG mice were treated *via i.p.* injection with Diphtheria Toxin (DT; Calbiochem) at 30 ug/kg body weight in sterile PBS at days 0, 2 and 5 (179). DT concentration had been titrated to limit DT-mediated weight loss to less than 20% during the experimental period. DEREG- littermates were used as control.

Treg cells used for adoptive transfer were isolated from spleens of *Foxp3*$^{Cre+}$ *Shp-1*$^{f/f}$ mice or *Foxp3*$^{Cre+}$*Shp-1*$^{wt/wt}$ control mice. 0.6 x 10^6 viable isolated Treg cells in 200 µl PBS were transferred into recipient mice *via* retro orbital injection, an alternative method for tail vein injection introducing less stress to the mice (180), using 30-gauge needles immediately following the first DT injection at day 0. Control mice were injected with 200µl plain PBS solution.

To assess IgE antibody levels, blood was sampled weekly *via* tail vein cut and at the end of the experiment *via* heart puncture. Blood was incubated at 4°C overnight before clearing at 10,000 g. IgE was measured in serum samples (diluted to 1:300) using a mouse IgE ELISA kit (BD biosciences) and 96-well high binding ELISA plates

(Corning Costar 9018) according to the manufacturer's protocol with duplicate data points, and concentrations were calculated based on standard curves.

Mice were euthanized 3 or 5 weeks following the initial DT injection. Stomachs were separated from esophagus and pyloric sphincter, and gastric lymph nodes were collected. Stomachs were sliced open following the inner curvature, and its content was gently washed away with ice-cold PBS. Samples were fixed with Bouin's fixative solution (RICCA Chemical Company) for 4 days, rinsed with PBS and soaked into 70% ethanol for further slides processing at the Research Histology Core (University of Virginia). Samples were embedded in paraffin, sectioned into slides, and stained by H&E or PAS plus Alcian blue as indicated. Slides were blindly scored with following parameters assessing for levels of gastritis: lymphocytes infiltration, epithelial hyperplasia, and parietal cell loss. All parameters were scored on a scale of 0 - 4 based on severity. For structural changes such as parietal cell loss and mucinous cell hyperplasia, which are possibly associated with loss of gastric function, the score was multiplied by 1.5 adding to a total AIG score between 0 and 16.

Seahorse analysis of metabolism

Isolated splenic CD4+CD25+ Treg cells from *Foxp3*$^{Cre+}$ *Shp-1*$^{f/f}$ mice or *Foxp3*$^{Cre+}$ *Shp-1*$^{wt/wt}$ control mice were stimulated (see above) or rested overnight at 37°C in RPMI complete followed by mitochondrial or glycolysis stress tests, which were performed on a Seahorse XF analyzer (Agilent technologies) following the manufacture's procedure. Briefly, cells were washed and plated in the 96-well seahorse XF cell culture microplates. To measure OCR in mitochondrial stress test, the assay media was

composed of non-buffered Seahorse base RPMI media (Agilent technologies), 2mM glutamine (Gibco), 10mM glucose (Sigma) and 1mM sodium pyruvate (Gibco) with a PH adjusted to 7.4. Following measuring baseline OCAR, 1 µM Oligomycin A, 1 µM FCCP and 0.5µM Rotenone & Antimycin A (Sigma) were sequentially added. For glycolysis stress tests, base RPMI media was only supplemented with glutamine. Following measuring baseline ECAR, 10mM Glucose, 1µM Oligomycin and 50 mM 2-DG (Sigma) were sequentially injected. Analyses were performed using WAVE software (Agilent technologies).

Statistical analysis

Statistical significance was determined using student's t test (one-tailed/two-tailed and paired/unpaired chosen according to the hypothesis and as indicated in the text) or other pairwise statistic test methods as indicated in text. One-way ANOVA or two-way ANOVA test were performed according to the test requirements. Equal variance was confirmed with residuals vs fit plot. A p-value of<0.05 was considered significant. Asterisks represent *$p<0.05$, **$p<0.01$, ***$p<0.001$, ****$p<0.0001$.

Chapter 3

Treg-specific deletion of the phosphatase SHP-1 impairs control of inflammation in vivo

This chapter contains data adapted from the published manuscript:
Gu Q, Tung KS and Lorenz UM (2023) Treg-specific deletion of the phosphatase SHP-1 impairs control of inflammation *in vivo*. *Front. Immunol.* 14:1139326. doi: 10.3389/fimmu.2023.1139326

We would like to thank Dr. Chris Medina for his support of the AAI studies, Dr. Anne Sperling for lending us her expertise in AAI models, Ms. Marissa Gonzales for technical advice for the metabolic studies, Dr. Ranjit Sahu for his support in the characterization of the mice, Dr. Mahmut Parlak for technical advice for protein studies, and Dr. Kodi Ravichandran for critical reading of the manuscript.

Results

Characterization of Foxp3^{Cre+}Shp-1$^{f/f}$ mice

We had previously demonstrated that Treg cells derived from mice with a global SHP-1 deficiency, so called *motheaten* mice, exhibited an overall activated phenotype (165). However, as *motheaten* mice have a complex phenotype, we wanted to assess whether SHP-1 has an intrinsic effect on the suppressive function of Treg cells by specifically deleting *shp1* in Treg cells. We crossed mice carrying the floxed alleles of *Ptpn6 (shp1)* (170) with mice that express the Cre recombinase under the control of the *Foxp3* promoter (171). We confirmed highly efficient and specific SHP-1 deletion in CD4+ CD25+ splenic Treg population at protein level (Figure 3.1A) and >99.9% deletion (p value< 0.001) at RNA expression level (Figure 3.1B). $CD8^+$ T cells from *Foxp3*$^{Cre+}$ *Shp-1*$^{f/f}$ mice showed no detectable SHP-1 deletion (Figure 3.1.2A), suggesting SHP-1 deletion is specific to Foxp3-expressing cells. Importantly, we observed no difference between *Foxp3*$^{Cre+}$ *Shp-1*$^{f/f}$ and *Foxp3*$^{Cre+}$ *Shp-1*$^{wt/wt}$ control mice in the total splenocytes numbers (Figure 3.1C) and relative CD4+ and CD8+ T cell populations in spleen or lymph nodes (Figures 3.1D, E). Moreover, we aged *Foxp3*$^{Cre+}$ *Shp-1*$^{f/f}$ mice under specific pathogen-free condition up to 15-month-old without any overt disease phenotypes emerging.

We had previously observed that due to changes in the thymic selection process, *motheaten* mice have a relative accumulation of Treg cells within the splenic CD4+ T cell compartment (158). However, using this Treg-specific SHP-1 depletion model, there is

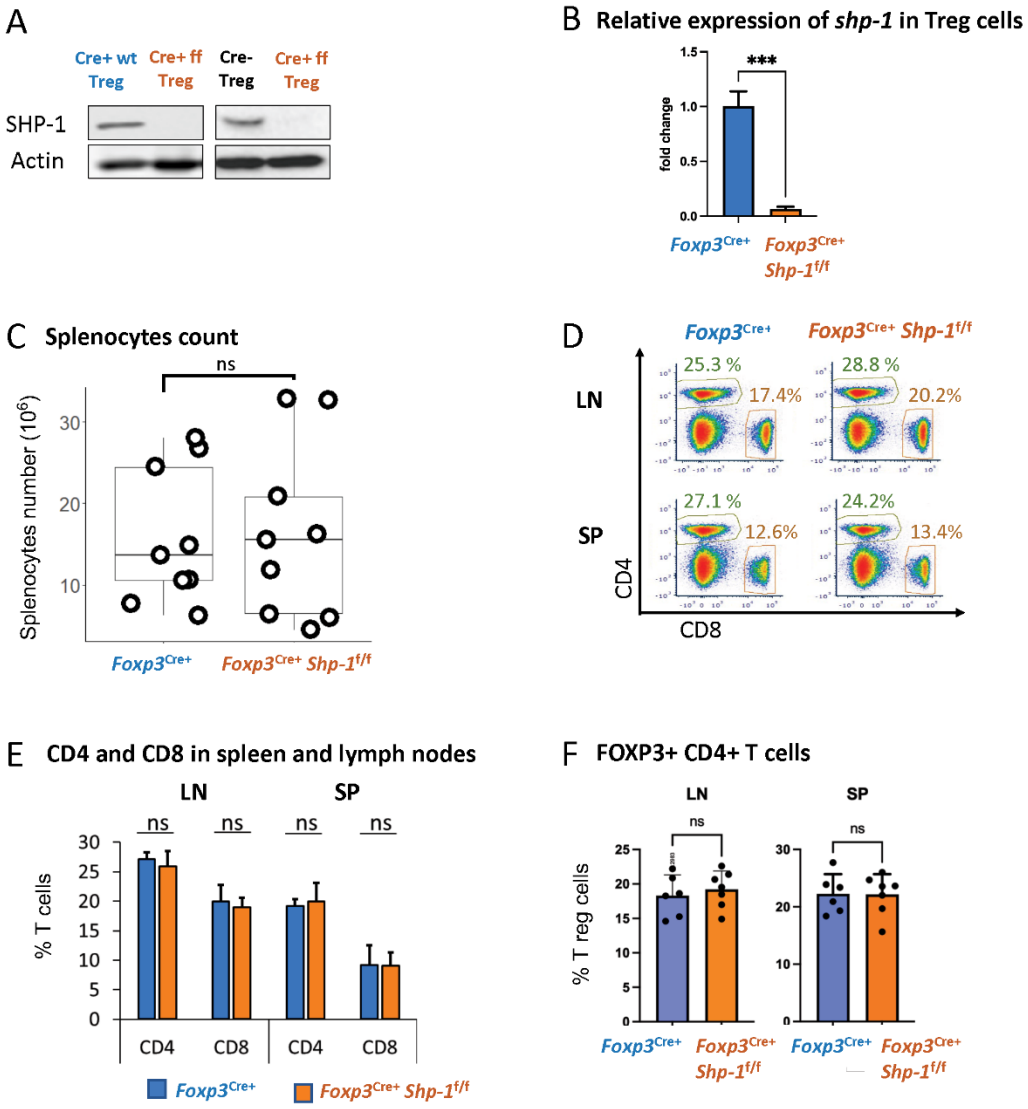

Figure 3.1 Foxp3^{Cre+} SHP-1$^{f/f}$ mice display normal T cell composition. (A) SHP-1 protein levels and **(B)** relative *shp1* mRNA expression levels in isolated CD4+ CD25+ Treg as measured by qPCR. *** p< 0.001 **(C)** Total numbers of splenocytes isolated from 6-8 weeks mice of indicated genotypes. Data are from 4 independent experiments with each dot representing one animal. ns, not subpopulations significant **(D)** Representative flow cytometry data. Percentages of CD4+ and CD8+ are indicated. **(E)** Average percentages of CD4+ and CD8+ T cells in lymph nodes and spleens of mice with indicated genotypes. Data are gated: singlets → live cells. Data points collected

from 5 independent experiments with 6 mice of each genotype. **(F)** Percentages of Foxp3+ Treg cells within total CD4+ T cells derived from spleens and lymph nodes of mice with indicated genotypes. n=6 for each genotype. Data are gated: singlets→ live cells → CD3 → CD4. Each dot representing one animal.

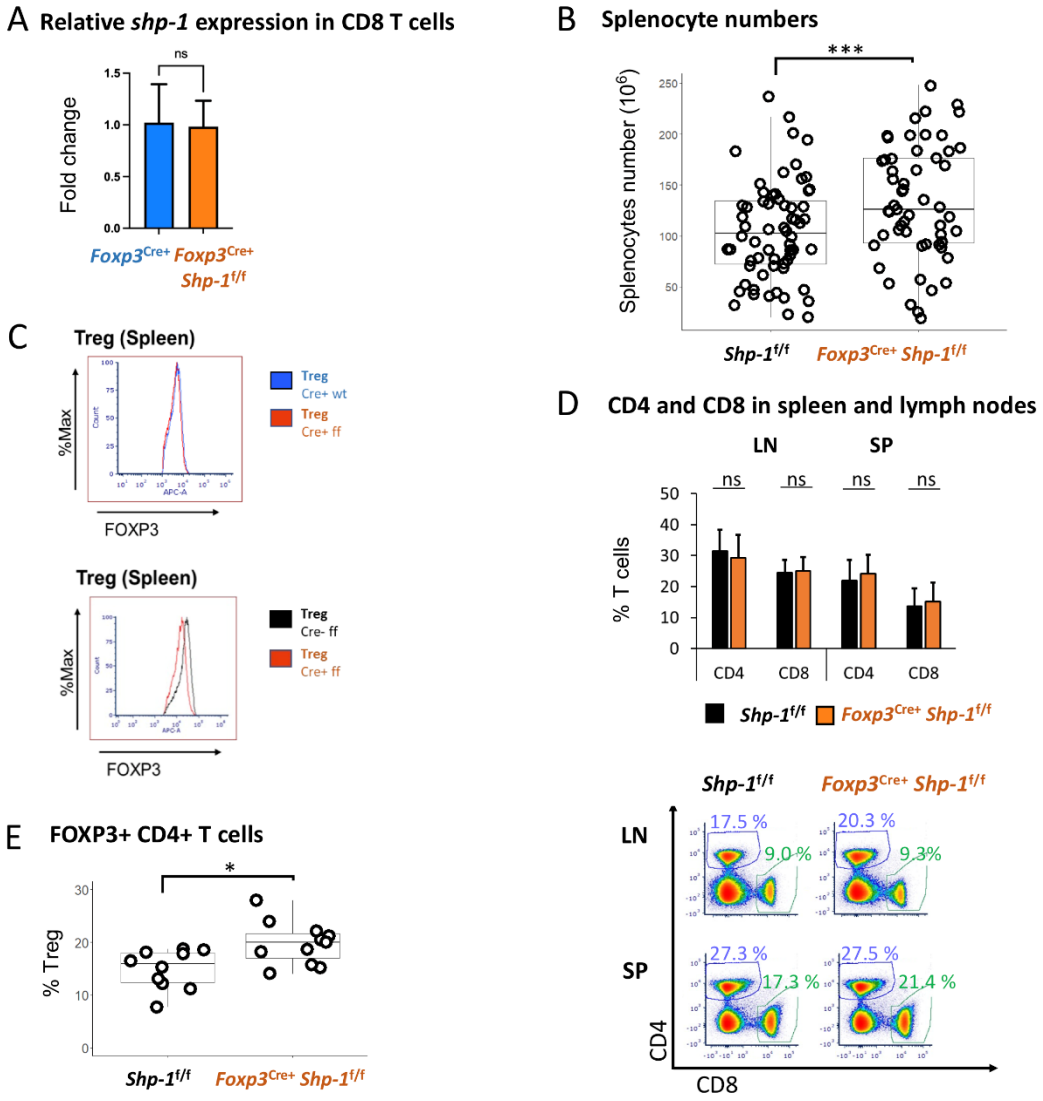

Figure 3.1.2 Foxp3-Cre confers slight phenotypic changes. (A) Relative shp-1 mRNA expression levels in CD8+ T cells as measured by qPCR. (B) Total number of splenocytes isolated from 6-8 weeks old mice of indicated genotypes. Data are derived from 14 independent experiments. Each dot represents an animal; n=52 and 67, p-value= 0.0043. (C) Representative FOXP3 expression levels were assessed on live CD4+ FOXP3+ cells by flow cytometry. Data are gated: singlets → live cells → CD3 → CD4 → FOXP3 (D) Representative flow cytometry data with indicated percentages of CD4+ and CD8+ subpopulations. Average percentages of CD4+ and CD8+ T cells in lymph nodes and

spleens of mice with indicated genotypes. Data are gated: singlets → live cells. Data points collected from 5 independent experiments with 8 mice/genotype. (E) Percentage of FOXP3+ Treg cells in total CD4+ T cells from cells. Data are gated: singlets → live cells →CD3 → CD4. Each dot represents an animal. p-value = 0.0102. n=11 for each genotype. ns = not significant.

no difference in the percentage of Foxp3+ Treg cells within the splenic CD4+ population (Figure 3.1F) or levels of Foxp3 expression in Treg cells (Figure 3.1.2C top panel) between *Foxp3*$^{Cre+}$ *Shp-1*$^{f/f}$ and control mice. Similarly, there is no difference in the number of Foxp3-expressing thymocytes in mutant and control mice (data not shown). Together, these results suggest that expression SHP-1 protein is not critical for the maintenance of the overall Treg population under steady state conditions.

An earlier report (181) suggested that due to the integration of Cre into the *Foxp3* promoter, there is hypomorphic Foxp3 expression; we also observed a decrease in Foxp3 protein expression in *Foxp3-Cre*$^{+}$ Treg cells, independent of SHP-1 expression (Figure 3.1.2C bottom panel). In addition, we observed increased total splenocytes numbers (Figure 3.1.2B) and relative percentages of Foxp3^{+} Treg cells within the CD4+ T cell population of Foxp3Cre+ Shp-1f/f mice (Figure 3.1.2E). However, relative CD4+ and CD8+ subpopulations remained comparable (Figure 3.1.2D). Decreased Foxp3 level have previously been linked to lower suppression function (182) and increased Treg proliferation (183-184) in vivo. To avoid any confounding issues from Foxp3-Cre, we have used Foxp3Cre+ Shp-1wt/wt as control in all the studies described below.

Characterization of Treg population within Foxp3Cre+Shp-1f/f mice

Next, we asked how the Treg population was affected by the loss of SHP-1 protein. When we analyzed proteins linked to Treg cell function and/or activation status (185–187), we observed slightly higher, yet statistically significant levels of folate receptor 4 (FR4), lymphocyte function-associated antigen 1 (LFA-1) and inducible T-cell co- stimulator (ICOS) protein expression on SHP-1-deficient Treg cells (Figure 3.2A) in the Foxp3Cre+ Shp-1f/f mice. Moreover, Foxp3Cre+ Shp-1f/f Treg cells appeared more proliferative *in*

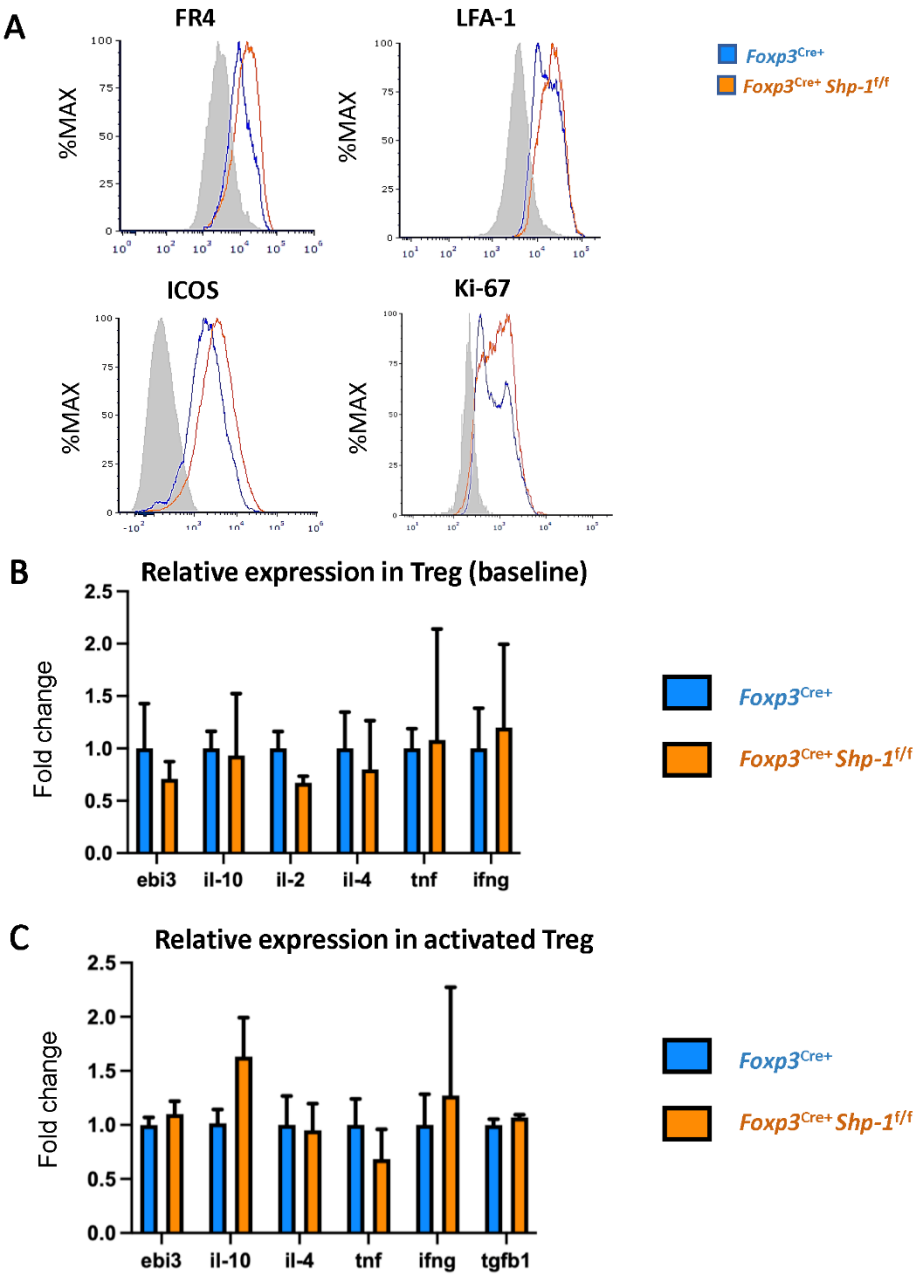

Figure 3.2 Phenotypic analyses of 6-8 weeks old Foxp3^{Cre+} Shp-1$^{f/f}$ and Foxp3^{Cre+} control mice. (A) Histograms depict representative protein expression levels of live splenic CD4+ FOXP3+ cells as assessed by flow cytometric analyses. Data are gated: singlets→ live cells → CD3 → CD4 → Foxp3. Statistical analyses of the MFIs (geometric mean) were performed using a two-way ANOVA test (FR4 – p=0.03878; LFA-1 – p=0.0154; ICOS – p=0.0133; Ki67 – p=0.0096) (**B**, **C**) Relative cytokine

expression of **(B)** freshly isolated and **(C)** stimulated splenic CD4+CD25+ Treg cells isolated from 6-8 weeks old mice of the indicated genotypes, **(B)** n = 3 for each genotype. **(C)** n= 5 for stimulated Treg. **(C)** Treg cells were incubated for 14-18 hrs. with plate bound anti-CD3 (150 ng/ml) and soluble anti-CD28 (500 ng/ml). Error bars represent SD.

vivo as measured by Ki-67 staining (Figure 3.2A). However, several Treg markers remained unchanged (CD54, CD80, OX-40, LAG-3, CD103, CD137, CD28, PD-1, CD127) or with a trend of slight increase (such as CD25, CTLA-4, GITR) in *Foxp3*$^{Cre+}$ *Shp-1*$^{f/f}$ mutant mice compared to *Foxp3*$^{Cre+}$ *Shp-1*$^{wt/wt}$ control mice at steady state (Figure 3.2.2A). Moreover, there was no spontaneous induction of a skewed T-bet, Gata-3 or RORγt-expressing Treg subpopulation in the *Foxp3*$^{Cre+}$ *Shp-1*$^{f/f}$ mutant mice (Figure 3.2.2B). Finally, there were no significant differences in cytokine expression in *Foxp3*$^{Cre+}$ *Shp-1*$^{f/f}$ Treg cells basally, with or without CD3/CD28 stimulation besides a trend of IL-10 increase in stimulated *Foxp3*$^{Cre+}$ *Shp-1*$^{f/f}$ Treg cells, (Figure 3.2B and Figure 3.2.2C). Thus, freshly isolated SHP-1-deficient Treg cells display certain features of an activated phenotype but show normal expression of numerous other Treg markers compared to control Treg cells.

Treg-specific SHP-1 deletion leads to greater AKT activation

Previous studies from our lab demonstrated that the SHP-1 inhibits the activation of the PI3K/AKT pathway in CD4+ Tcon cells (167). Moreover, PI3K/AKT activation has been linked to promoting proliferation in Tregs (188). As we noted that SHP-1 deficiency increased the percentage of Ki-67+ Treg cells indicating augmented proliferation *in vivo*, we explored whether the *Foxp3*$^{Cre+}$ *Shp-1*$^{f/f}$ Treg cells display an enhanced PI3K/AKT pathway activation. AKT phosphorylation at S473 was used as a surrogate measurement of AKT activation. Freshly isolated splenic *Foxp3*$^{Cre+}$ *Shp-1*$^{f/f}$ Tregs displayed an increased AKT phosphorylation compared to *Foxp3*$^{Cre+}$ and *Shp-1*$^{f/f}$ control Treg cells. Although not statistically significant when compared to *Foxp3*$^{Cre+}$, a trend towards an increase was also observed in lymph node derived Treg cells

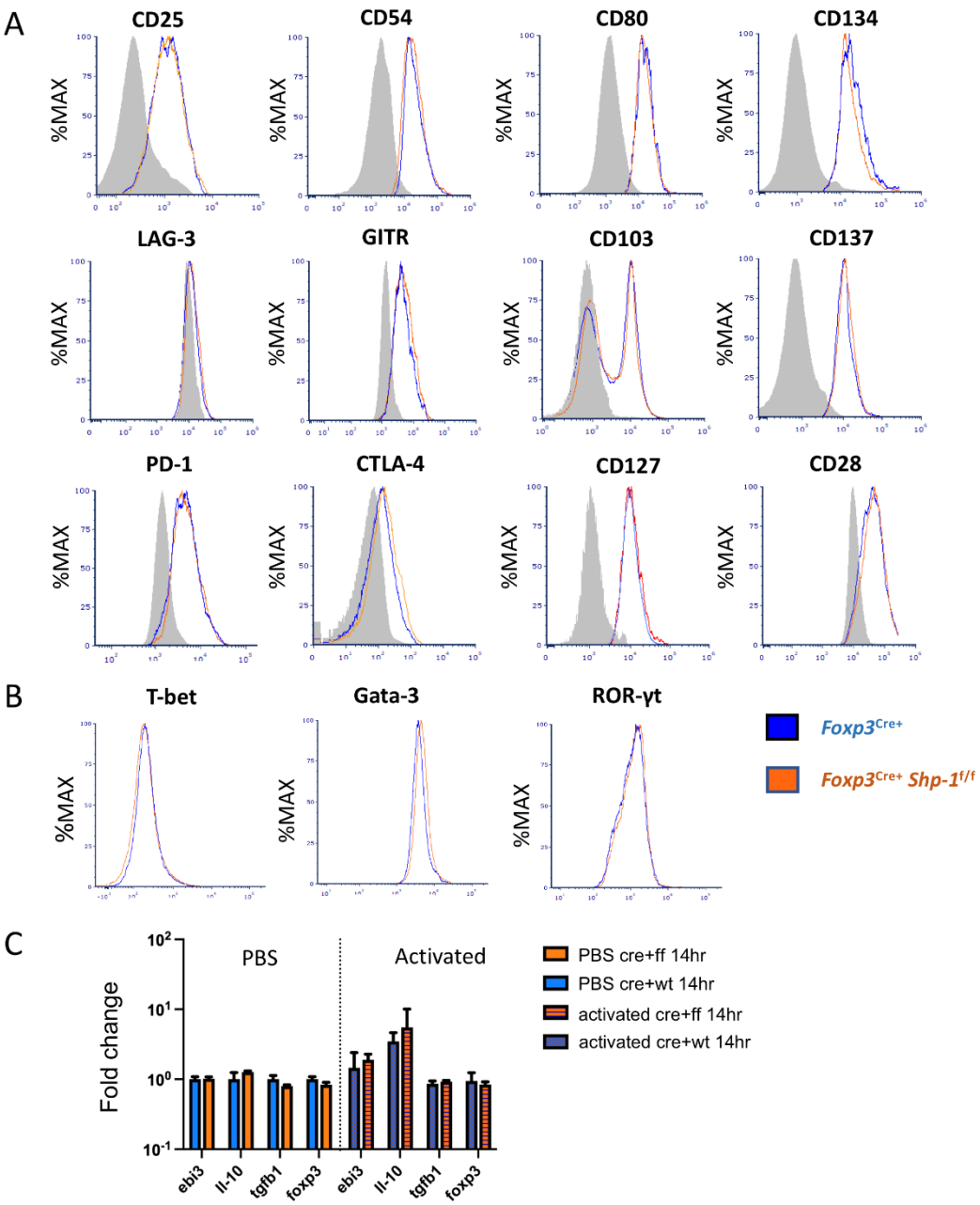

Figure 3.2.2 Phenotypic analyses of 6-8 weeks old Foxp3^{Cre+} Shp-1$^{f/f}$ and Foxp3^{Cre+} control mice. Histograms depict representative (A) surface and (B) intracellular protein expression levels of live CD4+ FoxP3+ cells as assessed by flow cytometric analyses. Data are gated: singlets → live cells → CD3 → CD4 → FOXP3. (C) Relative cytokine expression of PBS treated or CD3/CD28 overnight stimulated splenic CD4+CD25+ Treg cells isolated from 6-8 weeks old mice of the indicated genotypes, n= 3 for each genotype

treated with PBS, n= 5 for each genotype with overnight stimulation. Treg cells were incubated for 14-18 hours with plate-bound anti-CD3 (150 ng/ml) and soluble anti-CD28 (500 ng/ml). Error bars represent SD.

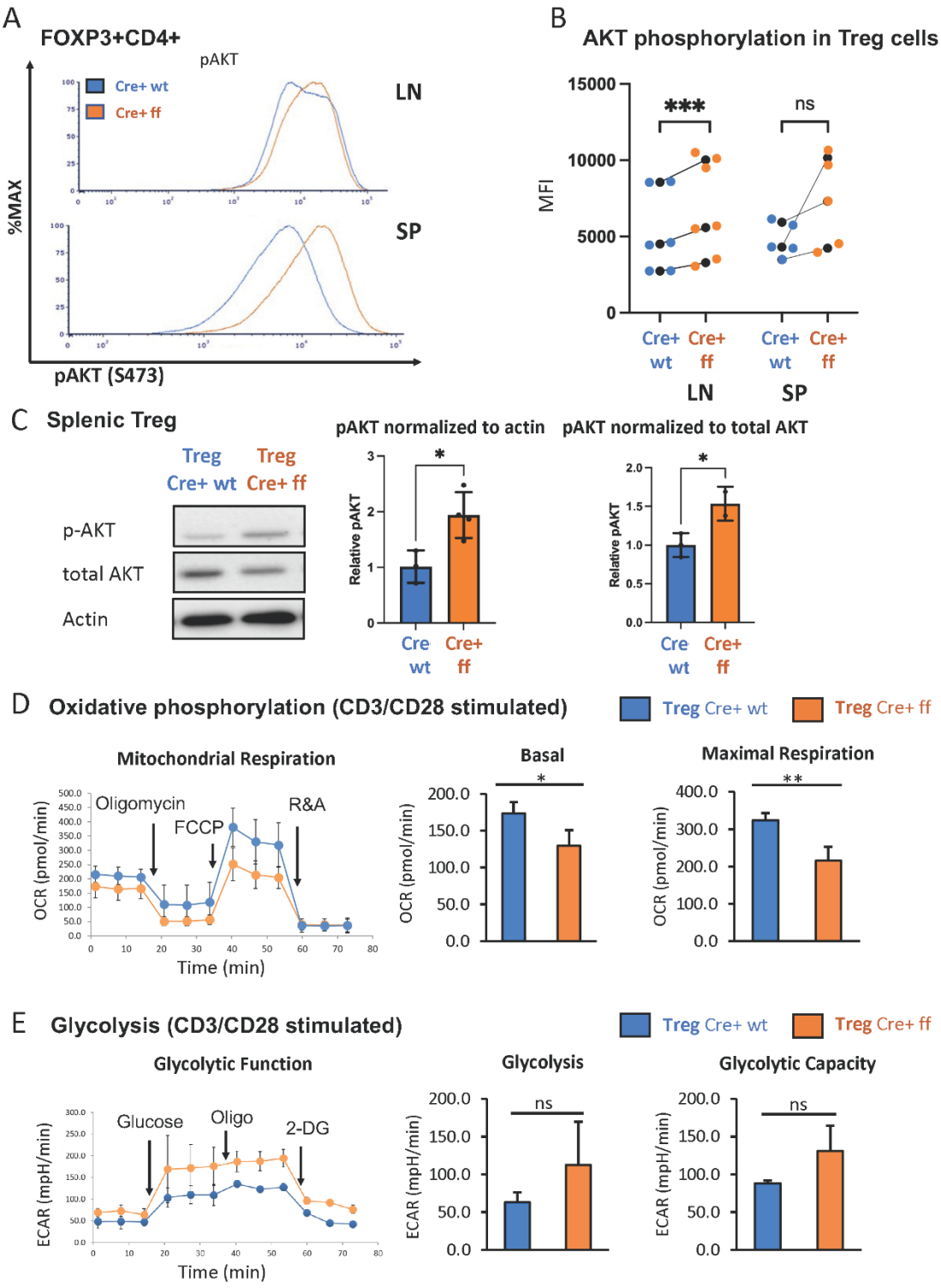

Figure 3.3 Treg specific SHP-1 deletion increases phosphorylation of AKT and affects cellular metabolism. (A) AKT phosphorylation (Ser473) in freshly isolated Treg

of 6-8 weeks old mice. Data are representative of 3 independent experiments. **(B)** MFIs of pAKT of *Foxp3*$^{Cre+}$ *Shp-1*$^{f/f}$ Treg cells and *Foxp3*$^{Cre+}$ control Treg cells from lymph node or spleen were plotted. Each colored dot represents one data point. Average values for each genotype from the same experiment are shown as black dot and matched by lines for each experiment. Two-way ANOVA test was performed for statistics. LN p-value = 0.0005, SP p-value = 0.0521. Data are gated singlets → live cells → CD3 → CD4 → Foxp3 **(C)** Immunoblot analysis of p-AKT(S473), total AKT and β-actin from control *Foxp3*$^{Cre+}$ ("cre wt") and *Foxp3*$^{Cre+}$ *Shp-1*$^{f/f}$ ("cre ff") mutant Treg cells stimulated with anti-CD3/CD28 beads + IL-2 (200U/ml) for 5 min. Relative pAKT quantity were normalized to actin and total AKT. Unpaired t test was used for statistics. pAKT/actin p-value = 0.0220, pAKT/total AKT p-value =0.0464. **(D, E)** CD4+CD25+ Treg cells of *Foxp3*$^{Cre+}$ *Shp-1*$^{f/f}$ or *Foxp3*$^{Cre+}$ control mice were stimulated with CD3/CD28 Dyna beads according to the manufacture's protocol overnight and using a Seahorse bioanalyzer. **(D)** Basal and maximal mitochondrial respiration and **(E)** glycolysis and glycolysis capacity were measured to assess **(D)** OCR and **(E)** ECAR respectively, n=3 for each genotype. Error bar represents **(B)** SD and (**D**, **E**) s.e.m., two-sided t test, *p<0.05, **p<0.01, ***p<0.001, ns, not significant.

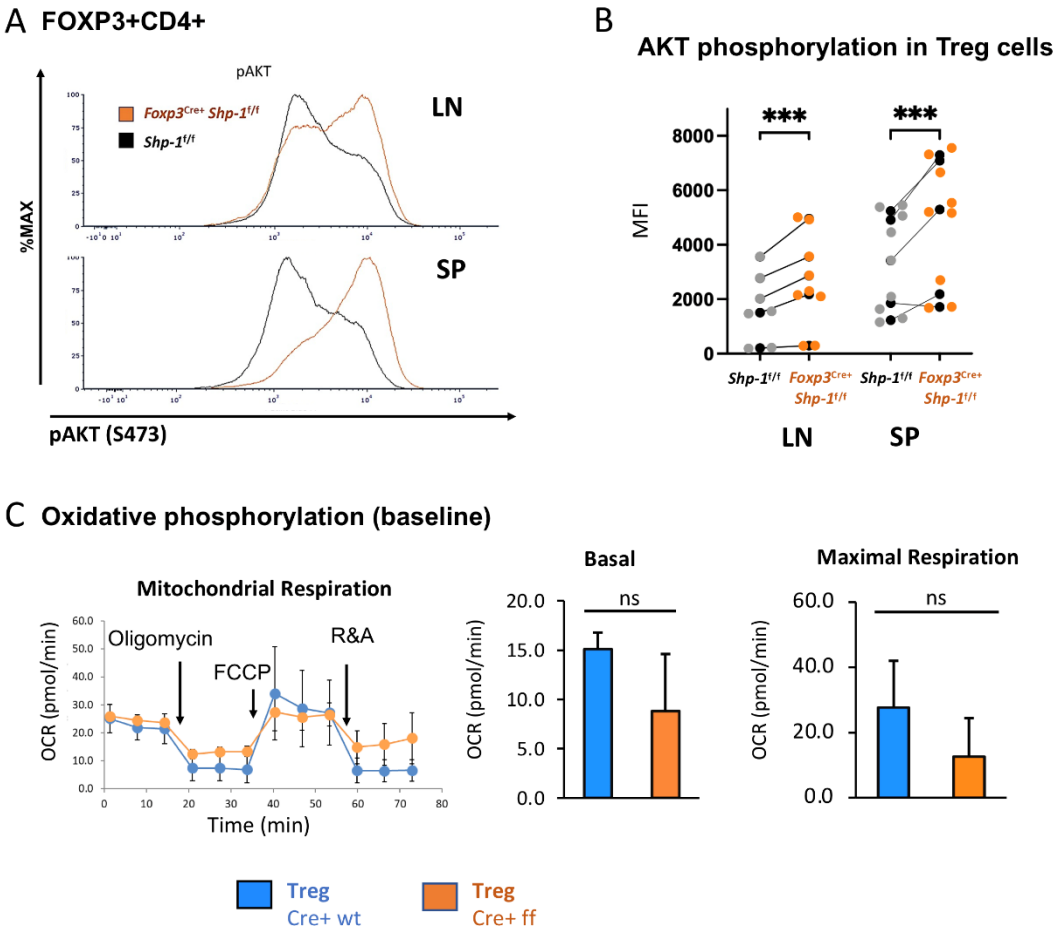

Figure 3.3.2 Treg specific SHP-1 deletion increases phosphorylation of AKT and affects cellular metabolism. (A) AKT phosphorylation (Ser473) in freshly isolated Treg of 6-8 weeks old Foxp3^{Cre+} Shp-1$^{f/f}$ or Shp-1$^{f/f}$ control mice. Data are representative of 4 independent experiments. (B) pAKT (Ser473) MFI of Foxp3^{Cre+} Shp-1$^{f/f}$ mutant and Shp-1f/f control Treg cells were measured. Colored dots represent each data point. Average value for each genotype in each experiment was indicated with black dots. Two-way ANOVA test was performed for statistics. P-values obtained for genotype effect was shown in figure. Data are gated singlets → live cells → CD3→ CD4 → FOXP3 (C) Basal and maximal mitochondrial respiration/OCR of freshly isolated CD4+CD25+ Treg cells of Foxp3^{Cre+} Shp-1$^{f/f}$ (“cre+ ff”) or Foxp3^{Cre+}

Shp-1$^{wt/wt}$ (“cre+ wt”) control mice were measured using a Seahorse bioanalyzer. Error bar represents (B) SD and (C) s.e.m., unpaired t test, *p <0.05, **p<0.01, ***p<0.001, ****p<0.0001. ns = not significant.

(Figures 3.3A, B and Figures 3.3.2A, B). This increase was even more pronounced upon *in vitro* anti-CD3/anti-CD28 stimulation (Figure 3.3C*).* Interestingly, we consistently observed a trend toward a small but not statistically significant decrease in total AKT protein levels in the mutant Treg cells despite the hyperphosphorylation. Together these data suggest that SHP-1 limits signaling along the PI3K/AKT/mTOR pathway in Treg cells.

We next asked whether the increased AKT phosphorylation may translate to a metabolic change, as AKT activation is linked to increased glycolytic activity (183). While the freshly isolated unstimulated Treg cells showed no significant oxygen consumption rate (OCR) difference between the *Foxp3*$^{Cre+}$ *Shp-1*$^{f/f}$ mutant and *Foxp3*$^{Cre+}$ *Shp-1*$^{wt/wt}$ control Treg cells (Figure 3.3.2C), TCR/CD3 stimulation showed decreased mitochondrial respiration, as measured by the OCR at both basal and maximal level (Figure 3.3D) in SHP-1-deficient Treg cells. Moreover, *Foxp3*$^{Cre+}$ *Shp-1*$^{f/f}$ Treg cells displayed a trend toward increased extracellular acidification rate (ECAR) compared to control Treg cells, suggesting higher glycolytic activity (Figure 3.3E). It should be noted that the link between AKT phosphorylation status and Treg cell plasticity and function is complex (189), and we address the Treg cell lineage stability and functionality in the *Foxp3*$^{Cre+}$ *Shp-1*$^{f/f}$ mice further below.

Treg-specific SHP-1 deletion affects other T cell populations *in vivo*

Next, we asked whether the Treg-specific loss of SHP-1 resulted in phenotypic changes in the non-Treg lymphocyte populations. We observed a significant increase in the CD44^{hi}CD62L^{lo} antigen-experienced CD4+ T cells within the non-Treg CD4+ Tcon

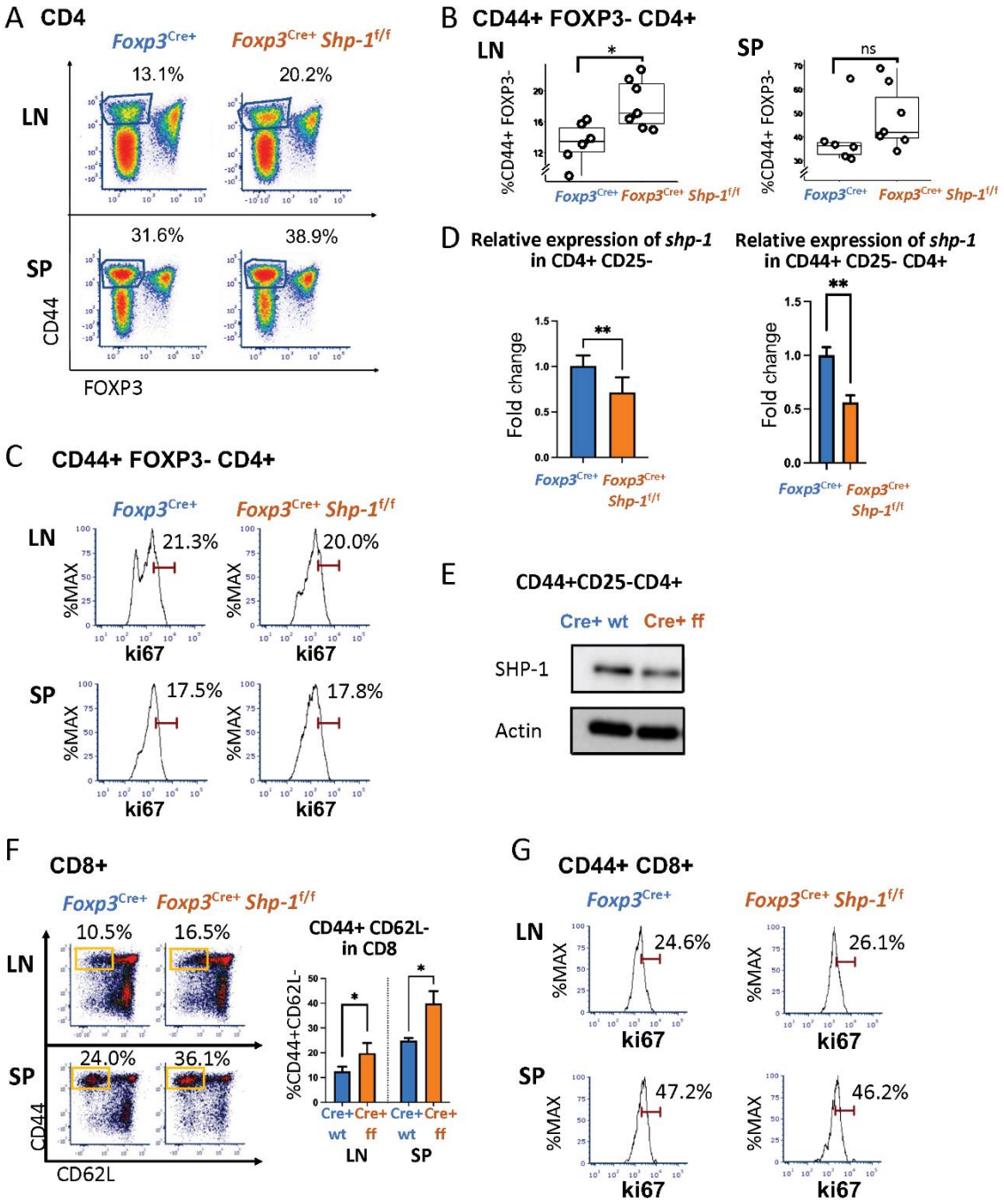

Figure 3.4 Treg specific SHP-1 deletion affects non-Treg T cell population. (A, B) Percentages of CD44^{hi} Foxp3- within CD4+ T cell population of lymph nodes and spleen of *Foxp3*$^{Cre+}$ *Shp-1*$^{f/f}$ or *Foxp3*$^{Cre+}$ mice. **(A)** Dot Plot is representative of 5 independent experiments. Percentages of CD44+ Foxp3- within CD4 populations are indicated. **(B)** Each dot represents one animal; lymph node p-value = 0.01, spleen p-value = 0.2537,

two-sided t test. Gated: singlets → live → CD4. Student T test were performed for statistics. **(C)** Percentages of Ki-67+ within $CD44^{hi}$ Foxp3- CD4+ T cells of lymph nodes and spleen of *Foxp3*$^{Cre+}$ *Shp-1*$^{f/f}$ or *Foxp3*$^{Cre+}$ mice. Data are representative of 3 independent experiments. Gated: Gated: singlets → live → CD4 → FOXP3- → CD44. (**D** *left panel*) CD4+ CD25- cells or (***D*** *right panel* and **E**) CD4+ $CD44^{hi}$ CD25- cells were magnetically sorted from *Foxp3*$^{Cre+}$ *Shp-1*$^{f/f}$ or *Foxp3*$^{Cre+}$ control mice and assessed for **(D)** mRNA expression via quantitative RT-PCR analysis of *shp-1* mRNA (n =3 for each genotype, p-value for left panel = 0.0017, p-value for right panel = 0.0067) and for **(E)** SHP-1 protein expression via immunoblotting. Percentages of **(F)** $CD44^{hi}$ $CD62L^{lo}$ (n= 3-4 for each genotype, p-value for LN=0.0379, p-value for SP=0.0282) and **(G)** Ki-67+ T cells within CD44+ CD8+ T cell population of lymph nodes and spleen of *Foxp3*$^{Cre+}$ *Shp-1*$^{f/f}$ or *Foxp3*$^{Cre+}$ mice. Data are representative of 3 independent experiments. Gated: **(C)** singlets → live → CD4 → FOXP3- →CD44. **(F)** singlets → live → CD8. **(G)** singlets → live → CD8 →CD44. Unpaired t test. *, $p<0.05$, **, $p<0.01$. (**D**, **E**) CD4+ $CD44^{hi}$ CD25- cells were magnetically sorted from *Foxp3*$^{Cre+}$ *Shp-1*$^{f/f}$ or *Foxp3*$^{Cre+}$ control mice and assessed for SHP-1 protein levels and mRNA expression *via* **(D)** Immunoblot and **(E)** Quantitative RT-PCR analysis of *shp-1* mRNA. Percentages of **(F)** $CD44^{hi}$ $CD62L^{lo}$ and **(G)** Ki-67+ T cells within CD8+ T cell population of lymph nodes and spleen of *Foxp3*$^{Cre+}$ *Shp-1*$^{f/f}$ or *Foxp3*$^{Cre+}$ mice. Data are representative of 3 independent experiments. Gated: singlets → live → CD8. ns, not significant.

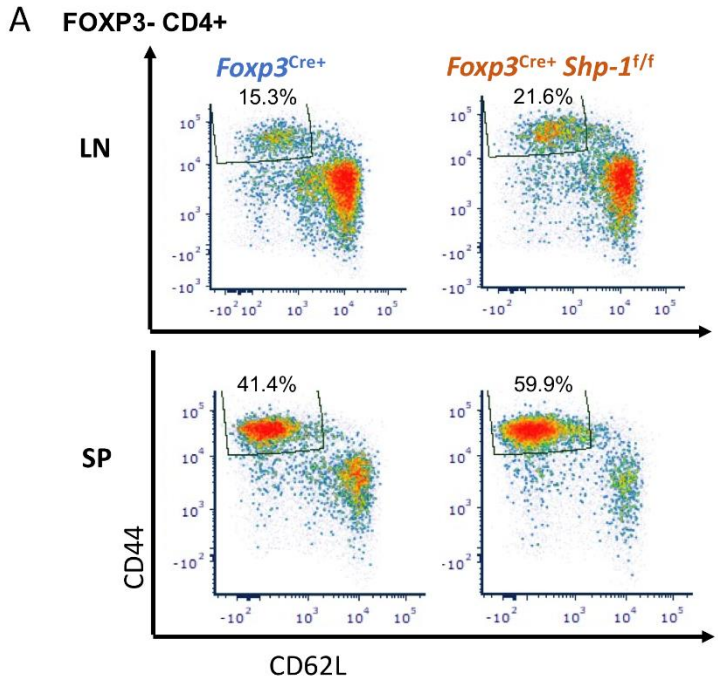

Figure 3.4.2 Treg-specific SHP-1 deletion affects CD4+ Tcon cell population.

Percentages of CD44^{hi} CD62L^{lo} cells within CD4+ FOXP3- Tcon cells in the lymph nodes and spleen of Foxp3^{Cre+} Shp-1$^{f/f}$ or Foxp3^{Cre+} mice. Data are representative of 2 independent experiments. Gated: singlets → live → CD4 → FOXP3-.

cell compartment derived from lymph nodes of naïve *Foxp3*$^{Cre+}$ *Shp-1*$^{f/f}$ mutant mice as well as a trend towards an increased CD44^{hi}CD4+ splenic T cell population in mutant mice (Figures 3.4A, B and Figure 3.4.2). This CD4+ CD44^{hi} Tcon cell population from *Foxp3*$^{Cre+}$ *Shp-1*$^{f/f}$ mutant express Ki-67 at levels comparable to control mice, indicating similar degrees of proliferation (Figure 3.4C). However, an analysis of the *shp-1* mRNA expression levels in CD25-CD4+ Tcon and the CD44^{hi} CD25-CD4+ T cell subsets derived from *Foxp3*$^{Cre+}$ *Shp-1*$^{f/f}$ mutant mice showed a significant decrease compared to control mice (Figure 3.4D), which was also confirmed at the protein level (Figure 3.4E), suggesting that at least some of the CD44^{hi} antigen experienced populations in the CD4+ Tcon cell compartment might be exTreg cells, which we address below.

Interestingly, CD8+ T cells isolated from spleen or lymph nodes of naive *Foxp3*$^{Cre+}$ *Shp-1*$^{f/f}$ mice also contain higher CD44^{hi}CD62^{lo} subpopulations (Figure 3.4F), indicating a basal increase in antigen-experienced CD8+ T cells. As we had observed for the CD4+ T cell lineage, Ki-67 staining of the CD44^{hi} CD8+ T cell population was comparable between *Foxp3*$^{Cre+}$ *Shp-1*$^{f/f}$ mutant and control mice (Figure 3.4G), indicating that the overall increase in CD44^{hi} non-Treg T cells is not driven by hyper-proliferation. We confirmed the lineage specificity of *Foxp3*$^{Cre+}$ by assessing *shp1* mRNA levels in the CD8+ T cell population using RT-PCR, a population that should not be directly affected by *Foxp3*$^{Cre+}$ and found comparable *shp1* mRNA levels in CD8 cells derived from mutant and control mice (Figure 3.1.2A) suggesting that SHP-1-deficient Treg cells affect the phenotype of the CD8 T cell lineage.

Treg-specific SHP-1 deletion increases ex-Treg compartment *in vivo*

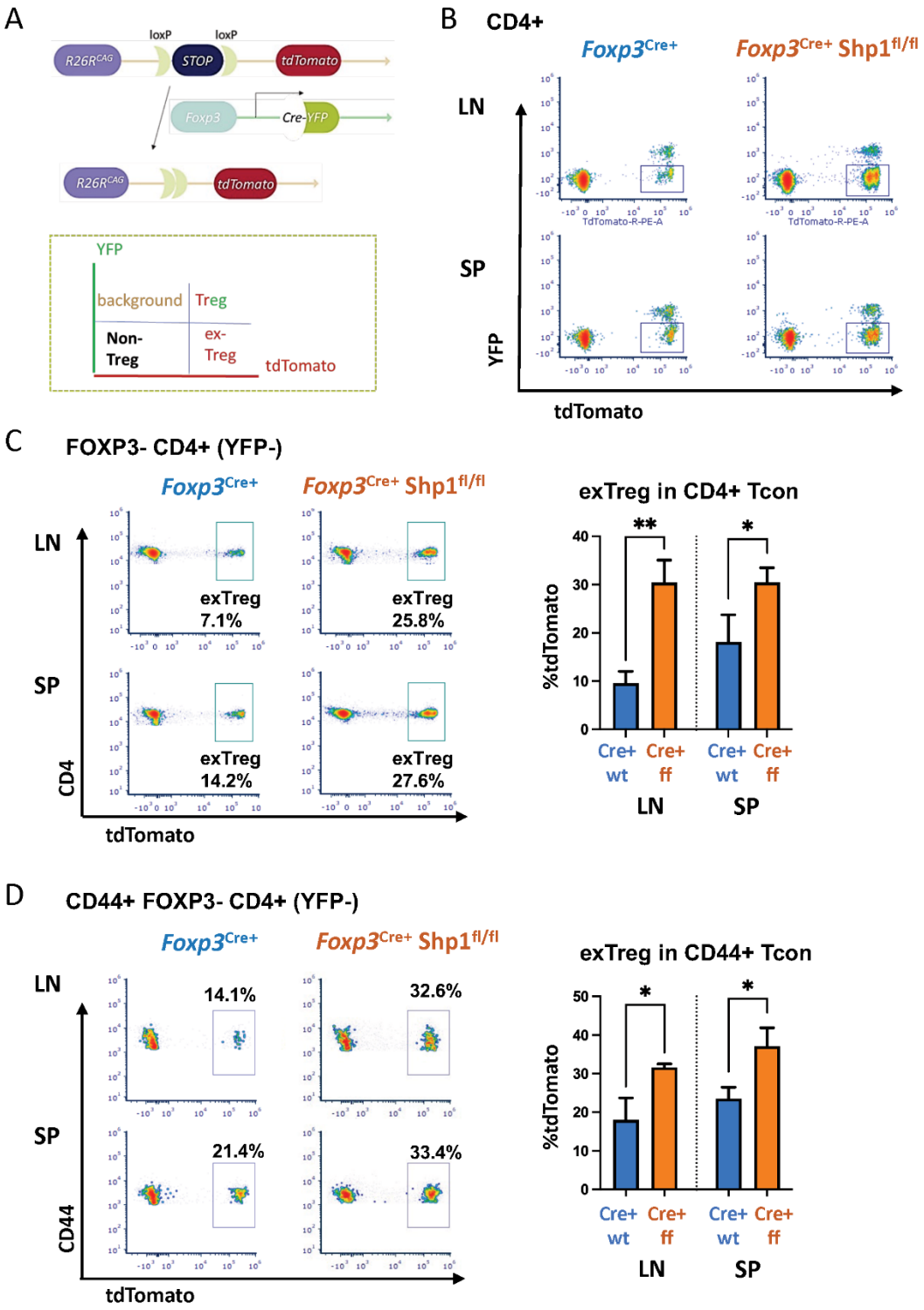

Figure 5 SHP-1 promotes Treg cell lineage stability. (A) Schematic diagram and **(B)** flow cytometry representation of Treg lineage tracing model. Gates for tdTomato+ YFP- (exTreg) cells are indicated throughout the panels. tdTomato (cre-inducible expression)

were crossed with *Foxp3*$^{YFP\text{-}cre}$/*Shp-1*$^{f/f}$ and *Foxp3*$^{YFP\text{-}cre}$ control mice. **(C**, **D)** Plot depicts T cell subpopulations based on YFP and tdTomato expression. Flow cytometric analyses of **(C)** tdTomato+ (exTreg) within CD4+ FOXP3 (YFP)- Tcon (LN p-value =0.0023, SP p-value = 0.0449) and **(D)** tdTomato+ (exTreg) within CD44+FOXP3-CD4+ T cells in 8 weeks old mice (LN p-value = 0.0146, SP p-value = 0.0388). Percentages of exTreg cells within each subpopulation are indicated. Gated: **(B)** singlets → live → CD4 **(C)** singlets → live → CD4 → FOXP3-(YFP-) **(D)** singlets → live → CD4 → FOXP3-(YFP-) →CD44. Data are from 2 experiments with each 2-3 mice per genotype. *, $p<0.05$, **, $p<0.01$.

As some of the CD4+ CD44^{hi} Tcon cells seen above might represent the previously reported 'ex-Treg cells' that have lost Foxp3 expression, we next asked whether SHP-1 may help maintain Treg cell lineage stability. To test this, we turned to a lineage tracing model that expresses a Cre-inducible tdTomato by crossing *Foxp3*$^{YFP\text{-}Cre+}$ *Shp-1*$^{f/f}$ or *Foxp3*$^{YFP\text{-}Cre+}$ *Shp-1*$^{wt/wt}$ onto the *Rosa26*^{tdTomato} strain (173) (Figure 3.5A). We expected that if the CD44^{hi} Tcon cells were to be ex-Treg cells, then the Foxp3-Cre would have been active in these cells at one point, leading to tdTomato expression, even if they have since lost the Cre-YFP expression. This can then be distinguished from the non-Treg-derived Tcon cells (which would be negative for both tdTomato and YFP fluorescence) and the Treg cells (which continue to express both tdTomato and YFP) (Figure 3.5B). We found that loss of SHP-1 in Treg cells caused an increase in exTregs (tdTomato^{+} but YFP^{-}) within the CD4+ Tcon cell population in both the spleen and lymph nodes (Figure 3.5C). This suggested that SHP-1-deficient Treg cells might be less stable leading to an accumulation of an exTreg population. It is noteworthy that not all CD4+ CD44^{hi} Tcon cells are exTreg cells, but that the population is enriched in the *Foxp3*$^{YFP\text{-}Cre+}$ *Shp-1*$^{f/f}$ mice compared to *Foxp3*$^{YFP\text{-}Cre+}$ control mice (Figure 3.5D). This suggests that the overall increase in the CD44^{hi} antigen-experienced population in *Foxp3*$^{YFP\text{-}Cre+}$ *Shp-1*$^{f/f}$ mice might come from both reduced Treg stability as well as additional secondary factors leading to further accumulation of the CD4+ CD44^{hi} Tcon population.

SHP-1-deficient Treg cells demonstrate increased suppressive activity *in vitro*

To address whether SHP-1-deficient Treg cells are functional, we first tested the suppressive capacity *ex vivo*. Using *in vitro* suppression assays, SHP-1-deficient Treg

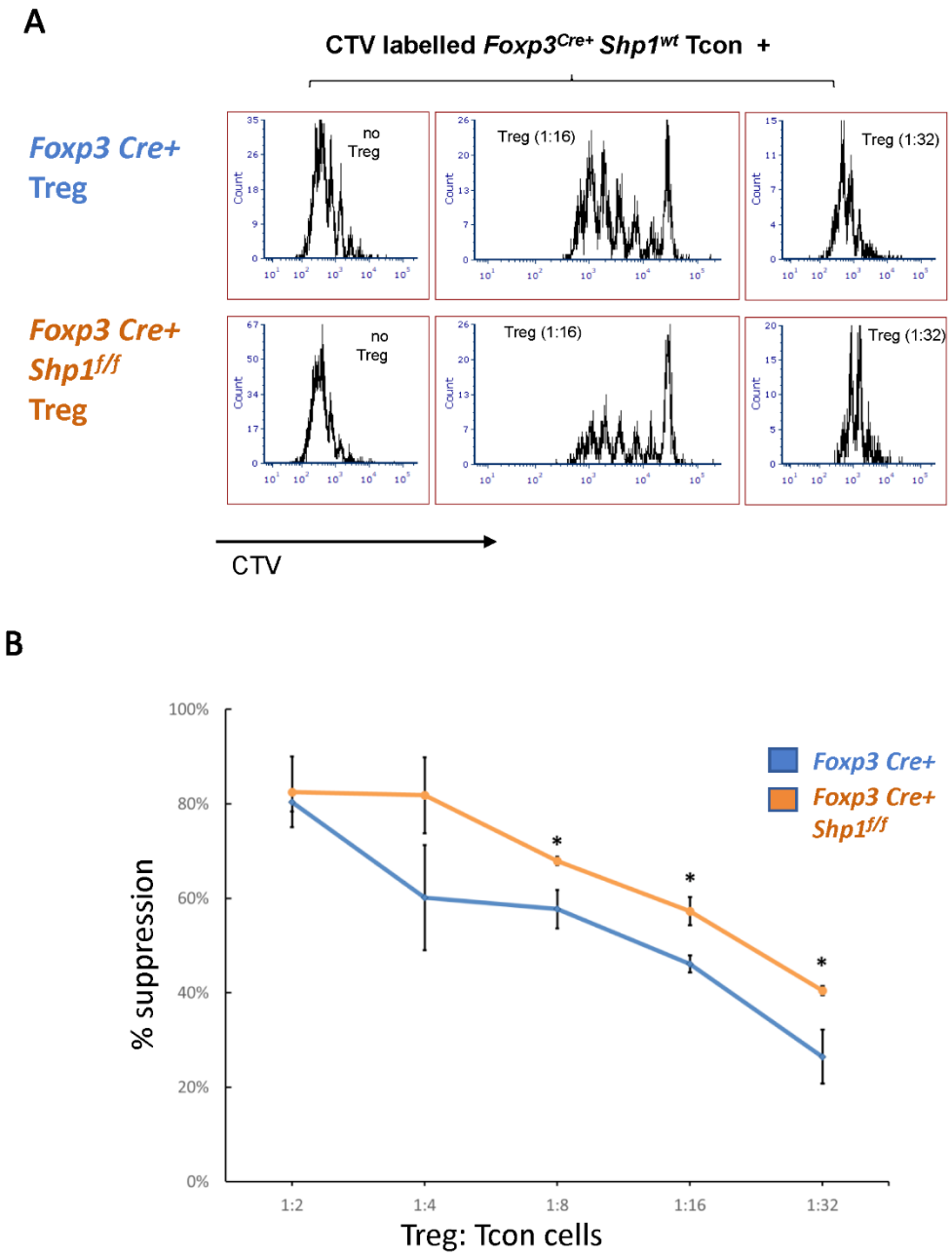

Figure 3.6 SHP-1-deficient Treg cells display increased suppressive activity in vitro. **(A, B)** Treg (CD4+CD25+ isolated from *Foxp3*$^{Cre+}$ *Shp-1*$^{f/f}$ mutant or *Foxp3*$^{Cre+}$ control mice) and CTV-labeled Tcon (CD4+CD25- from control mice) cells were co-cultured at the indicated ratios. **(A)** Histogram depicts CTV-dilution of Tcon cells as a measurement of proliferation. Data are representative of 3 independent experiments with each n= 1 - 3

mice (6-9 weeks) per genotype. **(B)** Suppression capacity of Treg cells based on data obtained in **(A)** Error bar represents SD. *, $p \leq 0.05$.

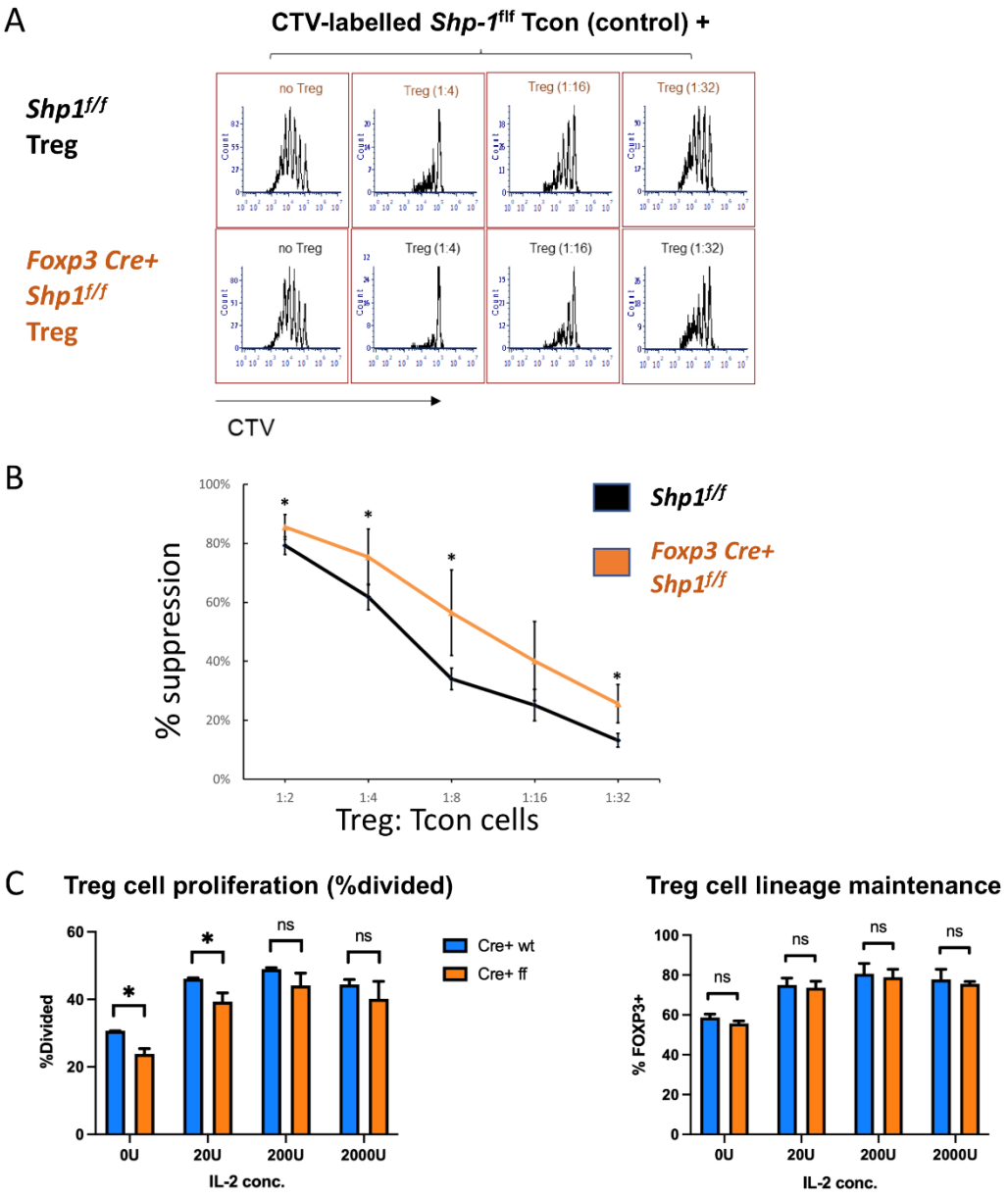

Figure 3.6.2 SHP-1-deficient Treg cells display increased suppressive activity in vitro. (A and B) Treg (CD4+CD25+ isolated from Foxp3^{Cre+} Shp-1$^{f/f}$ mutant or Shp-1$^{f/f}$ control mice) and CTV-labeled Tcon (CD4+CD25- from control mice) cells were co-cultured at the indicated ratios. (A) Histogram depicts CTV dilution within Tcon cells as a measurement of proliferation. Data are representative of 5 independent experiments with n= 2 to 3 mice (6-9 weeks old) of each genotype for each experiment. (B)

Suppression capacity of Treg cells based on data obtained in A. (C) (Left) Treg cell proliferation after 3 days of IL-2 stimulation (0 U, 20 U, 200 U, 2000 U). Treg cells were derived from $Foxp3^{Cre+}$ $Shp\text{-}1^{f/f}$ mutant or $Foxp3^{Cre+}$ control mice. (Right) Percentage of Treg cells that maintain Foxp3 expression following 3 days of IL-2 stimulation. n= 3 mice for each bar. Error bar represents SD. *, $p \leq 0.05$. ns = not significant.

cells showed increased suppressive capacity toward wild type CD4+ Tcon cells compared to *Foxp3*$^{Cre+}$ or *Shp-1*$^{f/f}$ control Treg cells, which was most evident at lower Treg : Tcon ratios (Figures 3.6A, B and Figures 3.6.2A, B).

To assess whether SHP-1-deficient Treg cells might hyper-proliferate in response to IL-2, we stimulated Treg cells in culture with 0, 20, 200 and 2000 Unit of IL-2 for 4 days. Both Foxp3Cre+ control and Foxp3Cre+ Shp-1f/f mutant Treg proliferated at similar levels when given medium to high level of IL-2 stimulation, while mutant Treg cells show less proliferation at low or no IL-2 condition (Figure 3.6.2C left). Treg from both genotypes show comparable viability and maintain similar percentages of Foxp3+ cells within the culture under the same IL-2 concentration (Figure 3.6.2C right), demonstrating that the observed increase in suppressive activity mediated by SHP-1-deficient Treg cells is not due to increased Treg proliferation in an *in vitro* setting. These data indicate that SHP-1-deficient Treg cells have the potential not only to be functional but are hyper-suppressive in a short-term *ex vivo* setting. However, we interpret these *ex vivo* results with caution, as it is well recognized that Treg functionality measured *in vitro* may not reflect the general Treg functionality/biology *in vivo*.

Mice with SHP-1-deficient Treg cells show impaired control of inflammation *in vivo*

We next tested the functionality of SHP-1-deficient Treg cells in vivo by comparing the abilities of SHP-1-deficient and -sufficient Treg cells to control inflammation in vivo. First, we employed a model of allergic airways inflammation (AAI), which is acutely induced through exposure to the common allergens from the house dust mite (HDM) (Figure 3.7A) (177). A comparison of mutant and control mice

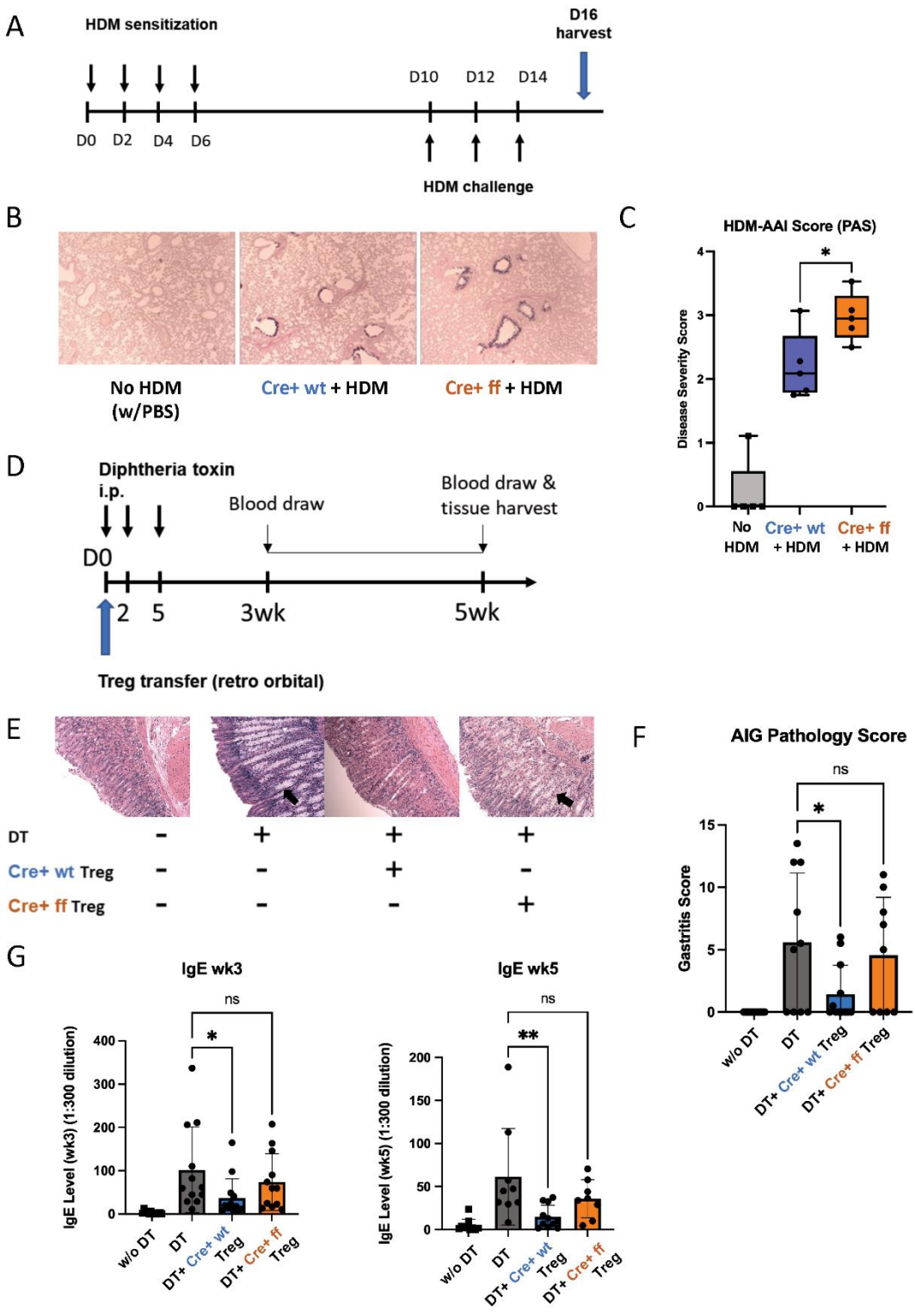

Figure 3.7 SHP-1 is required for the suppressive functionality of Treg cells in vivo.

(A) Schematic diagram depicts HDM-AAI experimental setup. **(B)** Representative

images of lung histology (PAS/Alcian blue staining) of *Foxp3*$^{Cre+}$ control and *Foxp3*$^{Cre+}$ *Shp-1*$^{f/f}$ mice 5 weeks after HDM or PBS treatment. Magnification: 4x **(C)** HDM-induced AAI disease severity represented by score based on PAS stained mucous. n= 6 (*Foxp3*$^{Cre+}$ control), 6 (*Foxp3*$^{Cre+}$ *Shp-1*$^{f/f}$ mutant), 5 (PBS treated no HDM), **(D)** Schematic diagram of DEREG model. Treg cells are depleted by consecutive Diphtheria toxin (DT) injections causing an AIG phenotype that can be rescued *via* adoptive transfer of Treg cells. **(E)** Representative images of stomach histology (H&E staining) of indicated experimental groups. Magnification: 10X. Arrows indicate epithelia hyperplasia/metaplasia. **(F)** AIG disease severity score based on H&E and PAS-stained histology images. n= 12 (no DT), 10 (DT), 12 (*Foxp3*$^{Cre+}$ control), 9 (*Foxp3*$^{Cre+}$ *Shp-1*$^{f/f}$ mutant). ns = not significant. **(G)** Serum IgE level of the indicated experimental groups at 3 and 5 wks. Data are from three independent experiments with 2-3 mice per experimental group for each experiment. *, $p<0.05$, **, $p<0.01$. One-way ANOVA, followed by Fisher's LSD test **(C**, **G)**, or Brown-Forsythe and Welch ANOVA test followed by Welch test **(F)** for multiple comparisons. ns, not significant.

following HDM treatment showed higher lung mucous production in Foxp3Cre+ Shp-1f/f mutant mice (Figure 3.7B), when assessed by a semiquantitative severity score (178) based on PAS stain (Figure 3.7C). This suggested that Treg cells in Foxp3Cre+ Shp-1f/f mice have a decreased capacity to suppress inflammation in the AAI model in vivo, despite their greater ability to suppress in vitro. Nevertheless, there were no significant differences in the T cell populations derived from draining lymph nodes, bronchoalveolar lavage fluid, or lung tissues and consistent with this finding, the levels of bronchiolar and vascular inflammation were comparable (Figure 3.7.2A). This decrease in suppressive ability was surprising, as we had initially expected the greater suppressive activity *in vitro* to translate to reduced disease severity *in vivo*.

To complement the AAI model, where inflammation is induced in response to a foreign antigen, we employed the DEREG (DEpletion of REGulatory T cells) model, in which mice develop inflammatory disease in the form of autoimmune gastritis (AIG) upon Treg cell depletion (179). The phenotype can be rescued through adoptive transfer of Treg cells allowing to compare the suppressive capacities of Treg cells in a genetically identical background (Figure 3.7D) (175). Diphtheria toxin (DT)-mediated Treg depletion has been shown to cause a Th2-skewed immune response as evidenced by elevated serum IgE level (179). AIG-induced mice rescued with *Foxp3*$^{Cre+}$ *Shp-1*$^{wt/wt}$ control Treg cells showed a reduced inflammation as reflected by pathology score, with reduced lymphocyte infiltration, epithelia hyperplasia/metaplasia, and parietal cell loss (Figure 3.7E). However, transfer with *Foxp3*$^{Cre+}$ *Shp-1*$^{f/f}$ Treg cells failed to rescue the AIG pathology score (Figures 3.7E, F). With respect to serum IgE levels, at 3- and 5-week post transfer, adoptive transfer of wild type Treg cells significantly reduced the

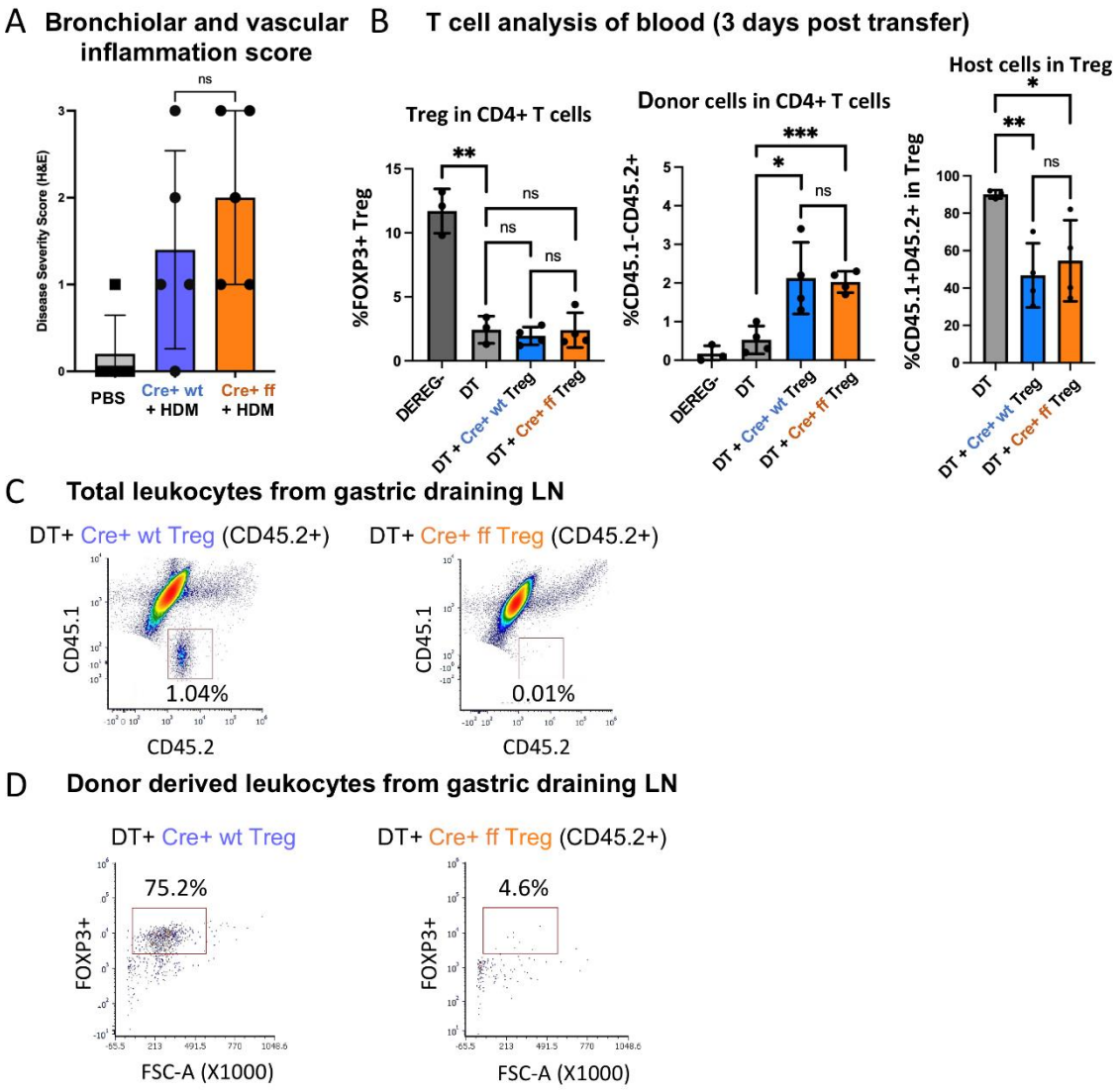

Figure 3.7.2 SHP-1 is required for the suppressive functionality of Treg cells in vivo. (A) HDM-induced AAI disease severity score based on bronchiolar and vascular inflammation (H&E histology). (B) To assess the presence of total (left panel), donor-derived (CD45.1-CD45.2+) (middle panel), and host-derived (CD45.1+CD45.2+) Treg cells (right panel), blood was drawn at day 3 post transfer and analyzed by flow cytometry (*note: % of donor cells (CD45.1- CD45.2+) in DEREG- and DT represents baseline autofluorescence*). n = 3 (DEREG- mice), 4 (DT), 4 (cre+ wt control Treg), 4

(cre+ ff mutant Treg). (C) Representative flow cytometric data of CD45.2+ CD45.1- donor cells of indicated genotype 3 weeks post transfer. Host cells are CD45.2+ CD45.1+. Percentages indicate donor-derived T cells within gastric draining lymph nodes. Data are gated on singlets → live cells → CD45 (D) Representative flow cytometric data of FOXP3 expression within CD45.2+ CD45.1- donor cell population. Data are gated on singlets → live cells → CD45 → CD45.2+ CD45.1-. (A) One-way ANOVA test was applied followed by Fisher's LSD for comparison across multiple conditions. (B) Unpaired t test. *p <0.05, **p<0.01, ***p<0.001. Error bar represents SD. ns = not significant.

serum IgE levels, while *Foxp3*$^{Cre+}$ *Shp-1*$^{f/f}$ Treg cells failed to do so (Figure 3.7G). In the DEREG induced AIG model, host-derived Treg cells reappear within a few days following DT-mediated Treg depletion (179) *(*Figure 3.7.2B *left panel)*. To precisely distinguish between host and donor Treg cells, we crossed the B6 CD45.1 allele mice (172–174) onto the DEREG background. We found comparable levels of donor *(CD45.1-CD45.2+) Foxp3*$^{Cre+}$ *Shp-1*$^{f/f}$ mutant and *Foxp3*$^{Cre+}$ control Treg cells *(*Figure 3.7.2B, *middle panel*), and both experimental groups limited the reappearance of host-derived Treg cells (CD45.1+CD45.2+) at a comparable level (Figure 3.7.2B*, right panel)* confirming that there was no difference between the adoptive transfer of the two experimental groups. It also indicates that this early effect of homeostatic expansion of the host Treg population was not affected by the loss of SHP-1 in the donor Treg cells.

Since we had observed that loss of SHP-1 causes an instability of the Treg lineage commitment (Figure 3.5B), we next assessed whether adoptively transferred donor Treg cells are localized to the site of inflammation. 3 weeks after the adoptive Treg transfer, there were no detectable donor *Foxp3*$^{Cre+}$ *Shp-1*$^{f/f}$ cells (CD45.2+ CD45.1-) in the host gastric draining lymph nodes, while in the *Foxp3*$^{Cre+}$ control donor group, about 1% of the CD45+ leukocytes were donor-derived. Within this population, about 70-80% remained Foxp3+ (Figures 3.7.2C, D). These finding suggest that although *Foxp3*$^{Cre+}$ *Shp-1*$^{f/f}$ Treg cells are initially able to control the homeostatic expansion of host Treg cells, they fail to sufficiently migrate and/or survive at the site of inflammation in the *in vivo* AIG model. Neither *Foxp3*$^{Cre+}$ *Shp-1*$^{f/f}$ nor *Foxp3*$^{Cre+}$ control donor group-derived cells could be detected in the spleen 3 weeks post transfer. This failure of SHP-1-deficient Treg cells to efficiently control inflammation in two different models of

inflammatory disease suggests a critical role for SHP-1 in the in vivo functionality of Treg cells.

Chapter 4

Summary, discussion and future directions

This section contains both published and unpublished data.

Summary of major findings

In the present study, we aimed to understand the functional role of SHP-1 in Treg cells to gain a better mechanistic understanding of how SHP-1 coordinates the immune homeostasis/response under physiological and pathophysiological conditions. Based on Treg-specific deletion of SHP-1, our findings revealed previously unappreciated roles for this tyrosine phosphatase in regulating Treg function and homeostasis. We generated a Treg-specific SHP-1 deletion model, Foxp3Cre+ Shp-1$^{f/f}$ (65, 66) to address how SHP-1 affects Treg function and thereby contributes to T cell homeostasis. While the loss of SHP-1 *via* the *Foxp3*$^{Cre+}$ *Shp-1*$^{f/f}$ approach does not quantitatively affect the thymic Treg selection process under such conditions, qualitative differences remain between *Foxp3*$^{Cre+}$ control and *Foxp3*$^{Cre+}$ mutant Treg cell populations.

Our *ex vivo* studies support a model where SHP-1 negatively regulates the suppressive activity of Treg cells. However, our *in vivo* models demonstrate that the role SHP-1 plays in Treg-mediated suppression is complicated. Treg cells appear less stable *in vivo*, and tend to lose Foxp3 expression and a significant fraction of these cells transition to ex-Treg cells at the steady state.

Further, when *Foxp3*$^{Cre+}$ *Shp-1*$^{f/f}$ mice were challenged in inflammatory models (induced by exogenous antigens or in autoimmune settings), the Treg cells failed to control the inflammation effectively. Loss of SHP-1 decreases the effectiveness of Treg cells to suppress inflammation in a model of acute airway inflammation and a model of acutely induced autoimmunity. Moreover, mechanistically, our data indicate that SHP-1 plays a crucial role in Treg plasticity, the AKT-mTOR pathway, and metabolism. Thus, SHP-1 has critical functions in Treg cells in inflammation mitigation.

Discussion

Our data demonstrate an increase in the suppressive activity of SHP-1-deficient Treg cells *in vitro*. However, when assessed *in vitro*, the expression of suppressive cytokines such as IL-10 or IL-35 (Figures 3.2B&C) were comparable between mutant and control Treg cells suggesting SHP-1 regulates Treg cell suppressive activity through mechanisms other than suppressive cytokine productions. Further, while a higher percentage of *Foxp3*$^{Cre+}$ *Shp-1*$^{f/f}$ Treg cells are proliferating *in vivo* based on Ki-67 expression levels (Figure 3.2A), in the *in vitro* suppression assays, Treg numbers from both *Foxp3*$^{Cre+}$ *Shp-1*$^{f/f}$ and control groups are comparable after 4 days in culture (data not shown). *In vitro* suppression assays measure the potential suppressive capacity of Treg cells under optimal conditions. As these assays only partially reflect the *in vivo* setting, which integrates additional factors that directly and indirectly modulate Treg-mediated suppression, including trafficking and maintenance of Treg cells, we utilized two mouse models: the HDM antigen-induced AAI model and the DT-induced AIG model. In both models, *Foxp3*$^{Cre+}$ *Shp-1*$^{f/f}$ Treg performed worse when challenged and failed to protect the host from both allergic response and autoimmune disease.

In the AAI model, the discrepancy between *in vitro* and *in vivo* suppressive function might be partially explained by the resistance to Treg suppression arising from the Tcon compartment: *Foxp3*$^{Cre+}$ *Shp-1*$^{f/f}$ mice contain an increase in the CD44^{hi} CD62L^{low} CD4+ T cell population (Figure 3.4A and Figure 3.4.2), which expresses lower levels of SHP-1 (Figure 3.4D) and potentially arise from a subpopulation of SHP-1-deficient ex-Treg cells. We have previously shown that loss of SHP-1 in Tcon cells promotes resistance to suppression (167). At steady state, *Foxp3*$^{Cre+}$ *Shp-1*$^{f/f}$ mice have

absolute thymic (data not shown) and peripheral cell numbers as well as relative CD4+, CD8+, Foxp3+ T cell numbers (Figure 3.1E) comparable to control mice and exhibit no spontaneous disease phenotypes. This data suggests that with Treg-specific SHP-1 knockout, mutant mice maintain both central and peripheral tolerance at homeostatic conditions. However, upon challenge, this otherwise dormant $CD44^{hi}$ $CD62L^{lo}$ population may become not only less suppressible, but also more readily activated upon any inflammatory signals to carry out a robust response.

In the transient Treg-depletion in the DEREG system, the host Treg cells quickly come back, although they cannot control autoimmune gastritis (AIG). Interestingly, these quickly resurrected host Treg cells exhibit normal *in vitro* suppressive capacity (179). The reappearance of the host Treg cells is reduced upon the adoptive transfer of Treg cells. In our studies, we detected comparable levels of returning host Treg cells in the spleen and lymph nodes upon transfer of SHP-1-deficient or -sufficient Treg cells indicating that this Treg-mediated control of homeostasis is unaffected by the presence of absence of SHP-1 (Figure 3.7.2B). However, the transferred SHP-1-deficient Treg cells failed to control AIG, while control Treg cells were able to limit AIG. Interestingly, *Foxp3*$^{Cre+}$ *Shp-1*$^{f/f}$ Treg can be found at similar levels as the control Treg in the blood on day 4 after the transfer. However, at 3 weeks post transfer, the SHP-1-deficient Treg cells are not detectable in the gastric draining lymph nodes (Figures 3.7.2C&D). In contrast, *Foxp3*$^{Cre+}$ control Treg cells are maintained as a small but functionally significant population. The inability of *Foxp3*$^{Cre+}$ *Shp-1*$^{f/f}$ Treg cells to suppress AIG, is not due to the loss of Foxp3 expression or conversion to ex-Treg cells, since no *Foxp3*$^{Cre+}$ *Shp-1*$^{f/f}$ donor cells were detectable at 3 weeks, regardless of Foxp3 expression. Impaired Treg

functions during recruitment, retention, or survival at stomach mucosa may contribute to the disappearance of transferred SHP-1-deficient Treg cells. Interestingly, it has previously been reported that SHP-1-deficient Treg cells might actively contribute to an increased response to food-mediated allergies via a reprogramming towards a TH2 phenotype (190). Although in both of the two studies, SHP-1-deficient Treg cells were inefficient in preventing/mitigating inflammatory diseases, the underlying mechanisms are likely different.

Similar to our previous findings in Tcon cells (167), SHP-1 regulates AKT phosphorylation in Treg cells. The role of AKT activation and the AKT-mTOR pathway in Treg cells is complex. Early studies noted that strong TCR activation promotes AKT phosphorylation, which then inhibits FOXO transcription factors promoting FOXO localization out of the nucleus thereby inhibiting the generation of peripherally induced Treg cells (184, 191–194). These studies either stimulated the AKT/mTOR pathway through TLR (184), rapamycin (191), used TCR agonist peptides in TCR transgenic T cells (192, 195), or Raptor knockout mice with strong autoimmune phenotype (192). Although these results seem to contrast our findings that *Foxp3*$^{Cre+}$ *Shp-1*$^{f/f}$ Treg cells display a higher AKT phosphorylation while also exhibiting a more robust suppression *in vitro*, it is worth noting that conditional SHP-1 deletion, as done in our study, presents a more subtle modulation of TCR activation, which does not affect the overall Foxp3 expression and may not impair the Treg suppressive function.

Foxp3^{Cre+} *Shp-1*$^{f/f}$ mice show an expanded CD44^{hi} CD62L^{lo} CD4+ Tcon population (Figure 3.4A and Figure 3.4.2). A similar increase of antigen-experienced cells in the CD4 and CD8 compartments had previously been reported by Johnson et al.

in CD4-Cre SHP1$^{f/f}$ mice (196). We have previously performed an extensive series of studies in our lab using dLck-Cre SHP-1$^{f/f}$ mice but did not find a similar effect (167). A possible explanation for these differences might be the timing of the SHP-1 depletion. While CD4-Cre and Foxp3-Cre drive Cre expression at the double positive stage during the thymic selection process, Cre driven by the distal LCK promoter begins to express post-selection at the single positive stage (197), allowing for physiological SHP-1 expression during thymic selection. The TCR repertoire generated during thymic T cell development is the product of positive and negative selections and is directed by the strength of signaling downstream of the TCR, a signaling pathway regulated by SHP-1. SHP-1 has been shown to be crucial for the differentiation between low-affinity versus high-affinity altered peptide ligands using OT-I *CD4-Cre SHP1*$^{f/f}$ transgenic mice (198), albeit Martinez et al. found a decreased naïve CD4 population (198) rather than an increased CD44^{hi} CD62L^{lo} population in their transgenic mice. It has also been shown that a complete Treg repertoire with sufficient recognition power for autoreactive molecules is required for maintaining intestinal homeostasis (199). In the current study, SHP-1 is deleted at a distinct Treg developmental timeframe coinciding with the formation of the TCR repertoire. Although there was no apperant overall defect of positive and negative selection, Treg cells might have developed expressing an alternative TCR repertoire, which may be less diversified or lacking recognition of specific endogenous antigens, thereby less equipped for controlling autoantigen-driven T cell activation *in vivo*. This defect might manifest in increased levels of antigen-experienced Tcon cells, as we have observed in the *Foxp3*$^{Cre+}$ *Shp-1*$^{f/f}$ mice. Whether

there is a critical developmental time point for SHP-1 expression to control the size of the $CD44^{hi}CD62L^{lo}$ population remains to be elucidated.

Independently, an alternative possibility would be that the enlarged $CD44^{hi}$ $CD62L^{lo}$ population derived from increased ex-Treg cells. We, therefore, assessed Treg lineage stability *in vivo* using the tdTomato lineage tracing model. We found that SHP-1-deficient Treg cells are more likely to lose Foxp3 expression and become ex-Tregs, which is consistent with the potential fragile Treg paradigm, as indicated by increased AKT phosphorylation, suggesting a previously unappreciated new role for SHP-1 in Treg cells. We tested whether this "ex-Treg" population was due to a loss of IL-2-stabilized Foxp3 expression. *Foxp3*$^{Cre+}$ *Shp-1*$^{f/f}$ Treg cells showed comparable levels of CD25 expression to control Treg cells (Figure 3.2.2A). Moreover, when stimulated with IL-2 *in vitro*, both *Foxp3*$^{Cre+}$ *Shp-1*$^{f/f}$ and *Foxp3*$^{Cre+}$ Treg cells maintain comparable levels of Foxp3-expressing T cells (Figure 3.6.2C). This data suggests SHP-1 does not affect the IL-2 signaling required to maintain Foxp3/Treg lineage. However, while ex-Treg cells might contribute to the increased antigen-experienced CD4 T cell population, ex-Treg cells alone cannot explain the expansion of all antigen-experienced T cells in the *Foxp3*$^{Cre+}$ *Shp-1*$^{f/f}$ mice, since there is also an increase in the percentage of $CD44^{hi}$ $CD62L^{lo}$ within the CD8 population.

As a third alternative possibility besides being antigen-experienced potentially auto-reactive T cells or ex-Treg, these $CD44^{hi}$ $CD62L^{lo}$ cells may belong to the "virtual memory" category. SHP-1 deficiency in Treg might promote the accumulation of these virtual memory T cells, in which some naive CD4 and CD8 T cells express $CD44^{hi}$ $CD62L^{lo}$ memory-like phenotype before encountering their cognate antigen (200–202).

These three possible explanations are not mutually exclusive and may all contribute to the observed increase in $CD44^{hi}$ $CD62L^{lo}$ CD4+ T cells.

In summary, our data reveal a previously unrecognized role of SHP-1 in mediating the functionality of Treg cells under physiological and patho-physiological conditions. Our data demonstrate that SHP-1 regulates AKT phosphorylation and Foxp3 stability in Treg cells. Moreover, our *in vivo* data suggest that SHP-1 is critical for optimal Treg-mediated suppression in an inflammatory environment. Since our findings are based on acute models of inflammation, it remains to be tested on how SHP-1 is involved in the control of chronic inflammation. Interestingly, deficient SHP-1 expression has been associated with chronic inflammatory diseases such as psoriasis (203) and multiple sclerosis (204), potentially pointing to a similar loss of function associated with SHP-1 insufficiency. Future studies are required to explore whether inducing SHP-1 expression in Treg cells would alleviate the diseases. On the contrary, functionally unstable and less suppressive Treg cells may be therapeutically preferrable in a tumor environment. Since the loss of SHP-1 results in resistance to suppression in effector T cells (167) as well as the functionality of Treg cells, SHP-1 inhibition may be a promising target for tumor clearance. While two phase I trials for malignant melanoma and advanced cancer malignancies using the SHP-1 inhibitor sodium stibogluconate (SSG) have failed due to the lack of efficacy on tumor burden while inducing strong toxic side effects (205), retroviral SHP-1 knockdown together with immune checkpoint blockade has been effective in recruiting low-affinity T cells for antitumor function (206). The resulting resurrection of SHP-1 as a potential drug target in the context of

cancer emphasizes the need to gain a better functional understanding of the role of SHP-1 in various cellular subsets.

Future directions

While our study added to the mechanistic understanding of Treg biology, it also raised new questions that will require further investigation and analyses. By delving into these aspects, we may uncover additional insights and knowledge that could contribute to advancing our understanding of SHP-1 in Treg immunity.

Repertoire

One hypothesis that arose from the existence of the increased CD4+ CD44+ $CD62L^{lo}$ population in mice with SHP-1-deficient Treg is that loss of SHP-1 in Treg cells during thymic development led to an altered Treg repertoire. Since FOXP3-driven Cre is expressed in the thymus during the selection process, SHP-1-deficient Treg cells may express an altered TCR repertoire, which lacks self-antigen-driven activation in the host AIG mice, which are therefore incapable of maintaining this population. This observation would be consistent with the finding that SHP-1-deficient Treg might have a survival disadvantage in the AIG environment, as they were not detected after 3 weeks post-transfer (Figures 3.7.2 D&C).

The interaction between the TCR and MHC-peptide complex is crucial for T cell survival, activation, and function. Some studies have indicated that enhancing the binding between TCR and MHC-peptide would increase the functional attributes of T cells (208). This enhanced binding can be achieved by increasing the affinity and half-life of the TCR-MHC-peptide interactions (208, 209). The affinity hypothesis for Treg development suggests that in the thymus, TCRs with higher affinity will preferably drive the precursor cells towards a Treg differentiation pathway rather than towards conventional CD4 T cells fate (82,114, 210) Vahl et al.'s finding also emphases the importance of TCR, such

that TCR ablation left the Treg with impaired suppression function, even if the master Treg regulator FOXP3 is still expressed (211),.

While in the mature Treg cell population, a variety of TCRs with distinctive affinities can support Treg function, the diversity of TCR affinities expressed by Tregs may also contribute to modulation of their responses following recognition of a wide range of self-antigens thereby maintaining immune tolerance. For example, Sprouse et al. suggested that murine Tregs expressing TCRs of different affinities support distinct functions in a type 1 diabetes autoimmune environment (210): where high-affinity Treg cells upregulating *Gzmb, Il10, Tigit,* and *Lag3* mRNA and expressing high level of CTLA-4 and GITR protein, low affinity Treg cells upregulate *Ebi3* and *Areg.* They also pointed out that the high affinity 4-8 TCR, but not low affinity 12-4.4m1 TCR expressing Treg cells accumulated at the inflammatory site of pancreatic draining lymph node and presented an actively proliferating phenotype, as evidenced by the increased expression of Ki67 (210). However, when facing the Teff cells from a polyclonal environment, produced by the polyclonal bone marrow cells transfer, Treg cells with lower affinity TCR proliferates better (210). These findings suggest that having a wide range of repertoire could reduce the pressure for Treg cells carrying lower affinity TCR to compete with their higher affinity colleagues for antigens, thus leading to a more favorable environment for low-affinity Treg proliferation. In our AIG mice, besides the potential defect in Treg homing, the altered repertoire might reduce the fitness of transferred mutant *Foxp3*$^{Cre+}$ *Shp-1*$^{f/f}$ Treg, thus contributing to the failure of maintaining mutant Tregs and controlling the autoimmune disease.

As discussed above, using OT-I CD4-Cre SHP1$^{f/f}$ transgenic mice, SHP-1 has been reported to influence the generation T cells expressing TCRs with high and low-affinity repertoire (93). SHP-1 has also been reported to affect cellular TCR affinity perception under partial knockdown of SHP-1 in OT-I mice, where OT-I CD8+ cell infiltration was altered in the context of a low antigen affinity tumor, but not higher affinity ones (206). Interestingly, SHP-1 can also counterbalance a too strong response evoked by the increase of TCR affinity toward tumor antigen HLA-A2/NY-ESO-1 in engineered CD8+ T cells (209). This balanced regulation might also be required for any *in vivo* Treg function during the inflammatory setting and would have been absent in our murine model of SHP-1-deficient Treg cells.

Therefore, analysis of the repertoire of mutant *Foxp3*$^{Cre+}$ *Shp-1*$^{f/f}$ Treg will help to dissect SHP-1 function during the tTreg differentiation in thymus while also providing further information for how SHP-1 regulates mature Treg function under the steady state or inflammatory condition in response to the continuously TCR signaling, which maintains Treg suppression. Overall, this future Treg repertoire analysis will allow progress toward a better understanding of the role of SHP-1 in defining Treg function.

CD44^{hi} CD62L^{lo} population in CD4 T cell

Another interesting finding is the increased CD4 CD44^{hi} CD62L^{lo} population. Our study suggests that Treg cells that lose their FOXP3 expression and their Treg cell lineage commitment potentially contribute to the CD4 T cells accumulation (Figure 3.5). We have also observed upon activation a 2-fold increased *il-4* mRNA expression in *ex vivo* CD44^{hi} Foxp3- CD4+ T cells from *Foxp3*$^{Cre+}$ *Shp-1*$^{f/f}$ mutant mice compared to T cells from Foxp3^{Cre+} control mice (data not shown). However, based on flow cytometric

analyses, no difference in GATA3 expression was observed in this CD44^{hi} Foxp3- CD4+ population suggesting no general skewing toward the Th2 pathway under the steady state. This result might indicate that this CD4 CD44^{hi} CD62L^{lo} population is primed to be skewed toward Th2 but requires an extra stimulus.

Atopic asthma, a chronic inflammatory disease involving airway remodeling which HDM-induced AAI models aimed to study, has been reported to be a Th2 mediated, IL-4 and IL-5 associated disease in human beings (212, 213,124). When HDM allergens are inhaled, they are taken up by dendritic cells in the airway and presented to T cells, and the IL-6 is produced by macrophages (215). IL-6 in the environment triggers the activation of transcription through the nuclear factor of activated T cells (NFAT), leading to the IL-4 production in T cells and the activation and differentiation of CD4+ T helper 2 (Th2) cells (212, 215). Th2 cells then secrete a variety of cytokines, including IL-4, that stimulate the differentiation and activation of other immune cells, such as eosinophils, mast cells, and B cells.

In our study, the mutant Treg cells performed worse in controlling AAI, possibly due to resistance from the expanded CD4 CD44^{hi} CD62L^{lo} population. When we tested IgE or IL-4 levels at day 16 in the serum, there was no increase in response to the HDM (data not shown), which is consistent with Woo et al's report that IgE production in serum was not evident at 2 weeks, but will start to show in the 3-or 4-weeks HDM AAI (212, 216). However, it is also possible that the sensitivity of the ELISA was not sufficient to detect changes in systemic cytokine levels at that time point. A direct measurement of IL-4 and IL-5 levels in purified T cells upon in vitro re-stimulation with

HDM might allow detection at earlier time points due to increased sensitivity as suggested by Johnson et al (216).

The current AAI model tests the functional outcome of Treg-specific SHP-1 depletion in the context of a genetically modified animal. To test whether the possible resistance from the CD4 $CD44^{hi}$ $CD62L^{lo}$ population prevents the Treg immune modulation in this AAI model, models using adoptive cell transfer of individual subsets could be employed to identify the specific contributions of each T cell subset.

CD44 expression has been linked to CD4 Th cell differentiation into the cell fate of Th1 memory, and loss of CD44 drives the activated and expanding Th 1 cells to upregulate caspase-8 and undergo apoptosis after the peak of the primary immune response, as in the case of influenza infection (217). Thus, the increased $CD44^{hi}$ CD4 population might facilitate Th1 memory formation and provide a survival benefit for mutant mice. Further experiments in a Th1-driven murine disease model are required.

Another question that has come out of our research is whether differences in the timing of SHP-1 depletion affect the accumulation of the CD4 $CD44^{hi}$ $CD62L^{lo}$ population in *Foxp3*$^{Cre+}$ *Shp-1*$^{f/f}$ mutant mice. As discussed above, we attribute the sole appearance of the CD4 $CD44^{hi}$ $CD62L^{lo}$ in *Foxp3*$^{Cre+}$ *Shp-1*$^{f/f}$ mutant mice but not in the dLck-Cre SHP-$1^{f/f}$ mice to the differences in earlier SHP-1 deletion timing in the *Foxp3*-Cre bearing mice. To approach this question, our first critical target would be to determine the outcome when SHP-1 deletion occurred post thymic development. Small molecule inhibitors may be an option. While SHP-1 was sensitive to SSG, which selectively inhibits protein tyrosine phosphatases (217), the off-target effect of SSG renders the effect of other protein tyrosine phosphatases, such as SHP-2, hard to rule out.

Viral transduction, CRISPR/cas9 system, tamoxifen-inducible Cre/loxP system, and RNA interference provide potential methods for knockdown or knockout of the SHP-1 and allow the silencing of SHP-1 at a controlled timepoint. While all the above methods have their benefits but also weaknesses, our lab recently generated an inducible and reversible *in vivo* protein degradation (IRIP) system, which may be helpful in expanding our knowledge of SHP-1 function at different stages of thymocytes and mature T cells, and informing us whether the modulation is reversible.

CD44^{hi} CD62L^{lo} population in CD8 T cell

Our finding showed an expanded CD44^{hi} CD62L^{lo} population within the CD8 cytotoxic T cell in mice with SHP-1-deficient Treg cells. Previous studies have shown that SHP-1 limits the number of CD8 short-lived effector cells, and at the same time does not affect the memory precursor effector cell population during the peak of CD8 expansion after the primary or secondary instance of antigen experiences (207). However, in our study, the relative *shp-1* expressions are comparable in the CD8 T cells from the mutant *Foxp3*$^{Cre+}$ *Shp-1*$^{f/f}$ and *Foxp3*$^{Cre+}$ control mice. Instead of intrinsic SHP-1 depletion in the mutant group of CD8, this expanded CD44^{hi} CD62L^{lo} population is most likely regulated by cell-extrinsic factors secondary to Treg-specific SHP-1 deletion.

Another interesting topic of future studies would be a better characterization of this CD44^{hi} CD62L^{lo} CD8+ population and how SHP-1 depletion in a different T cell lineage contributes to the emergence of this CD8 subpopulation. One possibility is that this is a virtual memory (Tvm) CD8 population. The Tvm cells are a group of CD8 T cells defined as memory-like, with the ability to mount a rapid and robust IFN-γ mediated response upon encounter with the antigens. However, these cells had no prior antigen

exposure and, instead, developed under the homeostatic condition (219,220,221). Traditionally, Tvm cells have been found in unimmunized mice and germ-free mice and can be characterized with surface expression $CD44^{hi}$, $CD122^{hi}$, and $CD49d^{lo}$ (219, 222). Induced by IL-15 mediated cytokine stimulation, previous studies have shown these Tvm cells provide bystander protection during the influenza virus and *Listeria monocytogenes* invasion (222).

Tvm cells are originated from CD8 T cells with a higher affinity for self-antigens (222). Although no studies have ever reported any link between intrinsic or extrinsic SHP-1 and Tvm cells, expression of CD5, the potential binding partner for SHP-1 on cell surface, can be used as an indicator for the TCR self-antigen affinity and is therefore correlated with identifying potential naïve CD8 T cell candidates for Tvm cells (222). We hypothesize a potential role of SHP-1 in modulating pre-Tvm antigen affinity. However, in the current scenario, the $CD44^{hi}$ CD8 T cell showed intact SHP-1, and SHP-1 regulation of Tvm would have been carried out through environmental factors secondary to the SHP-1 deficiency in Treg cells.

Treg cells have been reported to limit the population of Tvm. Treg cells expressing β1-integrin interrupt the interaction between pre-Tvm and CD11b+ IL-15 producing dendritic cells (221). In our case, it is possible that the SHP-1 deficiency in Treg cells facilitate the interaction between CD11b+ IL-15 producing DCs, which then drive the Tvm production in mice under the steady state.

Since our mice are kept in a pathogen-free (SPF) facility instead of a Germ-free facility, there remains the possibility that these mice, although not actively immunized or infected, might still experience antigens without our notice. Thus, to test whether these

are virtual memory cells, we first would confirm the high expression of CD122 and low CD49d on the surface of these $CD44^{hi}$ CD8 T cells and then determine whether SHP-1 helps Treg regulate the IL-15 production in DC or alters Tvm affinity as can be indicated with CD5 marker upregulated on Tvn cell surface. It is also possible that the accumulated population is antigen-experienced memory CD8 T cells coming from previous infections or antigen exposure. These studies should contribute to our knowledge of how SHP-1 influences Treg-mediated effects on memory CD8 T cells.

LFA-1

LFA-1 surface protein expression is elevated on the *Foxp3*$^{Cre+}$ *Shp-1*$^{f/f}$ mutant Treg cell surface (Figure 3.2A). LFA-1 on Treg may increase suppressive activity by promoting Treg-APC immune-synapse formation via LFA-1-ICAM-1 interaction. SHP-1 has previously been reported to negatively control LFA-1-mediated adhesion function in mouse T cells (223). On the resting T cells, by default, LFA-1 is at a low-affinity state, and the activation of LFA-1 requires the "inside-out" signal to induce LFA-1 clustering, which boosts the LFA-1 binding avidity with its ligands (224). After TCR/CD3 antigen-receptor complex engagement, TCR signaling cascade promotes the SLP-76 interaction with the adaptor protein ADAP further stimulating LFA-1 clustering. Specifically, Sauer et al. found that SHP-1 dephosphorylates the tyrosine motif YDGI on the ADAP to suppress the binding between SLP-76 and ADAP (223). Oppositely, Azoulay-Alfaguter et al. found that SHP-1 dephosphorylates CrkII and localizes CrkII from central supramolecular activation cluster (c-SMACs) to peripheral (p)-SMACs to recruit C3G and thus cause Rap1 activation and positively redistribute LFA-1 leading edge and

increase LFA-1 affinity to ICAM-1(163). Therefore, the role of SHP-1 in LFA-1 function seems to be less understood.

Our lab has demonstrated that SHP-1-deficient Treg cells derived from *motheaten* mice have an increased ability to form binding conjugates with bone marrow DCs (165). Thus, we hypothesize that the increase of LFA-1 protein on *Foxp3*$^{Cre+}$ *Shp-1*$^{f/f}$ mutant Treg contributes to better suppression performance *in vitro*.

Our preliminary study tests whether the upregulated LFA-1 on mutant Treg surface facilitates binding function. We coated goat anti-rabbit IgG magnetic bead with recombinant ICAM-1-Fc, and added pre-activated Treg to access binding with flow cytometry after 20 min. Although only a low level of Treg cells binds to the ICAM-1 beads in this binding assay, Treg cells from *Foxp3*$^{Cre+}$ *Shp-1*$^{f/f}$ mutant mice show a small but statistically significant increased binding (Figure 4.1).

Because higher LFA-1 binding affinity does not necessarily translate to an enhancement in Treg-APC binding or increased Treg suppression. For example, strong LFA-1 activation can also drive FAK1/PYK2 activation and generate LAT-GRB2-SKAP1 complexes, which then negatively regulate the T cell contact time with DCs (225). Next, we want to test whether LFA-1 blockade ablates the increased *in vitro* suppression in mutant Treg. With Treg cells pre-treated with LFA-1 blocking ab, we expect APCs in the suppression assay to reduce their contact time with Treg under single-cell imaging and the suppression activity of mutant Treg decrease.

However, because LFA-ICAM-1 formation is essential for immune-synapses formation, it is also possible that blocking LFA-1 can prevent in *vitro* Treg suppression

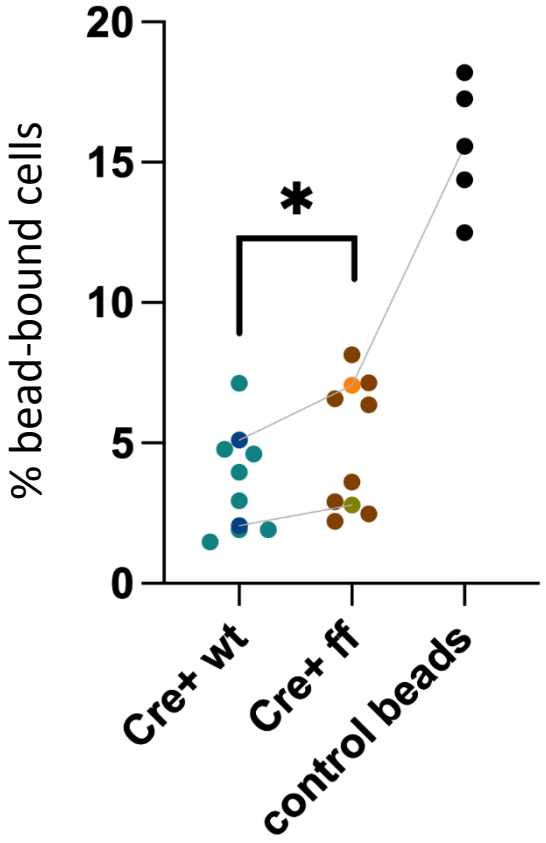

Figure 4.1 LFA-1 on Treg surface promotes Treg binding with ICAM-1 coated beads. Data are combined from 2 experiments, n= 4 for each genotype per experiment. The average percentage from each genotype in the experiment is shown in different color and linked with thin lines. Magnetic Dyna beads were coated with recombinant ICAM-1 -Fc and Treg cells from *Foxp3*$^{Cre+}$ (Cre+ wt) control mice, *Foxp3*$^{Cre+}$ *Shp-1*$^{f/f}$ (Cre+ ff) mice. A 1:1 mixture of Cre+ wt and Cre+ ff Treg cells was added to control beads. After 2 hours, cells went through flow cytometry to determine doublet. 2-way ANOVA was performed for statistics, p-value = 0.0233 phenotypes.

altogether, which suggests that mutant Treg cells carry out their suppression in a LFA-1-mediated contact-dependent manner.

Aging

We have observed an accumulation of $CD44^{hi}$ $CD62L^{lo}$ population in CD4 and CD8 in *Foxp3*$^{Cre+}$ *Shp-1*$^{f/f}$ mutant mice (Figure 4 3.4B&F). These populations seem to be benign at homeostatic condition. Although CD4 and CD8 $CD44^{hi}$ cells in mutant mice seem to be equally proliferative as $CD44^{hi}$ $CD62L^{lo}$ cells, as measured by Ki-67, in the control mice (Figure 3.4C&G), considering the increased $CD44^{hi}$ $CD62L^{lo}$ population in 6-8-week-old mutant mice, we hypothesize there might be some defects such as splenomegaly when these mice get aged. Therefore, we kept *Foxp3*$^{Cre+}$ *Shp-1*$^{f/f}$ mutant mice, *Foxp3*$^{Cre+}$ control mice, and *Shp-1*$^{f/f}$ control mice for 15 months and harvested the tissue.

Over-accumulation of splenocytes was indeed observed in some of these 15-month mice (Figure 4.2). However, the occurrence of these overgrown spleens is almost uniform for all genotype groups.

The phenotype of the 15-month-aged mice appears similar to what has been observed in the younger mice. No differences were observed in CD4 and CD8 percentages among live cells and FOXP3+ percentage in CD4+ T cells (Figures 4.2.2.A, B&C). As these mice age, the $CD44^{hi}$ percentage differences in *Foxp3*$^{Cre+}$ *Shp-1*$^{f/f}$ mutant and *Foxp3*$^{Cre+}$ control mice CD4 FOXP3+ population seems to decrease and become no longer significant (Figure 4.2.2 D), suggesting the existence of potential self-limiting mechanism among these $CD44^{hi}$ FOXP3+CCD4 cells.

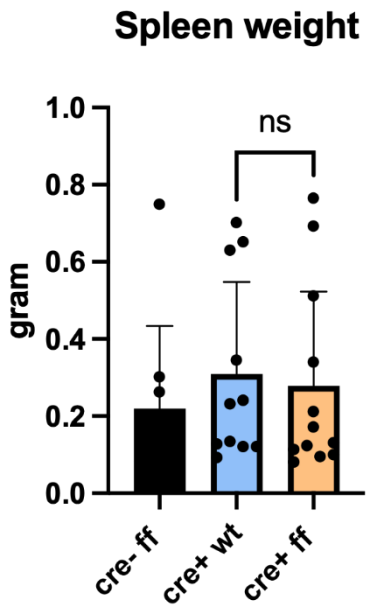

Figure 4.2 Spleen weight of 15-month-old Foxp3^{Cre+} Shp-1$^{f/f}$ mutant mice, Foxp3^{Cre+} control mice, and Shp-1$^{f/f}$ control mice. Whole spleens were harvested, rinsed with PBS, and weighed. 1-way ANOVA, followed by the unpaired test for pair-wise comparison. p-value = 0.7631, ns, not significant.

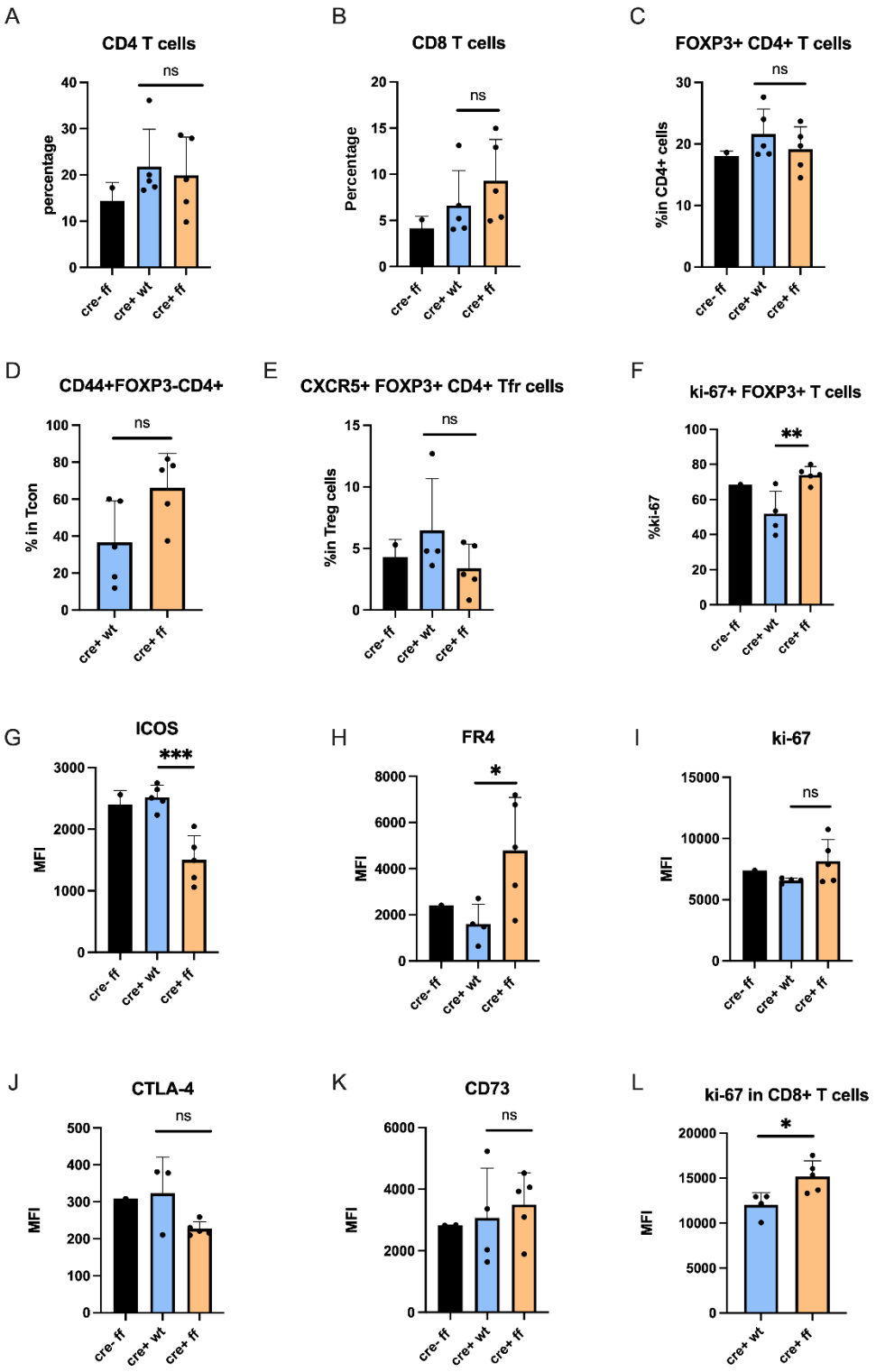

Figure 4.2.2 15-month-old CD4+ CD8+ Treg cells show a phenotype similar to the characters in 6–8-week-old mice. Spherocytes from *Shp-1*$^{f/f}$ (Cre- ff) control mice, *Foxp3*$^{Cre+}$ (Cre+ wt) control mice, *Foxp3*$^{Cre+}$ *Shp-1*$^{f/f}$ (Cre+ ff) mice were harvested and

accessed with flow cytometry. *n* = 4-5 for each genotype. Average percentages of (A) CD4 (p= 0.5526), and (B) CD8 (p =0.3073) in live cell, (C) %FOXP3 in CD4+ cells (p = 0.4401), (D) %CD44+ in CD4+ FOXP3- cells (p = 0.0533), (E) %CXCR5+ FOXP3+ in CD4 T cells (p = 0.3401), and (F) %Ki-67 in FOXP3+ Treg cells (p = 0.0083). Average MFI of (G) ICOS (p = 0.0009), (H) FR4 (p =0.0360), (I) Ki-67 (p = 0.1286), (J) CTLA-4 (p =0.0655), (K)CD73 (p =0.7790) in FOXP3+ Treg cells. (L) Ki-67 in CD8+ Tcells (p = 0.0212). ns, not significant.

Meanwhile, the Ki-67+ population remains higher in SHP-1 deficient Treg (Figure 4.2.2 F). However, the average Ki-67 expression of mutant mice no longer differs from that in control mice (Figure 4.2.2.I), in contrast to Ki-67 expression in CD8 T cell. (Figure 4.2.2 L). While FR4 remains higher when these mutant mice age (Figure 4.2.2 H), ICOS expression interestingly drops (Figure 4.2.2.G).

ICOS has been demonstrated to help maintain the $CD44^{hi}$ $CD62L^{lo}$ effector Treg sub-population at the homeostatic condition (230). Raynor et al. have shown that during the aging process, the majority of Treg cells become effector Treg cells; ICOS limits cell death and promotes effector Treg cells by inhibiting Bim in the homeostasis (231).

Despite being statistically not different, there is a visible trend suggesting that the %FOXP3+ in CD4 T cells in *Foxp3*$^{Cre+}$ *Shp-1*$^{f/f}$ mutant is slightly less than that percentage in *Foxp3*$^{Cre+}$ control mice (Figure 4.2.2 C). It is possible that these aged *Foxp3*$^{Cre+}$ *Shp-1*$^{f/f}$ mutant mice have a defect in ICOS, and therefore, the $CD44^{hi}$ $CD62L^{lo}$ effector FOXP3+ Treg failed to be maintained.

A longer aging process might be desirable to manifest the loss of FOXP3+ Treg cell population. To test this hypothesis, we want to define the population of Treg in our aged mouse with RNAseq. We can determine whether the Bim expression is upregulated in our Treg by western blot or flow cytometry. We could also inhibit Bim in mutant mice to see whether this inhibition compensates for the loss of FOXP3+ cells. We could also inhibit ICOSL in younger or control Treg cells to mimic the loss of foxp3 in aged *Foxp3*$^{Cre+}$ *Shp-1*$^{f/f}$ mutant mice.

References

1. Cooper MD, Herrin BR. How did our complex immune system evolve? Nat Rev Immunol. 2010 Jan;10(1):2–3.

2. Buchmann K. Evolution of Innate Immunity: Clues from Invertebrates via Fish to Mammals. Front Immunol [Internet]. 2014 [cited 2023 Mar 1];5. Available from: https://www.frontiersin.org/articles/10.3389/fimmu.2014.00459

3. Brown GD. Dectin-1: a signaling non-TLR pattern-recognition receptor. Nat Rev Immunol. 2006 Jan;6(1):33–43.

4. Murphy K (Kenneth M) author. Janeway's immunobiology. Ninth edition. New York, NY : Garland Science/Taylor & Francis Group, LLC, [2017]

5. Iwasaki A, Medzhitov R. Control of adaptive immunity by the innate immune system. Nat Immunol. 2015 Apr;16(4):343–53.

6. Flajnik MF, Kasahara M. Origin and evolution of the adaptive immune system: genetic events and selective pressures. Nat Rev Genet. 2010 Jan;11(1):47–59.

7. Boehm T, Swann JB. Origin and Evolution of Adaptive Immunity. Annu Rev Anim Biosci. 2014;2(1):259–83.

8. Flajnik MF. A cold-blooded view of adaptive immunity. Nat Rev Immunol. 2018 Jul;18(7):438–53.

9. Sun H, Sun C, Xiao W, Sun R. Tissue-resident lymphocytes: from adaptive to innate immunity. Cell Mol Immunol. 2019 Mar;16(3):205–15.

10. Smith K. Toward a molecular understanding of adaptive immunity: a chronology, part I. Front Immunol [Internet]. 2012 [cited 2023 Mar 10];3. Available from: https://www.frontiersin.org/articles/10.3389/fimmu.2012.00369

11. Minervina A, Pogorelyy M, Mamedov I. T-cell receptor and B-cell receptor repertoire profiling in adaptive immunity. Transpl Int. 2019;32(11):1111–23.

12. McHeyzer-Williams M, Okitsu S, Wang N, McHeyzer-Williams L. Molecular programming of B cell memory. Nat Rev Immunol. 2012 Jan;12(1):24–34.

13. Bevan MJ. Memory T cells as an occupying force. Eur J Immunol. 2011;41(5):1192–5.

14. Rosato PC, Beura LK, Masopust D. Tissue resident memory T cells and viral immunity. Curr Opin Virol. 2017 Feb;22:44–50.

15. Fan X, Rudensky AY. Hallmarks of Tissue-Resident Lymphocytes. Cell. 2016 Mar 10;164(6):1198–211.

16. Lugli E, Hudspeth K, Roberto A, Mavilio D. Tissue-resident and memory properties of human T-cell and NK-cell subsets. Eur J Immunol. 2016;46(8):1809–17.

17. Turner DL, Bickham KL, Thome JJ, Kim CY, D'Ovidio F, Wherry EJ, et al. Lung niches for the generation and maintenance of tissue-resident memory T cells. Mucosal Immunol. 2014 May 1;7(3):501–10.

18. Di Santo JP, Rodewald HR. In vivo roles of receptor tyrosine kinases and cytokine receptors in early thymocyte development. Curr Opin Immunol. 1998 Apr 1;10(2):196–207.

19. Corbeaux T, Hess I, Swann JB, Kanzler B, Haas-Assenbaum A, Boehm T. Thymopoiesis in mice depends on a Foxn1-positive thymic epithelial cell lineage. Proc Natl Acad Sci. 2010 Sep 21;107(38):16613–8.

20. Bajoghli B, Aghaallaei N, Hess I, Rode I, Netuschil N, Tay BH, et al. Evolution of Genetic Networks Underlying the Emergence of Thymopoiesis in Vertebrates. Cell. 2009 Jul 10;138(1):186–97.

21. Calderón L, Boehm T. Three chemokine receptors cooperatively regulate homing of hematopoietic progenitors to the embryonic mouse thymus. Proc Natl Acad Sci. 2011 May 3;108(18):7517–22. b

22. Thome JJC, Bickham KL, Ohmura Y, Kubota M, Matsuoka N, Gordon C, et al. Early-life compartmentalization of human T cell differentiation and regulatory function in mucosal and lymphoid tissues. Nat Med. 2016 Jan;22(1):72–7.

23. Kumar BV, Connors TJ, Farber DL. Human T Cell Development, Localization, and Function throughout Life. Immunity. 2018 Feb 20;48(2):202–13.

24. Thome JJC, Yudanin N, Ohmura Y, Kubota M, Grinshpun B, Sathaliyawala T, et al. Spatial Map of Human T Cell Compartmentalization and Maintenance over Decades of Life. Cell. 2014 Nov 6;159(4):814–28.

25. Gaudino SJ, Kumar P. Cross-Talk Between Antigen Presenting Cells and T Cells Impacts Intestinal Homeostasis, Bacterial Infections, and Tumorigenesis. Front Immunol [Internet]. 2019 [cited 2023 Mar 14];10. Available from: https://www.frontiersin.org/articles/10.3389/fimmu.2019.00360

26. Hwang JR, Byeon Y, Kim D, Park SG. Recent insights of T cell receptor-mediated signaling pathways for T cell activation and development. Exp Mol Med. 2020 May;52(5):750–61.

27. Daniels MA, Teixeiro E. TCR Signaling in T Cell Memory. Front Immunol [Internet]. 2015 [cited 2023 Mar 14];6. Available from: https://www.frontiersin.org/articles/10.3389/fimmu.2015.00617

28. Kim C, Wilson T, Fischer KF, Williams MA. Sustained Interactions between T Cell Receptors and Antigens Promote the Differentiation of CD4+ Memory T Cells. Immunity. 2013 Sep 19;39(3):508–20.

29. Kong KF, Yokosuka T, Canonigo-Balancio AJ, Isakov N, Saito T, Altman A. A motif in the V3 domain of the kinase PKC-θ determines its localization in the immunological synapse and functions in T cells via association with CD28. Nat Immunol. 2011 Nov;12(11):1105–12.

30. Jogdand GM, Mohanty S, Devadas S. Regulators of Tfh Cell Differentiation. Front Immunol [Internet]. 2016 [cited 2023 Mar 14];7. Available from: https://www.frontiersin.org/articles/10.3389/fimmu.2016.00520

31. Ruterbusch M, Pruner KB, Shehata L, Pepper M. In Vivo CD4 $^{+}$ T Cell Differentiation and Function: Revisiting the Th1/Th2 Paradigm. Annu Rev Immunol. 2020 Apr 26;38(1):705–25.

32. Walker JA, McKenzie ANJ. TH2 cell development and function. Nat Rev Immunol. 2018 Feb;18(2):121–33.

33. Neurath MF, Kaplan MH. Th9 cells in immunity and immunopathological diseases. Semin Immunopathol. 2017 Jan 1;39(1):1–4.

34. Licona-Limón P, Arias-Rojas A, Olguín-Martínez E. IL-9 and Th9 in parasite immunity. Semin Immunopathol. 2017 Jan 1;39(1):29–38.

35. Chen T, Guo J, Cai Z, Li B, Sun L, Shen Y, et al. Th9 Cell Differentiation and Its Dual Effects in Tumor Development. Front Immunol [Internet]. 2020 [cited 2023 Mar 15];11. Available from: https://www.frontiersin.org/articles/10.3389/fimmu.2020.01026

36. Yang Y, Torchinsky MB, Gobert M, Xiong H, Xu M, Linehan JL, et al. Focused specificity of intestinal TH17 cells towards commensal bacterial antigens. Nature. 2014 Jun;510(7503):152–6.

37. Szabo SJ, Kim ST, Costa GL, Zhang X, Fathman CG, Glimcher LH. A Novel Transcription Factor, T-bet, Directs Th1 Lineage Commitment. Cell. 2000 Mar 17;100(6):655–69.

38. Zheng W ping, Flavell RA. The Transcription Factor GATA-3 Is Necessary and Sufficient for Th2 Cytokine Gene Expression in CD4 T Cells. Cell. 1997 May 16;89(4):587–96.

39. Ivanov II, McKenzie BS, Zhou L, Tadokoro CE, Lepelley A, Lafaille JJ, et al. The Orphan Nuclear Receptor RORγt Directs the Differentiation Program of Proinflammatory IL-17+ T Helper Cells. Cell. 2006 Sep 22;126(6):1121–33.

40. Yu D, Rao S, Tsai LM, Lee SK, He Y, Sutcliffe EL, et al. The Transcriptional Repressor Bcl-6 Directs T Follicular Helper Cell Lineage Commitment. Immunity. 2009 Sep 18;31(3):457–68.

41. Johnston RJ, Poholek AC, DiToro D, Yusuf I, Eto D, Barnett B, et al. Bcl6 and Blimp-1 Are Reciprocal and Antagonistic Regulators of T Follicular Helper Cell Differentiation. Science. 2009 Aug 21;325(5943):1006–10.

42. Fontenot JD, Gavin MA, Rudensky AY. Foxp3 programs the development and function of CD4+CD25+ regulatory T cells. Nat Immunol. 2003 Apr;4(4):330–6.

43. Hori S, Nomura T, Sakaguchi S. Control of Regulatory T Cell Development by the Transcription Factor Foxp3. Science. 2003 Feb 14;299(5609):1057–61.

44. Zhou L, Chong MMW, Littman DR. Plasticity of CD4+ T Cell Lineage Differentiation. Immunity. 2009 May 22;30(5):646–55.

45. Mirlekar B. Co-expression of master transcription factors determines CD4+ T cell plasticity and functions in auto-inflammatory diseases. Immunol Lett. 2020 Jun 1;222:58–66.

46. Oestreich KJ, Weinmann AS. Master regulators or lineage-specifying? Changing views on CD4+ T cell transcription factors. Nat Rev Immunol. 2012 Nov;12(11):799–804.

47. Chowdhury D, Lieberman J. Death by a Thousand Cuts: Granzyme Pathways of Programmed Cell Death. Annu Rev Immunol. 2008;26(1):389–420.

48. Spicer BA, Conroy PJ, Law RHP, Voskoboinik I, Whisstock JC. Perforin—A key (shaped) weapon in the immunological arsenal. Semin Cell Dev Biol. 2017 Dec 1;72:117–23.

49. Sparrow E, Bodman-Smith MD. Granulysin: The attractive side of a natural born killer. Immunol Lett. 2020 Jan 1;217:126–32.

50. Martínez-Lorenzo MJ, Anel A, Gamen S, Monleón I, Lasierra P, Larrad L, et al. Activated Human T Cells Release Bioactive Fas Ligand and APO2 Ligand in Microvesicles1. J Immunol. 1999 Aug 1;163(3):1274–81.

51. Green DR, Llambi F. Cell Death Signaling. Cold Spring Harb Perspect Biol. 2015 Dec;7(12):a006080.

52. Cassioli C, Baldari CT. The Expanding Arsenal of Cytotoxic T Cells. Front Immunol. 2022 Apr 20;13:883010.

53. Martínez-Lorenzo MJ, Anel A, Alava MA, Piñeiro A, Naval J, Lasierra P, et al. The human melanoma cell line MelJuSo secretes bioactive FasL and APO2L/TRAIL on the surface of microvesicles. Possible contribution to tumor counterattack. Exp Cell Res. 2004 May 1;295(2):315–29.

54. Bálint Š, Müller S, Fischer R, Kessler BM, Harkiolaki M, Valitutti S, et al. Supramolecular attack particles are autonomous killing entities released from cytotoxic T cells. Science. 2020 May 22;368(6493):897–901.

55. Chang HF, Schirra C, Ninov M, Hahn U, Ravichandran K, Krause E, et al. Identification of distinct cytotoxic granules as the origin of supramolecular attack particles in T lymphocytes. Nat Commun. 2022 Feb 24;13(1):1029.

56. McLane LM, Abdel-Hakeem MS, Wherry EJ. CD8 T Cell Exhaustion During Chronic Viral Infection and Cancer. Annu Rev Immunol. 2019;37(1):457–95.

57. Cui W, Kaech SM. Generation of effector CD8+ T cells and their conversion to memory T cells. Immunol Rev. 2010;236(1):151–66.

58. Park SL, Zaid A, Hor JL, Christo SN, Prier JE, Davies B, et al. Local proliferation maintains a stable pool of tissue-resident memory T cells after antiviral recall responses. Nat Immunol. 2018 Feb;19(2):183–91.

59. Kratchmarov R, Magun AM, Reiner SL. TCF1 expression marks self-renewing human CD8+ T cells. Blood Adv. 2018 Jul 18;2(14):1685–90.

60. Wherry EJ. T cell exhaustion. Nat Immunol. 2011 Jun;12(6):492–9.

61. Schietinger A, Greenberg PD. Tolerance and exhaustion: defining mechanisms of T cell dysfunction. Trends Immunol. 2014 Feb 1;35(2):51–60.

62. Doering TA, Crawford A, Angelosanto JM, Paley MA, Ziegler CG, Wherry EJ. Network Analysis Reveals Centrally Connected Genes and Pathways Involved in CD8+ T Cell Exhaustion versus Memory. Immunity. 2012 Dec 14;37(6):1130–44.

63. Hosokawa H, Rothenberg EV. How transcription factors drive choice of the T cell fate. Nat Rev Immunol. 2021 Mar;21(3):162–76.

64. Hosokawa H, Rothenberg EV. Cytokines, Transcription Factors, and the Initiation of T-Cell Development. Cold Spring Harb Perspect Biol. 2018 May 1;10(5):a028621.

65. Yui MA, Rothenberg EV. Developmental gene networks: a triathlon on the course to T cell identity. Nat Rev Immunol. 2014 Aug;14(8):529–45.

66. Yang Q, Jeremiah Bell J, Bhandoola A. T-cell lineage determination. Immunol Rev. 2010;238(1):12–22.

67. Rothenberg EV, Moore JE, Yui MA. Launching the T-cell-lineage developmental programme. Nat Rev Immunol. 2008 Jan;8(1):9–21.

68. Carpenter AC, Bosselut R. Decision checkpoints in the thymus. Nat Immunol. 2010 Aug;11(8):666–73.

69. Germain RN. T-cell development and the CD4–CD8 lineage decision. Nat Rev Immunol. 2002 May;2(5):309–22.

70. Lu M, Tayu R, Ikawa T, Masuda K, Matsumoto I, Mugishima H, et al. The Earliest Thymic Progenitors in Adults Are Restricted to T, NK, and Dendritic Cell

Lineage and Have a Potential to Form More Diverse TCRβ Chains than Fetal Progenitors1. J Immunol. 2005 Nov 1;175(9):5848–56.

71. Oestreich KJ, Mohn SE, Weinmann AS. Molecular mechanisms that control the expression and activity of Bcl-6 in TH1 cells to regulate flexibility with a TFH-like gene profile. Nat Immunol. 2012 Apr;13(4):405–11.

72. Pepper M, Pagán AJ, Igyártó BZ, Taylor JJ, Jenkins MK. Opposing Signals from the Bcl6 Transcription Factor and the Interleukin-2 Receptor Generate T Helper 1 Central and Effector Memory Cells. Immunity. 2011 Oct 28;35(4):583–95.

73. Godfrey DI, Kennedy J, Suda T, Zlotnik A. A developmental pathway involving four phenotypically and functionally distinct subsets of CD3-CD4-CD8- triple-negative adult mouse thymocytes defined by CD44 and CD25 expression. J Immunol. 1993 May 15;150(10):4244–52.

74. Shinkai Y, Koyasu S, Nakayama K ichi, Murphy KM, Loh DY, Reinherz EL, et al. Restoration of T Cell Development in RAG-2-Deficient Mice by Functional TCR Transgenes. Science. 1993;259(5096):822–5.

75. Groettrup M, Ungewiss K, Azogui O, Palacios R, Owen MJ, Hayday AC, et al. A novel disulfide-linked heterodimer on pre—T cells consists of the T cell receptor β chain and a 33 kd glycoprotein. Cell. 1993 Oct 22;75(2):283–94.

76. Kreslavsky T, Gleimer M, Miyazaki M, Choi Y, Gagnon E, Murre C, et al. β-Selection-Induced Proliferation Is Required for αβ T Cell Differentiation. Immunity. 2012 Nov 16;37(5):840–53.

77. Wu Z, Zheng Y, Sheng J, Han Y, Yang Y, Pan H, et al. CD3+CD4-CD8- (Double-Negative) T Cells in Inflammation, Immune Disorders and Cancer. Front Immunol

[Internet]. 2022 [cited 2023 Mar 15];13. Available from: https://www.frontiersin.org/articles/10.3389/fimmu.2022.816005

78. Chapman JC, Chapman FM, Michael SD. The production of alpha/beta and gamma/delta double negative (DN) T-cells and their role in the maintenance of pregnancy. Reprod Biol Endocrinol. 2015 Jul 12;13(1):73.

79. von Boehmer H. Unique features of the pre-T-cell receptor α-chain: not just a surrogate. Nat Rev Immunol. 2005 Jul;5(7):571–7.

80. Tran DQ, Ramsey H, Shevach EM. Induction of FOXP3 expression in naive human CD4+FOXP3− T cells by T-cell receptor stimulation is transforming growth factor-β–dependent but does not confer a regulatory phenotype. Blood. 2007 Oct 15;110(8):2983–90.

81. Savage PA, Klawon DEJ, Miller CH. Regulatory T Cell Development. Annu Rev Immunol. 2020;38(1):421–53.

82. Li MO, Rudensky AY. T cell receptor signalling in the control of regulatory T cell differentiation and function. Nat Rev Immunol. 2016 Apr;16(4):220–33.

83. Qi Y, Zhang R, Lu Y, Zou X, Yang W. Aire and Fezf2, two regulators in medullary thymic epithelial cells, control autoimmune diseases by regulating TSAs: Partner or complementer? Front Immunol [Internet]. 2022 [cited 2023 Mar 24];13. Available from: https://www.frontiersin.org/articles/10.3389/fimmu.2022.948259

84. Abramson J, Anderson G. Thymic Epithelial Cells. Annu Rev Immunol. 2017;35(1):85–118.

85. Takaba H, Morishita Y, Tomofuji Y, Danks L, Nitta T, Komatsu N, et al. Fezf2 Orchestrates a Thymic Program of Self-Antigen Expression for Immune Tolerance. Cell. 2015 Nov 5;163(4):975–87.

86. DeVoss JJ, LeClair NP, Hou Y, Grewal NK, Johannes KP, Lu W, et al. An Autoimmune Response to Odorant Binding Protein 1a Is Associated with Dry Eye in the Aire-Deficient Mouse. J Immunol. 2010 Apr 15;184(8):4236–46.

87. Akirav EM, Ruddle NH, Herold KC. The role of AIRE in human autoimmune disease. Nat Rev Endocrinol. 2011 Jan;7(1):25–33.

88. Weng X, Kumar A, Cao L, He Y, Morgun E, Visvabharathy L, et al. Mitochondrial metabolism is essential for invariant natural killer T cell development and function. Proc Natl Acad Sci. 2021 Mar 30;118(13):e2021385118.

89. Bendelac A, Savage PB, Teyton L. The Biology of NKT Cells. Annu Rev Immunol. 2007;25(1):297–336.

90. White AJ, Lucas B, Jenkinson WE, Anderson G. Invariant NKT-cells And Control Of The Thymus Medulla. J Immunol Baltim Md 1950. 2018 May 15;200(10):3333–9.

91. Josefowicz SZ, Lu LF, Rudensky AY. Regulatory T Cells: Mechanisms of Differentiation and Function. Annu Rev Immunol. 2012;30(1):531–64.

92. Noval Rivas M, Chatila TA. Regulatory T cells in allergic diseases. J Allergy Clin Immunol. 2016 Sep 1;138(3):639–52.

93. Dominguez-Villar M, Hafler DA. Regulatory T cells in autoimmune disease. Nat Immunol. 2018 Jul;19(7):665–73.

94. Hatzioannou A, Boumpas A, Papadopoulou M, Papafragkos I, Varveri A, Alissafi T, et al. Regulatory T Cells in Autoimmunity and Cancer: A Duplicitous Lifestyle. Front

Immunol [Internet]. 2021 [cited 2022 Dec 6];12. Available from: https://www.frontiersin.org/articles/10.3389/fimmu.2021.731947

95. Feuerer M, Herrero L, Cipolletta D, Naaz A, Wong J, Nayer A, et al. Lean, but not obese, fat is enriched for a unique population of regulatory T cells that affect metabolic parameters. Nat Med. 2009 Aug;15(8):930–9.

96. Arpaia N, Green JA, Moltedo B, Arvey A, Hemmers S, Yuan S, et al. A Distinct Function of Regulatory T Cells in Tissue Protection. Cell. 2015 Aug 27;162(5):1078–89.

97. Ali N, Zirak B, Rodriguez RS, Pauli ML, Truong HA, Lai K, et al. Regulatory T cells in Skin Facilitate Epithelial Stem Cell Differentiation. Cell. 2017 Jun 1;169(6):1119-1129.e11.

98. Burzyn D, Kuswanto W, Kolodin D, Shadrach JL, Cerletti M, Jang Y, et al. A Special Population of Regulatory T Cells Potentiates Muscle Repair. Cell. 2013 Dec 5;155(6):1282–95.

99. Fontenot JD, Dooley JL, Farr AG, Rudensky AY. Developmental regulation of Foxp3 expression during ontogeny. J Exp Med. 2005 Oct 3;202(7):901–6.

100. Khattri R, Cox T, Yasayko SA, Ramsdell F. An essential role for Scurfin in CD4+CD25+ T regulatory cells. Nat Immunol. 2003 Apr;4(4):337–42.

101. Yagi H, Nomura T, Nakamura K, Yamazaki S, Kitawaki T, Hori S, et al. Crucial role of FOXP3 in the development and function of human CD25+CD4+ regulatory T cells. Int Immunol. 2004 Nov 1;16(11):1643–56.

102. Roncador G, Brown PJ, Maestre L, Hue S, Martínez-Torrecuadrada JL, Ling KL, et al. Analysis of FOXP3 protein expression in human CD4+CD25+ regulatory T cells at the single-cell level. Eur J Immunol. 2005;35(6):1681–91.

103. Du Y, Fang Q, Zheng SG. Regulatory T Cells: Concept, Classification, Phenotype, and Biological Characteristics. In: Zheng SG, editor. T Regulatory Cells in Human Health and Diseases [Internet]. Singapore: Springer; 2021 [cited 2022 Dec 6]. p. 1–31. (Advances in Experimental Medicine and Biology). Available from: https://doi.org/10.1007/978-981-15-6407-9_1

104. Wang J, Ioan-Facsinay A, van der Voort EIH, Huizinga TWJ, Toes REM. Transient expression of FOXP3 in human activated nonregulatory CD4+ T cells. Eur J Immunol. 2007;37(1):129–38.

105. Miyara M, Yoshioka Y, Kitoh A, Shima T, Wing K, Niwa A, et al. Functional Delineation and Differentiation Dynamics of Human CD4+ T Cells Expressing the FoxP3 Transcription Factor. Immunity. 2009 Jun 19;30(6):899–911.

106. Sakaguchi S, Mikami N, Wing JB, Tanaka A, Ichiyama K, Ohkura N. Regulatory T Cells and Human Disease. Annu Rev Immunol. 2020;38(1):541–66.

107. Kondělková K, Vokurková D, Krejsek J, Borská L, Fiala Z, Ctirad A. Regulatory T cells (TREG) and their roles in immune system with respect to immunopathological disorders. Acta Medica (Hradec Kralove). 2010 Jan 1;53(2):73–7.

108. Gagliani N, Magnani CF, Huber S, Gianolini ME, Pala M, Licona-Limon P, et al. Coexpression of CD49b and LAG-3 identifies human and mouse T regulatory type 1 cells. Nat Med. 2013 Jun;19(6):739–46.

109. Meiler F, Zumkehr J, Klunker S, Rückert B, Akdis CA, Akdis M. In vivo switch to IL-10–secreting T regulatory cells in high dose allergen exposure. J Exp Med. 2008 Nov 10;205(12):2887–98.

110. Robb RJ, Lineburg KE, Kuns RD, Wilson YA, Raffelt NC, Olver SD, et al. Identification and expansion of highly suppressive CD8+FoxP3+ regulatory T cells after experimental allogeneic bone marrow transplantation. Blood. 2012 Jun 14;119(24):5898–908.

111. Beres AJ, Haribhai D, Chadwick AC, Gonyo PJ, Williams CB, Drobyski WR. CD8+ FOXP3+ REGULATORY T CELLS ARE INDUCED DURING GRAFT VERSUS HOST DISEASE AND MITIGATE DISEASE SEVERITY. J Immunol Baltim Md 1950. 2012 Jul 1;189(1):464–74.

112. Sawamukai N, Satake A, Schmidt AM, Lamborn IT, Ojha P, Tanaka Y, et al. Cell-autonomous role of TGFβ and IL-2 receptors in CD4+ and CD8+ inducible regulatory T-cell generation during GVHD. Blood. 2012 Jun 7;119(23):5575–83.

113. Ohkura N, Kitagawa Y, Sakaguchi S. Development and Maintenance of Regulatory T cells. Immunity. 2013 Mar 21;38(3):414–23.

114. Santamaria JC, Borelli A, Irla M. Regulatory T Cell Heterogeneity in the Thymus: Impact on Their Functional Activities. Front Immunol. 2021 Feb 11;12:643153.

115. Lee HM, Bautista JL, Scott-Browne J, Mohan JF, Hsieh CS. A Broad Range of Self-Reactivity Drives Thymic Regulatory T Cell Selection to Limit Responses to Self. Immunity. 2012 Sep 21;37(3):475–86.

116. Ohkura N, Sakaguchi S. Transcriptional and epigenetic basis of Treg cell development and function: its genetic anomalies or variations in autoimmune diseases. Cell Res. 2020 Jun;30(6):465–74.

117. Ono M, Shimizu J, Miyachi Y, Sakaguchi S. Control of Autoimmune Myocarditis and Multiorgan Inflammation by Glucocorticoid-Induced TNF Receptor Family-Related

Proteinhigh, Foxp3-Expressing CD25+ and CD25− Regulatory T Cells1. J Immunol. 2006 Apr 15;176(8):4748–56.

118. Kim HJ, Barnitz RA, Kreslavsky T, Brown FD, Moffett H, Lemieux ME, et al. Stable inhibitory activity of regulatory T cells requires the transcription factor Helios. Science. 2015 Oct 16;350(6258):334–9.

119. Lio CWJ, Hsieh CS. A Two-Step Process for Thymic Regulatory T Cell Development. Immunity. 2008 Jan 18;28(1):100–11.

120. Dikiy S, Li J, Bai L, Jiang M, Janke L, Zong X, et al. A distal Foxp3 enhancer enables interleukin-2 dependent thymic Treg cell lineage commitment for robust immune tolerance. Immunity. 2021 May 11;54(5):931-946.e11.

121. Burchill MA, Yang J, Vang KB, Moon JJ, Chu HH, Lio CWJ, et al. Linked T Cell Receptor and Cytokine Signaling Govern the Development of the Regulatory T Cell Repertoire. Immunity. 2008 Jan 18;28(1):112–21.

122. Hadis U, Wahl B, Schulz O, Hardtke-Wolenski M, Schippers A, Wagner N, et al. Intestinal Tolerance Requires Gut Homing and Expansion of FoxP3+ Regulatory T Cells in the Lamina Propria. Immunity. 2011 Feb 25;34(2):237–46.

123. Worbs T, Bode U, Yan S, Hoffmann MW, Hintzen G, Bernhardt G, et al. Oral tolerance originates in the intestinal immune system and relies on antigen carriage by dendritic cells. J Exp Med. 2006 Mar 13;203(3):519–27.

124. Liu M, Li S, Li MO. TGF-β Control of Adaptive Immune Tolerance: a Break from Treg Cells. BioEssays News Rev Mol Cell Dev Biol. 2018 Nov;40(11):e1800063.

125. Campbell C, McKenney PT, Konstantinovsky D, Isaeva OI, Schizas M, Verter J, et al. Bacterial metabolism of bile acids promotes generation of peripheral regulatory T cells. Nature. 2020 May;581(7809):475–9.

126. Josefowicz SZ, Niec RE, Kim HY, Treuting P, Chinen T, Zheng Y, et al. Extrathymically generated regulatory T cells control mucosal TH2 inflammation. Nature. 2012 Feb;482(7385):395–9.

127. Kawakami R, Kitagawa Y, Chen KY, Arai M, Ohara D, Nakamura Y, et al. Distinct Foxp3 enhancer elements coordinate development, maintenance, and function of regulatory T cells. Immunity. 2021 May 11;54(5):947-961.e8.

128. Gershon RK, Kondo K. Cell interactions in the induction of tolerance: the role of thymic lymphocytes. Immunology. 1970 May;18(5):723–37.

129. Bacchetta R, Passerini L, Gambineri E, Dai M, Allan SE, Perroni L, et al. Defective regulatory and effector T cell functions in patients with *FOXP3* mutations. J Clin Invest. 2006 Jun 1;116(6):1713–22.

130. Amoozgar Z, Kloepper J, Ren J, Tay RE, Kazer SW, Kiner E, et al. Targeting Treg cells with GITR activation alleviates resistance to immunotherapy in murine glioblastomas. Nat Commun. 2021 May 11;12(1):2582.

131. Pandiyan P, Zheng L, Ishihara S, Reed J, Lenardo MJ. CD4+CD25+Foxp3+ regulatory T cells induce cytokine deprivation–mediated apoptosis of effector CD4+ T cells. Nat Immunol. 2007 Dec;8(12):1353–62.

132. Thornton AM, Shevach EM. CD4+CD25+ Immunoregulatory T Cells Suppress Polyclonal T Cell Activation In Vitro by Inhibiting Interleukin 2 Production. J Exp Med. 1998 Jul 20;188(2):287–96.

133. Chinen T, Kannan AK, Levine AG, Fan X, Klein U, Zheng Y, et al. An essential role for the IL-2 receptor in Treg cell function. Nat Immunol. 2016 Nov;17(11):1322–33.

134. Li MO, Wan YY, Flavell RA. T Cell-Produced Transforming Growth Factor-β1 Controls T Cell Tolerance and Regulates Th1- and Th17-Cell Differentiation. Immunity. 2007 May 25;26(5):579–91.

135. Chaudhry A, Samstein RM, Treuting P, Liang Y, Pils MC, Heinrich JM, et al. Interleukin-10 Signaling in Regulatory T Cells Is Required for Suppression of Th17 Cell-Mediated Inflammation. Immunity. 2011 Apr 22;34(4):566–78.

136. Collison LW, Workman CJ, Kuo TT, Boyd K, Wang Y, Vignali KM, et al. The inhibitory cytokine IL-35 contributes to regulatory T-cell function. Nature. 2007 Nov;450(7169):566–9.

137. Sullivan JA, Tomita Y, Jankowska-Gan E, Lema DA, Arvedson MP, Nair A, et al. Treg-Cell-Derived IL-35-Coated Extracellular Vesicles Promote Infectious Tolerance. Cell Rep. 2020 Jan 28;30(4):1039-1051.e5.

138. Aiello S, Rocchetta F, Longaretti L, Faravelli S, Todeschini M, Cassis L, et al. Extracellular vesicles derived from T regulatory cells suppress T cell proliferation and prolong allograft survival. Sci Rep. 2017 Sep 14;7:11518.

139. Tung SL, Fanelli G, Matthews RI, Bazoer J, Letizia M, Vizcay-Barrena G, et al. Regulatory T Cell Extracellular Vesicles Modify T-Effector Cell Cytokine Production and Protect Against Human Skin Allograft Damage. Front Cell Dev Biol [Internet]. 2020 [cited 2022 Dec 6];8. Available from: https://www.frontiersin.org/articles/10.3389/fcell.2020.00317

140. Lin C, Guo J, Jia R. Roles of Regulatory T Cell-Derived Extracellular Vesicles in Human Diseases. Int J Mol Sci. 2022 Sep 23;23(19):11206.

141. Tung SL, Boardman DA, Sen M, Letizia M, Peng Q, Cianci N, et al. Regulatory T cell-derived extracellular vesicles modify dendritic cell function. Sci Rep. 2018 Apr 17;8:6065.

142. Chen J, Huang F, Hou Y, Lin X, Liang R, Hu X, et al. TGF-β-induced CD4+ FoxP3+ regulatory T cell-derived extracellular vesicles modulate Notch1 signaling through miR-449a and prevent collagen-induced arthritis in a murine model. Cell Mol Immunol. 2021 Nov;18(11):2516–29.

143. Bopp T, Becker C, Klein M, Klein-Heßling S, Palmetshofer A, Serfling E, et al. Cyclic adenosine monophosphate is a key component of regulatory T cell–mediated suppression. J Exp Med. 2007 May 14;204(6):1303–10.

144. Ring S, Karakhanova S, Johnson T, Enk AH, Mahnke K. Gap junctions between regulatory T cells and dendritic cells prevent sensitization of CD8+ T cells. J Allergy Clin Immunol. 2010 Jan 1;125(1):237-246.e7.

145. Su W, Chen X, Zhu W, Yu J, Li W, Li Y, et al. The cAMP–Adenosine Feedback Loop Maintains the Suppressive Function of Regulatory T Cells. J Immunol. 2019 Sep 15;203(6):1436–46.

146. Deaglio S, Dwyer KM, Gao W, Friedman D, Usheva A, Erat A, et al. Adenosine generation catalyzed by CD39 and CD73 expressed on regulatory T cells mediates immune suppression. J Exp Med. 2007 May 14;204(6):1257–65.

147. Maj T, Wang W, Crespo J, Zhang H, Wang W, Wei S, et al. Oxidative stress controls regulatory T cell apoptosis and suppressor activity and PD-L1-blockade resistance in tumor. Nat Immunol. 2017 Dec;18(12):1332–41.

148. Cederbom L, Hall H, Ivars F. CD4+CD25+ regulatory T cells down-regulate co-stimulatory molecules on antigen-presenting cells. Eur J Immunol. 2000;30(6):1538–43.

149. Qureshi OS, Zheng Y, Nakamura K, Attridge K, Manzotti C, Schmidt EM, et al. Trans-Endocytosis of CD80 and CD86: A Molecular Basis for the Cell-Extrinsic Function of CTLA-4. Science. 2011 Apr 29;332(6029):600–3.

150. Akkaya B, Oya Y, Akkaya M, Al Souz J, Holstein AH, Kamenyeva O, et al. Regulatory T cells mediate specific suppression by depleting peptide–MHC class II from dendritic cells. Nat Immunol. 2019 Feb;20(2):218–31.

151. Chen J, Ganguly A, Mucsi AD, Meng J, Yan J, Detampel P, et al. Strong adhesion by regulatory T cells induces dendritic cell cytoskeletal polarization and contact-dependent lethargy. J Exp Med. 2017 Jan 12;214(2):327–38.

152. Gondek DC, DeVries V, Nowak EC, Lu LF, Bennett KA, Scott ZA, et al. Transplantation Survival Is Maintained by Granzyme B+ Regulatory Cells and Adaptive Regulatory T Cells. J Immunol. 2008 Oct 1;181(7):4752–60.

153. Koyama S, Nishikawa H. Mechanisms of regulatory T cell infiltration in tumors: implications for innovative immune precision therapies. J Immunother Cancer. 2021 Jul 1;9(7):e002591.

154. Neel BG, Gu H, Pao L. The ‘Shp’ing news: SH2 domain-containing tyrosine phosphatases in cell signaling. Trends Biochem Sci. 2003 Jun 1;28(6):284–93.

155. Lorenz U. SHP-1 and SHP-2 in T cells: two phosphatases functioning at many levels. Immunol Rev. 2009 Mar;228(1):342–59.

156. Štefanová I, Hemmer B, Vergelli M, Martin R, Biddison WE, Germain RN. TCR ligand discrimination is enforced by competing ERK positive and SHP-1 negative feedback pathways. Nat Immunol. 2003 Mar;4(3):248–54.

157. Plas DR, Johnson R, Pingel JT, Matthews RJ, Dalton M, Roy G, et al. Direct Regulation of ZAP-70 by SHP-1 in T Cell Antigen Receptor Signaling. Science. 1996;272(5265):1173–6.

158. Carter JD, Calabrese GM, Naganuma M, Lorenz U. Deficiency of the Src Homology Region 2 Domain-Containing Phosphatase 1 (SHP-1) Causes Enrichment of CD4+CD25+ Regulatory T Cells. J Immunol. 2005 Jun 1;174(11):6627–38.

159. Zhang J, Somani AK, Yuen D, Yang Y, Love PE, Siminovitch KA. Involvement of the SHP-1 Tyrosine Phosphatase in Regulation of T Cell Selection1. J Immunol. 1999 Sep 15;163(6):3012–21.

160. Johnson KG, LeRoy FG, Borysiewicz LK, Matthews RJ. TCR Signaling Thresholds Regulating T Cell Development and Activation Are Dependent upon SHP-11. J Immunol. 1999 Apr 1;162(7):3802–13.

161. Stanford SM, Rapini N, Bottini N. Regulation of TCR signalling by tyrosine phosphatases: from immune homeostasis to autoimmunity. Immunology. 2012;137(1):1–19.

162. Mauldin IS, Tung KS, Lorenz UM. The tyrosine phosphatase SHP-1 dampens murine Th17 development. Blood. 2012 May 10;119(19):4419–29.

163. Azoulay-Alfaguter I, Strazza M, Peled M, Novak HK, Muller J, Dustin ML, et al. The tyrosine phosphatase SHP-1 promotes T cell adhesion by activating the adaptor protein CrkII in the immunological synapse. Sci Signal. 2017 Aug 8;10(491):eaal2880.

164. Wo Tsui H, Siminovitch KA, de Souza L, Tsui FWL. Motheaten and viable motheaten mice have mutations in the haematopoietic cell phosphatase gene. Nat Genet. 1993 Jun;4(2):124–9.

165. Iype T, Sankarshanan M, Mauldin IS, Mullins DW, Lorenz U. The Protein Tyrosine Phosphatase SHP-1 Modulates the Suppressive Activity of Regulatory T Cells. J Immunol. 2010 Nov 15;185(10):6115–27.

166. Shultz LD, Schweitzer PA, Rajan TV, Yi T, Ihle JN, Matthews RJ, et al. Mutations at the murine motheaten locus are within the hematopoietic cell protein-tyrosine phosphatase (Hcph) gene. Cell. 1993 Jul 2;73(7):1445–54.

167. Mercadante ER, Lorenz UM. T Cells Deficient in the Tyrosine Phosphatase SHP-1 Resist Suppression by Regulatory T Cells. J Immunol. 2017 Jul 1;199(1):129–37.

168. Mok SC, Kwok TT, Berkowitz RS, Barrett AJ, Tsui FWL. Overexpression of the Protein Tyrosine Phosphatase, Nonreceptor Type 6 (PTPN6), in Human Epithelial Ovarian Cancer. Gynecol Oncol. 1995 Jun 1;57(3):299–303.

169. Insabato L, Amelio I, Quarto M, Zannetti A, Tolino F, Mauro G de, et al. Elevated Expression of the Tyrosine Phosphatase SHP-1 Defines a Subset of High-Grade Breast Tumors. Oncology. 2009;77(6):378–84.

170. Pao LI, Lam KP, Henderson JM, Kutok JL, Alimzhanov M, Nitschke L, et al. B Cell-Specific Deletion of Protein-Tyrosine Phosphatase Shp1 Promotes B-1a Cell Development and Causes Systemic Autoimmunity. Immunity. 2007 Jul;27(1):35–48.

171. Rubtsov YP, Rasmussen JP, Chi EY, Fontenot J, Castelli L, Ye X, et al. Regulatory T Cell-Derived Interleukin-10 Limits Inflammation at Environmental Interfaces. Immunity. 2008 Apr 11;28(4):546–58.

172. Schluns KS, Williams K, Ma A, Zheng XX, Lefrançois L. Cutting edge: requirement for IL-15 in the generation of primary and memory antigen-specific CD8 T cells. J Immunol Baltim Md 1950. 2002 May 15;168(10):4827–31.

173. Yang G, Hisha H, Cui Y, Fan T, Jin T, Li Q, et al. A new assay method for late CFU-S formation and long-term reconstituting activity using a small number of pluripotent hemopoietic stem cells. Stem Cells Dayt Ohio. 2002;20(3):241–8.

174. Janowska-Wieczorek A, Majka M, Kijowski J, Baj-Krzyworzeka M, Reca R, Turner AR, et al. Platelet-derived microparticles bind to hematopoietic stem/progenitor cells and enhance their engraftment. Blood. 2001 Nov 15;98(10):3143–9.

175. Lahl K, Loddenkemper C, Drouin C, Freyer J, Arnason J, Eberl G, et al. Selective depletion of Foxp3+ regulatory T cells induces a scurfy-like disease. J Exp Med. 2007 Jan 22;204(1):57–63.

176. Madisen L, Zwingman TA, Sunkin SM, Oh SW, Zariwala HA, Gu H, et al. A robust and high-throughput Cre reporting and characterization system for the whole mouse brain. Nat Neurosci. 2010 Jan;13(1):133–40.

177. Medina CB, Chiu YH, Stremska ME, Lucas CD, Poon I, Tung KS, et al. Pannexin 1 channels facilitate communication between T cells to restrict the severity of airway inflammation. Immunity. 2021 Aug;54(8):1715-1727.e7.

178. George T, Bell M, Chakraborty M, Siderovski DP, Giembycz MA, Newton R. Protective Roles for RGS2 in a Mouse Model of House Dust Mite-Induced Airway Inflammation. PLOS ONE. 2017 Jan 20;12(1):e0170269.

179. Harakal J, Rival C, Qiao H, Tung KS. Regulatory T Cells Control Th2-Dominant Murine Autoimmune Gastritis. J Immunol. 2016 Jul 1;197(1):27–41.

180. Steel CD, Stephens AL, Hahto SM, Singletary SJ, Ciavarra RP. Comparison of the lateral tail vein and the retro-orbital venous sinus as routes of intravenous drug delivery in a transgenic mouse model. Lab Anim. 2008 Jan;37(1):26–32.

181. Franckaert D, Dooley J, Roos E, Floess S, Huehn J, Luche H, et al. Promiscuous Foxp3-cre activity reveals a differential requirement for CD28 in Foxp3 $^{+}$ and Foxp3 $^{-}$ T cells. Immunol Cell Biol. 2015 Apr;93(4):417–23.

182. Sawant DV, Vignali DAA. Once a Treg, always a Treg? Immunol Rev. 2014;259(1):173–91.

183. Gerriets VA, Kishton RJ, Johnson MO, Cohen S, Siska PJ, Nichols AG, et al. Foxp3 and Toll-like receptor signaling balance Treg cell anabolic metabolism for suppression. Nat Immunol. 2016 Dec;17(12):1459–66.

184. Zeng H, Chi H. Metabolic control of regulatory T cell development and function. Trends Immunol. 2015 Jan;36(1):3–12.

185. Yamaguchi T, Hirota K, Nagahama K, Ohkawa K, Takahashi T, Nomura T, et al. Control of Immune Responses by Antigen-Specific Regulatory T Cells Expressing the Folate Receptor. Immunity. 2007 Jul 27;27(1):145–59.

186. Kinoshita M, Kayama H, Kusu T, Yamaguchi T, Kunisawa J, Kiyono H, et al. Dietary Folic Acid Promotes Survival of Foxp3 $^{+}$ Regulatory T Cells in the Colon. J Immunol. 2012 Sep 15;189(6):2869–78.

187. Wohler J, Bullard D, Schoeb T, Barnum S. LFA-1 is critical for regulatory T cell homeostasis and function. Mol Immunol. 2009 Jul 1;46(11):2424–8.

188. Shi H, Chi H. Metabolic Control of Treg Cell Stability, Plasticity, and Tissue-Specific Heterogeneity. Front Immunol [Internet]. 2019 Dec 11 [cited 2020 May 29];10. Available from: https://www.ncbi.nlm.nih.gov/pmc/articles/PMC6917616/

189. Pompura SL, Dominguez-Villar M. The PI3K/AKT signaling pathway in regulatory T-cell development, stability, and function. J Leukoc Biol. 2018;103(6):1065–76.

190. Noval Rivas M, Burton OT, Wise P, Charbonnier LM, Georgiev P, Oettgen HC, et al. Regulatory T Cell Reprogramming toward a Th2-Cell-like Lineage Impairs Oral Tolerance and Promotes Food Allergy. Immunity. 2015 Mar 17;42(3):512–23.

191. Haxhinasto S, Mathis D, Benoist C. The AKT–mTOR axis regulates de novo differentiation of CD4 $^{+}$ Foxp3 $^{+}$ cells. J Exp Med. 2008 Mar 17;205(3):565–74.

192. Hawse WF, Boggess WC, Morel PA. TCR Signal Strength Regulates Akt Substrate Specificity To Induce Alternate Murine Th and T Regulatory Cell Differentiation Programs. J Immunol. 2017 Jul 15;199(2):589–97.

193. Zeng H, Yang K, Cloer C, Neale G, Vogel P, Chi H. mTORC1 couples immune signals and metabolic programming to establish Treg-cell function. Nature. 2013 Jul;499(7459):485–90.

194. Merkenschlager M, von Boehmer H. PI3 kinase signalling blocks Foxp3 expression by sequestering Foxo factors. J Exp Med. 2010 Jul 5;207(7):1347–50.

195. Gottschalk RA, Corse E, Allison JP. TCR ligand density and affinity determine peripheral induction of Foxp3 in vivo. J Exp Med. 2010 Aug 2;207(8):1701–11.

196. Johnson DJ, Pao LI, Dhanji S, Murakami K, Ohashi PS, Neel BG. Shp1 regulates T cell homeostasis by limiting IL-4 signals. J Exp Med. 2013 Jul 1;210(7):1419–31.

197. Chiang YJ, Hodes RJ. T cell development is regulated by the coordinated function of proximal and distal Lck promoters active at different developmental stages. Eur J Immunol. 2016 Oct;46(10):2401–8.

198. Martinez RJ, Morris AB, Neeld DK, Evavold BD. Targeted loss of SHP1 in murine thymocytes dampens TCR signaling late in selection. Eur J Immunol. 2016 Sep;46(9):2103–10.

199. Nishio J, Baba M, Atarashi K, Tanoue T, Negishi H, Yanai H, et al. Requirement of full TCR repertoire for regulatory T cells to maintain intestinal homeostasis. Proc Natl Acad Sci U S A. 2015 Oct 13;112(41):12770–5.

200. Akue AD, Lee JY, Jameson SC. Derivation and Maintenance of Virtual Memory CD8 T Cells. J Immunol. 2012 Mar 15;188(6):2516–23.

201. Marusina AI, Ono Y, Merleev AA, Shimoda M, Ogawa H, Wang EA, et al. CD4+ virtual memory: Antigen-inexperienced T cells reside in the naïve, regulatory, and memory T cell compartments at similar frequencies, implications for autoimmunity. J Autoimmun. 2017 Feb;77:76–88.

202. Chiu BC, Martin BE, Stolberg VR, Chensue SW. Cutting Edge: Central Memory CD8 T Cells in Aged Mice Are Virtual Memory Cells. J Immunol. 2013 Dec 15;191(12):5793–6.

203. Eriksen KW, Woetmann A, Skov L, Krejsgaard T, Bovin LF, Hansen ML, et al. Deficient SOCS3 and SHP-1 Expression in Psoriatic T Cells. J Invest Dermatol. 2010 Jun 1;130(6):1590–7.

204. Christophi GP, Hudson CA, Gruber RC, Christophi CP, Mihai C, Mejico LJ, et al. SHP-1 deficiency and increased inflammatory gene expression in PBMCs of multiple sclerosis patients. Lab Invest. 2008 Mar;88(3):243–55.

205. Varone A, Spano D, Corda D. Shp1 in Solid Cancers and Their Therapy. Front Oncol [Internet]. 2020 [cited 2022 Dec 8];10. Available from: https://www.frontiersin.org/articles/10.3389/fonc.2020.00935

206. Snook JP, Soedel AJ, Ekiz HA, O'Connell RM, Williams MA. Inhibition of SHP-1 Expands the Repertoire of Antitumor T Cells Available to Respond to Immune Checkpoint Blockade. Cancer Immunol Res. 2020 Apr 1;8(4):506–17.

207. Fowler CC, Pao LI, Blattman JN, Greenberg PD. SHP-1 in T Cells Limits the Production of CD8 Effector Cells without Impacting the Formation of Long-Lived Central Memory Cells. J Immunol. 2010 Sep 15;185(6):3256–67.

208. Stone JD, Chervin AS, Kranz DM. T-cell receptor binding affinities and kinetics: impact on T-cell activity and specificity. Immunology. 2009;126(2):165–76.

209. Hebeisen M, Baitsch L, Presotto D, Baumgaertner P, Romero P, Michielin O, et al. SHP-1 phosphatase activity counteracts increased T cell receptor affinity. J Clin Invest. 2013 Mar 1;123(3):1044–56.

210. Moran AE, Holzapfel KL, Xing Y, Cunningham NR, Maltzman JS, Punt J, et al. T cell receptor signal strength in Treg and iNKT cell development demonstrated by a novel fluorescent reporter mouse. J Exp Med. 2011 May 23;208(6):1279–89.

211. Vahl JC, Drees C, Heger K, Heink S, Fischer JC, Nedjic J, et al. Continuous T Cell Receptor Signals Maintain a Functional Regulatory T Cell Pool. Immunity. 2014 Nov 20;41(5):722–36.

212. Woo LN, Guo WY, Wang X, Young A, Salehi S, Hin A, et al. A 4-Week Model of House Dust Mite (HDM) Induced Allergic Airways Inflammation with Airway Remodeling. Sci Rep. 2018 May 2;8(1):6925.

213. Kim HY, DeKruyff RH, Umetsu DT. The many paths to asthma: phenotype shaped by innate and adaptive immunity. Nat Immunol. 2010 Jul;11(7):577–84.

214. Turato G, Barbato A, Baraldo S, Zanin ME, Bazzan E, Lokar-Oliani K, et al. Nonatopic Children with Multitrigger Wheezing Have Airway Pathology Comparable to Atopic Asthma. Am J Respir Crit Care Med. 2008 Sep;178(5):476–82.

215. Gubernatorova EO, Gorshkova EA, Namakanova OA, Zvartsev RV, Hidalgo J, Drutskaya MS, et al. Non-redundant Functions of IL-6 Produced by Macrophages and Dendritic Cells in Allergic Airway Inflammation. Front Immunol. 2018 Nov 26;9:2718.

216. Johnson JR, Wiley RE, Fattouh R, Swirski FK, Gajewska BU, Coyle AJ, et al. Continuous Exposure to House Dust Mite Elicits Chronic Airway Inflammation and Structural Remodeling. Am J Respir Crit Care Med. 2004 Feb;169(3):378–85.

217. Baaten BJG, Li CR, Deiro MF, Lin MM, Linton PJ, Bradley LM. CD44 Regulates Survival and Memory Development in Th1 Cells. Immunity. 2010 Jan 29;32(1):104–15.

218. Pathak MK, Yi T. Sodium Stibogluconate Is a Potent Inhibitor of Protein Tyrosine Phosphatases and Augments Cytokine Responses in Hemopoietic Cell Lines1. J Immunol. 2001 Sep 15;167(6):3391–7.

219. Savid-Frontera C, Viano ME, Baez NS, Lidon NL, Fontaine Q, Young HA, et al. Exploring the immunomodulatory role of virtual memory CD8+ T cells: Role of IFN gamma in tumor growth control. Front Immunol [Internet]. 2022 [cited 2023 Mar 24];13. Available from: https://www.frontiersin.org/articles/10.3389/fimmu.2022.971001

220. Lee JY, Hamilton SE, Akue AD, Hogquist KA, Jameson SC. Virtual memory CD8 T cells display unique functional properties. Proc Natl Acad Sci U S A. 2013 Aug 13;110(33):13498–503.

221. Da Costa AS, Graham JB, Swarts JL, Lund JM. Regulatory T cells limit unconventional memory to preserve the capacity to mount protective CD8 memory responses to pathogens. Proc Natl Acad Sci. 2019 May 14;116(20):9969–78.

222. White JT, Cross EW, Burchill MA, Danhorn T, McCarter MD, Rosen HR, et al. Virtual memory T cells develop and mediate bystander protective immunity in an IL-15-dependent manner. Nat Commun. 2016 Apr 21;7(1):11291.

223. Sauer MG, Herbst J, Diekmann U, Rudd CE, Kardinal C. SHP-1 Acts as a Key Regulator of Alloresponses by Modulating LFA-1-Mediated Adhesion in Primary Murine T Cells. Mol Cell Biol. 2016 Nov 28;36(24):3113–27.

224. Wang H, Wei B, Bismuth G, Rudd CE. SLP-76-ADAP adaptor module regulates LFA-1 mediated costimulation and T cell motility. Proc Natl Acad Sci. 2009 Jul 28;106(30):12436–41.

225. Raab M, Lu Y, Kohler K, Smith X, Strebhardt K, Rudd CE. LFA-1 activates focal adhesion kinases FAK1/PYK2 to generate LAT-GRB2-SKAP1 complexes that terminate T-cell conjugate formation. Nat Commun. 2017 Jul 12;8(1):16001.

226. Golubovskaya V, Wu L. Different Subsets of T Cells, Memory, Effector Functions, and CAR-T Immunotherapy. Cancers. 2016 Mar 15;8(3):36.

227. Liang B, Workman C, Lee J, Chew C, Dale BM, Colonna L, et al. Regulatory T Cells Inhibit Dendritic Cells by Lymphocyte Activation Gene-3 Engagement of MHC Class II1. J Immunol. 2008 May 1;180(9):5916–26.

228. Onodera T, Jang MH, Guo Z, Yamasaki M, Hirata T, Bai Z, et al. Constitutive Expression of IDO by Dendritic Cells of Mesenteric Lymph Nodes: Functional Involvement of the CTLA-4/B7 and CCL22/CCR4 Interactions1. J Immunol. 2009 Nov 1;183(9):5608–14.

229. Vignali DAA, Collison LW, Workman CJ. How regulatory T cells work. Nat Rev Immunol. 2008 Jul;8(7):523–32.

230. Smigiel KS, Richards E, Srivastava S, Thomas KR, Dudda JC, Klonowski KD, et al. CCR7 provides localized access to IL-2 and defines homeostatically distinct regulatory T cell subsets. J Exp Med. 2013 Dec 30;211(1):121–36.

231. Raynor J, Karns R, Almanan M, Li KP, Divanovic S, Chougnet CA, et al. IL-6 and ICOS antagonize Bim and promote Treg accrual with age. J Immunol Baltim Md 1950. 2015 Aug 1;195(3):944–52.